



## University of Bradford eThesis

This thesis is hosted in [Bradford Scholars](#) – The University of Bradford Open Access repository. Visit the repository for full metadata or to contact the repository team



© University of Bradford. This work is licenced for reuse under a [Creative Commons Licence](#).

**An Experimental Study on the Effects of Heat and  
Chemical Inhibitors on the Flow Behaviour of Waxy  
Crude Oils**

**The Effects of Heat and Chemical Inhibitors on the  
Rheological Properties of Waxy Crude Oils with  
regard to Pumping in Pipelines**

**Fathia Abdulwahed B. MOHAMED**

**Submitted for the Degree of Doctor of Philosophy**

**Faculty of Engineering and Informatics**

**University of Bradford**

**2019**

# ABSTRACT

Fathia Abdulwahed B. Mohamed

An experimental study on the effects of heat and chemical inhibitors on the flow behaviour of waxy crude oils

The effects of heat and chemical inhibitors on the rheological properties of waxy crude oils with regard to pumping in pipelines

**Keywords:** Waxy crude oil; Flow assurance; Pour point; Flow characteristic; gelled oil; Yield stress; Wax deposition; Chemical inhibitors; Morphology; Viscoelastic properties.

Waxy crude oils (1/3 of oil produced worldwide), pumping through pipelines considered risky operation due to the crude wax content (15-40 wt.%) and to the temperature at which wax supersaturates and precipitates, leading to the danger of pipe blockage, eventually resulting, in multimillion dollars loss in production and maintenance.

This research undertaken to develop operational strategy of waxy crude pipelines, considering the crude and crude gel properties and flow conditions. The research problem was approached by characterizing the crude gel with and without additives using chromatography (GC), differential scanning calorimetry (DSC), cross polarised microscopy (CPM), controlled stress and oscillatory shear rheology (CSR and OSR), the principal parameters being the crude temperature and the rate at which the crude was cooled. GC and DSC were useful in establishing wax composition, content and wax appearance temperature (WAT). Control stress rheometer proved to be the most appropriate as it measured the reduction in apparent viscosity at full production (10-50 s<sup>-1</sup> shear rate), near shutdown (1 s<sup>-1</sup>) and yielding when the oil was statically cooled. On this basis, it was established that the wax inhibitor was

the most effective. CPM revealed that only the wax inhibitor changed the structure of the gel, disrupting its otherwise knitted crystal network. Dilution with the light crude oil merely reduced the wax content and the pour point depressant reduced the gelling temperature. OSR provided a check on CSR and confirmed the gelation temperature measured. CSR provided the yield stress measured, it also provided comprehensive data that can be used for theoretical modelling of this complex flow.



## **ACKNOWLEDGEMENTS**

First and foremost, thanks to Almighty Allah who gave me the wit to execute this work.

I would like to express my sincere gratitude to my supervisor, Professor Hadj Benkreira for his help all the time, effort and encouragement. Also I would like to express my sincere thanks to my Industrial Supervisor, Dr Salah Al-Hengari for his great support during this work.

Thanks for my family especially my father for extra support, it is your great credit that I continued my graduate studies. I thank my wonderful husband “Mohamed” for providing unlimited support during my PhD studies. Without his love, patience and support, the completion of this work would not have been possible.

Thank you my friends, Laila, Abu baker and Attif for your never-ending support and encouragement throughout the process of completing this work.

This PhD research was financially supported by Libyan Petroleum Institute-Libya and I would like to take the opportunity to thank the management and all the staff of the institute, including workshop group.

## NOMENCLATURE

WAT & $T_{WA}$	Wax appearance temperature, °C
$\Delta P$	Restart pressure, Pa
PP	pour point, °C
$\dot{\gamma}$	Shear rate, 1/s
$\mu$	Apparent viscosity, Pa.s
$\tau_e$	Elastic yield stress, Pa
$\tau_s$	Static yield stress, Pa
$\tau_f$	Flow yield stress, Pa
$\tau_{rst}$	yield stress (restart), Pa
R	Pipe radius, mm
L	Pipe length, m
$\omega$	angular velocity
$\delta$	Phase angle, degree
f	Frequency, Hz
$G'$	Storage modulus, Pa
$G''$	Loss modulus, Pa
t	Time, s
LVE	Linear Viscoelastic range
n	Flow index
k	consistency index
$\rho$	Density, Kg/m <sup>3</sup>
BPD	barrels per day
CSR	Controlled shear rate rheometer
CSS	Controlled shear stress rheometer
OSR	Oscillatory stress rheometer

## List of Figures

Figure 1.1: Waxy crude oil gelation at (a) low and (b) high cooling rates. (Lee et al., Energy & Fuels 2008.....	2
Figure 1.2: Blockage of pipe following wax deposition ( <a href="http://www.subseaexpo.com">www.subseaexpo.com</a> ).....	2
Figure 1.3: Libya oil fields, pipelines and terminals. (Libya National Oil Corporation).....	4
Figure 1.4: Libya multitude of oil fields in the Sirte basin (Libya National Oil Corporation).....	5
Figure 1.5: Deformation-flow curve of waxy crude oil gels (Chang and Boger, 1998).....	7
Figure 2.2.1: Paraffins wax crystallising showing needles crystals (Edwards, 1957).....	12
Figure 2.2.2: General view of Abu-attifel crude oil crystals.....	12
Figure 2.3.1: Effect of cooling rate on crystal size and density for Abu-attifel crude oil at 30°C.....	14
Figure 2.4.1: Nucleation scheme.....	15
Figure 2.4.2: Formation of solid bridges between particles. (Beckmann, 2013).....	17
Figure 2.5.1: Common rheological viscous flow curve.....	21
Figure 2.5.2: Apparent viscosity plateaux.....	23
Figure 2.5.3: Dilatancy of 1.25µm PVC particles in dioctyl phthalate (Stickel and Powell, 2005).....	23
Figure 2.5.4: Flow curve for Abu-attifel crude oil untreated, shear stress vs shear rate at cooling rate of 1°C/min.....	24
Figure 2.5.5: Force Balance on a section of fluid in a pipe.....	26
Figure 2.5.6: Velocity distribution in the form of a parabola.....	28
Figure 2.5.7: Annulus of flow in a pipe.....	29
Figure 2.5.8: Yielding of waxy crude oil (Wardhaugh and Boger, 1991).....	33
Figure 2.5.9: Zoom into the controlled stress data for BPO at 15°C, cooling rate 0.5°C/min, stress sweep 0 -150 Pa at rate 30Pa/min (	

Fakroun, 2017).....	33
Figure 2.5.10: Schematic of atypical oscillatory rheometer setup.....	37
Figure 2.5.11: Applied strain and stress response on oscillatory shear flow.....	37
Figure 2.5.12a: Yielding in oscillatory flow: General Features.....	38
Figure 2.5.12b: Oscillatory test at 10Hz of a waxy crude oil gel (Mendez, 2015) .....	39
Figure 2.5.13: Yielding in creep flow (Chang et al., 1988).....	40
Figure 2.5.14a: Variations of $G'_E$ and $\gamma_E$ of 5 wt % gelled model waxy oil with concentration of precipitated wax crystals $\phi_w$ (Yang et al, 2013b) .....	44
Figure 2.5.14b: Variations of $G'_E$ and $\gamma_E$ of 10 wt % gelled model waxy oil with concentration of precipitated wax crystals $\phi_w$ . (Yang et al. 2013b).....	44
Figure 2.6.1: Treatment methods for wax deposition problems (Frenier et al., 2010).....	45
Figure 2.6.2: Typical wax inhibitors (Kelland, 2009).....	46
Figure 3.3.1: Oil samples conditioning rig and holding pots.....	58
Figure 3.4.1: Photograph of the the Thermal Analysis DSC Q20.....	59
Figure 3.4.2a: Typical DSC heat curves measured for Abu-attifel untreated crude .oil at cooling rate of 15°C/min.....	60
Figure 3.4.2b: Typical DSC heat curves measured for Abu-attifel crude oil treated with ROA500 PPM at cooling rate of 15°C/min.....	60
Figure 3.5.1: Varian Gas Chromatograph (CP3800).....	61
Figure 3.6.1: Axioskop 40 Cross-Polarised Microscope.....	62
Figure 3.6.2: Abu-attifel crude oil gel structure without and with a wax inhibitor ROA (1000 ppm, 22°C).....	63

Figure 3.7.1: Principle of SVM 3000 rotational viscometer.....	64
Figure 3.7.2: The Bohlin CVO 100 (Malvern).....	65
Figure 3.7.3: Typical controlled stress hysteresis loop of waxy crude oil.....	66
Figure 3.7.4: Typical Oscillatory G' and G'' variation with amplitude.....	69
Figure 3.7.5: Gel point for Abu-attifel crude oil.....	70
Figure 3.7.6: Set-up for pour point measurement.....	71
Figure 4.2.1: Carbon number distribution of Abu-attifel crude oil obtained with GC.....	76
Figure 4.2.2: Macro and micro crystalline paraffins wax structures.....	77
Figure 4.2.3: Carbon number distribution of Abu-attifel crude oil diluted with Sirtica.....	77
Figure 4.2.4: Carbon number distribution of Abu-attifel crude oil dosed with PPD.....	78
Figure 4.2.5: Carbon number distribution of Abu-attifel crude oil dosed with WI.....	78
Figure: 4.2.6: DSC traces for treated and untreated Abu-attifel crude oil.....	80
Figure 4.2.7a: Variation of WAT1 with cooling rates for treated and untreated Abu-attifel crude oil.....	81
Figure 4.2.7b: Variation of WAT2 with cooling rates for treated and untreated Abu-attifel crude oil.....	81
Figure 4.3.1: Variation of viscosity with temperatures for untreated Abu-attifel crude oil at 1°C/min.....	83
Figure 4.3.2a: Reduction in apparent viscosity after dilution with light crude oil Sirtica.....	84
Figure 4.3.2b: Reduction in apparent viscosity after dosing with WI ROA at 500 PPM.....	85
Figure 4.3.2c: Reduction in apparent viscosity after dosing with WI ROA at 1000 PPM.....	85

Figure 4.3.2d: Reduction in apparent viscosity upon dosing with PPD2000 down to 30°C.....	86
Figure 4.3.2e: Reduction in apparent viscosity upon dosing with PPD2000.....	86
Figure 4.3.2f: Reduction in apparent viscosity upon dosing with PPD2000. (Expanded scale in 40-30°C region).....	87
Figure 4.3.2g: Reduction in apparent viscosity after dilution with Sirtica light oil at the higher shear rate of 50 s <sup>-1</sup> .....	88
Figure 4.3.2h: Reduction in apparent viscosity after dosing with WI ROA at 500 PPM at the higher shear rate of 50 s <sup>-1</sup> .....	89
Figure 4.3.2i: Reduction in apparent viscosity upon dosing with 2000 PPM at the higher shear rate of 50 s <sup>-1</sup> .....	90
Figure 4.3.2j: Reduction in apparent viscosity upon dosing with 2000 PPM PPD at the higher shear rate of 50 s <sup>-1</sup> . (Expanding scale in 40-30°C range).....	90
Figure 4.4.1a: Reduction in apparent viscosity upon dilution with Sirtica at the low shear rate of 1 s <sup>-1</sup> and cooling rate of 1°C/min (a) 70-30 °C and (b) expanded scale in 40-30 °C range.....	92
Figure 4.4.1b: Reduction in apparent viscosity upon dosing with PPD1000 PPM at the low shear rate of 1 s <sup>-1</sup> and cooling rate of 1°C/min (a) 70-30 °C and (b) expanded scale in the 45-30°C range.....	93
Figure 4.4.1c: Apparent viscosity upon dosing with ROA at shear rate of 1 s <sup>-1</sup> and cooling rate of 1°C/min.....	94
Figure 4.4.1d: Reduction in apparent viscosity upon dosing with ROA at the low shear rate of 1 s <sup>-1</sup> and cooling rate of 1°C/min (70-30 °C and expanded scale in 40-30 °C range).....	95
Figure 4.4.1e: Reduction in apparent viscosity upon dosing with ROA and PPD at the low shear rate of 1 s <sup>-1</sup> and cooling rate of 1°C/min.....	95
Figure 4.4.1f: Reduction in apparent viscosity upon dosing with ROA and PPD at the low shear rate of 1 s <sup>-1</sup> and cooling rate of 1°C/min.....	96

Figure 4.5.1: Yielding of Abu-attifel crude oil at 30°C.....	97
Figure 4.5.2: Variation of shear stress with shear rate for Abu-attifel untreated crude oil at 1°C/min.....	99
Figure 4.5.3: Yielding of Abu-attifel crude oil at 40°C upon addition of Sirtica and ROA (cooling rate= 0.5°C/min and stress loading rate=25Pa/min.....	100
Figure 4.5.4: Yielding of Abu-attifel crude oil at 40°C upon addition of Sirtica, ROA and PPD (cooling rate= 0.5°C/min and stress loding rate=25Pa/min.....	101
Figure 4.5.5: Yielding of Abu-attifel crude oil at 35°C upon addition of Sirtica and ROA (cooling rate= 0.5°C/min and stress loding rate=25Pa/min.....	102
Figure 4.5.6: Yielding of Abu-attifel crude oil at 30°C upon addition of wax inhibitor ROA (cooling rate= 0.5°C/min and stress loding rate=25Pa/min.....	103
Figure 4.5.7: Yielding of Abu-attifel crude oil at 30°C upon addition of Sirtica and ROA at the higher cooling rate (cooling rate= 1°C/min and stress loading rate=25Pa/min).....	104
Figure 4.5.8: Yielding of Abu-attifel crude oil at 40°C upon addition of Sirtica, ROA and PPD at the higher cooling rate (cooling rate= 1°C/min and stress loading rate=25Pa/min).....	104
Figure 4.5.9: Yielding of Abu-attifel crude oil dosed with 1000 PPM ROA at 30°C (cooling rate= 1°C/min and stress loading rate=100Pa/min).....	105
Figure 4.6.1: Effect of cooling rate on crystal average area of Abu-attifel untreated crude oil. Scale: X100 magnification, whole width of the photographs covers 1380 µm.....	108
Figure 4.6.2: Microstructure and crystal average area of Abu-attifel crude oil diluted with 20% Sirtica at 30°C for a range of cooling rates. Scale: The whole width of the photographs covers 1380 µm and X100 magnification.....	109

Figure 4.6.3: Microstructure and crystal average area of Abu-attifel crude oil dosed with PPD 2000 PPM at 30°C for a range of cooling rates. Scale: The whole width of the photographs covers 1380 $\mu\text{m}$ and X100 magnification.....	110
Figure 4.6.4: Microstructure and crystal average area of Abu-attifel crude oil dosed with ROA 500 PPM at 30°C for a range of cooling rates. Scale: The whole width of the photographs covers 1380 $\mu\text{m}$ and X100 magnification.....	111
Figure 4.6.6: Microstructure and crystal average area of Abu-attifel crude oil dosed with ROA 500 PPM at 40°C. Scale: The whole width of the photographs covers 1380 $\mu\text{m}$ and X100 magnification.....	112
Figure 4.7.1: $G'$ and $G''$ as measured for Abu-attifel untreated crude oil at various temperatures. (Frequency= 0.5 Hz and cooling rate= 1°C).....	114
Figure 4.7.2: $G'$ and $G''$ as measured for Abu-attifel crude oil with 500 PPM ROA at various temperatures. (Frequency=0.5Hz and cooling rate=1°C/min)...	115
Figure 4.7.3: $G'$ and $G''$ as measured for Abu-attifel crude oil with 20% of Sirtica at various temperatures. (Frequency= 0.2 Hz, Shear stress= 0.3Pa and cooling rate= 1°C).....	115
Figure 4.7.4: Elastic modulus of Abu-attifel untreated crude oil.....	116
Figure 4.7.5: Elastic modulus of Abu-attifel crude oil treated with chemicals at 30°C and cooling rate of 1°C/min.....	118
Figure 4.7.6: Elastic modulus of Abu-attifel crude oil + 500 PPM ROA.....	118



## List of Tables

<b>Table 1.1:</b> Characteristic Properties of Abu-attifel crude oil.....	6
<b>Table 1.2:</b> Specifications & concentrations of wax inhibitors used.....	9
<b>Table 2.5.1:</b> Relationship of apparent viscosity with type of material behaviour.....	25
<b>Table 2.5.2:</b> Analytical solutions to pipe flow equations using viscometric models.....	30
<b>Table 2.5.3:</b> Various techniques for measuring the yield stress.....	36
<b>Table 3.2.1:</b> Physical properties of Abu-attifel crude oil.....	55
<b>Table 3.2.2:</b> Specifications & concentrations of wax inhibitors used.....	57
<b>Table 3.7.1:</b> Specifications of the Bohlin CVO100 (Operating manual).....	65
<b>Table 3.7.2:</b> Controlled Stress & Oscillatory Stress measurements testing conditions.(Initial temperature 75°C, oscillatory frequency 0.5 Hz)...	67
<b>Table 3.7.3:</b> Gel point determination using set Shear Stress (initial temperature 75°C, shear stress 0.3Pa).....	68
<b>Table 3.7.4:</b> Controlled Shear Rate measurements testing conditions.....	71
<b>Table 4.2.1:</b> Result of fractionation of Abu-attifel crude oil in HPLC.....	77
<b>Table 4.2.2:</b> Wax appearance temperature (WAT1 and WAT2) and wax content (WC2) of treated and untreated Abu-attifel crude oil at cooling rate of 1°C/min.....	80
<b>Table 4.5.1:</b> Comparative yielding of Abu-attifel crude oil treated with ROA1000 PPM (T=30°C and cooling rate=1°C/min) .....	106

# Table of Contents

ABSTRACT .....	i
ACKNOWLEDGEMENTS .....	iii
NOMENCLATURE .....	iv
List of Figures .....	v
List of Tables.....	xi
Table of Contents.....	xii
CHAPTER 1: INTRODUCTION .....	1
1.1 Waxy crude oils and remediation of wax precipitation .....	1
1.2 Case study context: Libyan waxy crude oils .....	4
1.2.1 Abu attifel’s current operation policy.....	5
1.3 Rheology: Principal focus of this Research.....	6
1.4 Aim and Objectives of the Research.....	7
1.5 Structure of the thesis .....	9
CHAPTER 2: LITERATURE REVIEW .....	11
2.1 Introduction.....	11
2.2 Wax and waxy crude oils .....	11
2.3 Paraffin Wax crystallisation .....	13
2.4 Crystallization .....	14
2.4.1 Nucleation.....	14
2.4.2 Crystal growth.....	16
2.4.3 Agglomeration .....	17
2.5 Rheology of Waxy crude oils .....	18
2.5.1 Fundamental concepts and definition.....	19
2.5.2 Application of Rheology to pipeflow .....	26
2.5.3 Yielding of Waxy crude oil gels .....	31
2.6 Hindered gelling with solvents or chemical wax Inhibitors.....	45
2.6.1 Wax Inhibitors types & wax inhibition mechanisms.....	45
2.6.2 Hindered gelling with chemical wax inhibitors.....	47
2.6.3 Hindered gelling with solvents (light crude oils, gas condensate and gas). ...	50

2.7	Conclusion .....	52
<b>CHAPTER 3: EXPERIMENTAL METHOD .....</b>		<b>53</b>
3.1	Introduction.....	53
3.2	Waxy crude oil and wax inhibitors used .....	54
3.3	Samples preparation and conditioning .....	57
3.4	Differential scanning calorimetry (DSC) .....	58
3.5	Wax composition determination.....	61
3.6	Microscopy .....	61
3.7	Rheometry .....	63
3.7.1	Anton Paar SVM 3000 .....	63
3.7.2	Bohlin CVO 100 .....	64
3.7.3	Pour Point determination .....	71
3.7.4	Measurement errors.....	72
<b>CHAPTER 4: RESULTS AND DISCUSSION.....</b>		<b>74</b>
4.1	Introduction.....	74
4.2	The characteristics of untreated and treated Abu-attifel crude oil .....	75
4.2.1	Chromatography Analysis .....	75
4.2.2	DSC Analysis .....	79
4.3	Rheology of treated and untreated Abu-attifel crude oil cooled under normal operating conditions, i.e. at $10\text{-}50\text{ s}^{-1}$ .....	82
4.3.1	Presentation of data .....	82
4.3.2	Conclusion.....	91
4.4	Rheology of treated and untreated Abu-attifel crude oil cooling under pipeline near shut down conditions, i.e. at very low shear rate here $1\text{ s}^{-1}$ .....	91
4.4.1	Presentation of data .....	92
4.4.2	Conclusion.....	96
4.5	Rheology of treated and untreated Abu-attifel crude oil cooled statically, i.e. during shut down conditions. ....	96
4.5.1	Presentation of data .....	98
4.5.2	Conclusion.....	106
4.6	Gel structure of treated and untreated Abu-attifel crude oil at shutdown. ....	107
4.6.1	Presentation of data .....	108

4.6.2	Conclusion.....	112
4.7	Oscillatory Rheology of treated and untreated Abu-attifel crude oil cooling statically, i.e. during shut down conditions. ....	113
4.7.1	Principles.....	113
4.7.2	Presentation of data .....	116
4.7.3	Conclusion.....	118
CHAPTER 5: CONCLUSION & RECOMMENDATIONS .....		119
5.1	Context .....	119
5.2	Research Strategy .....	119
5.3	Conclusions with recommendation imbedded .....	120
References.....		124
Appendix.....		142

# CHAPTER 1: INTRODUCTION

## 1.1 Waxy crude oils and remediation of wax precipitation

There is no doubt about the increasing importance of crude oil to our modern way of life. As a source of both energy and material, crude oil is the life blood of industry and modern society. It is not an understatement to say that without it, the world will stop functioning. Therefore, science and technology take the responsibility to develop, secure, and increase the supply of crude oil in all its forms, including the exploitation of waxy crude oils, oils which contain a significant amount of paraffin wax or naphthenic hydrocarbons, typically 15 to 40 wt. % (Venkatesan et al., 2003). Such crude oils are encountered throughout the world and have been produced for several decades in China, India, Egypt, Libya and North Sea, (Yang et al., 2013; Chanda et al., 1998; Al-Sabagh et al., 2013; Chen et al., 2007). Their exploitation is the more important as over the years as non-waxy crude oil reserves have declined due to heavy utilisation. They amount currently to 1/3 (Energy information administration (EIA), 2016, of the total oil being produced (97 million bbl/day). Also, the paraffin itself is valuable and waxy crude oils have the advantage of being low in sulphur content and this makes them more desirable from an environmental viewpoint.

There is however, a serious problem with the pumping and processing of waxy crude oils, the risk of the wax precipitating out of the solvent oil when the temperature drops below a critical temperature. Waxy crude oil in its original well state is hot, at temperature in the range 70-150°C, where all the wax is dissolved in the solvent oil. Once out of the ground, cooling occurs; so in normal pipeline operations and to enable them to flow, waxy crude oils are heated and maintained at temperatures above their wax appearance (precipitation) temperature ( $T_{WA}$ ). These  $T_{WA}$  (also called cloud point) are generally quite high compared with ambient conditions, for example 39°C in the case of North Sea oil, 43°C for China Daqing oil and as much as 67°C for Libya Remal oil (Singhal et al., 1991; Al Gamal et al., 1997; Ding et al., 2006). Correspondingly, their flow-ability (pour point) diminishes. When

accidentally, heating is cut off over prolonged periods of time or when the external ambient temperature drops drastically in the cold winter months, these oils cool rapidly, the solubility of the wax falls, the wax precipitates out and forms on the cold pipe wall a sponge like gel network of interlocking wax crystals trapping liquid oil. As with all crystallisation processes, cooling rates will dictate the number and sizes of the wax crystals formed, hence the strength of the gel structures (Lee et al., 2008) (Figure 1.1). If not quickly remedied, the gel ages overtime and hardens, reducing the cross-sectional area for flow and in severe cases nearly completely blocking the pipeline (Figure 1.2), very costly to the oil industry.

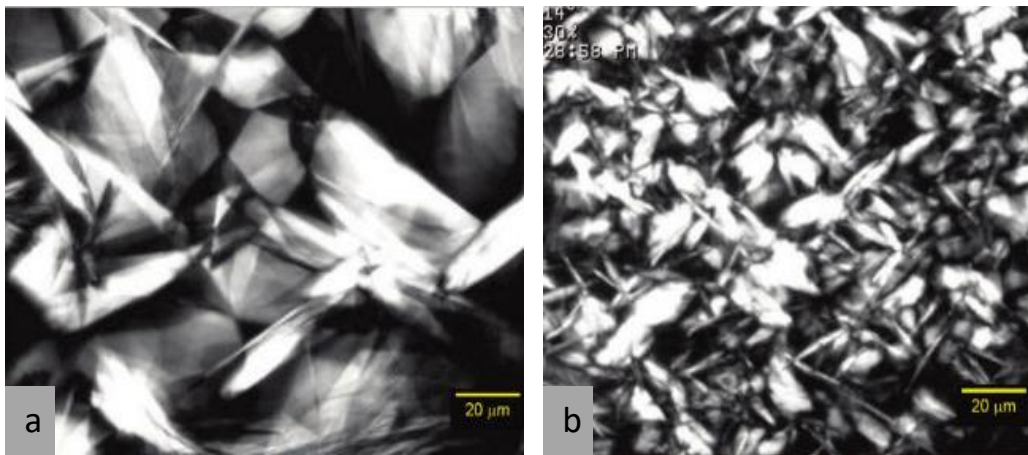


**Figure 1.1:** Waxy crude oil gelation at (a) low and (b) high cooling rates. (Lee et al., Energy & Fuels 2008).



**Figure 1.2:** Blockage of pipe following wax deposition ([www.subseaexpo.com](http://www.subseaexpo.com)).

Overcoming this problem, is at the heart of this thesis. Apart from drastic solution such as mechanical pigging or the injection of hot oil in the pipeline, in such situation, the gelled pipeline is optimally restarted if the yield stress of the gelled crude oil is known. The scientific importance of the problem can be seen in the context of rheology and the controversial concept of yield stress (see Barnes, 1999). Much research has been undertaken to measure and/or predict the yield stress of the gelled waxy crude oils (further details in the literature review in Chapter 2) by leading researchers, in particular by the eminent David Boger at the University Of Melbourne, Australia. In this research, rather than accepting the gelling problem, a solution that prevent wax precipitation or reduce its onset at much lower temperatures than normally is investigated by using one of two methods: blending with a lighter crude oil with very small wax content or adding chemical wax inhibitors. The blending with a little crude oil reduces the wax content hence the tendency of the mixture to form a strong gel. This approach is feasible is there are field nearby producing such light crude oil. The strategy then become purely logistical and the economic feasibility assessed against using wax inhibitors which come at a cost, often very expensive (1 IP). At minute concentrations, parts per million, wax inhibitors act at the molecular level to hinder the onset of crystallisation and formation of wax network. Essentially wax inhibitors are from two broad categories (Pederson and Rønningsen, 2003):

- a) wax crystals detergents or dispersants which are surface active agents that hinder the wax crystals that form from assembling into a gel network. Typical dispersants include alkyl sulfonates and fatty amine ethoxylates (Kelland, 2009].
- b) wax crystal modifiers, polymers dissolved in solvent, which insert themselves between the crystals formed thus hindering their assembly into a gel network. These crystal modifiers are also known as pour point depressants (PPD) because they reduce viscosity. Typical polymers used as crystal modifiers are ethylene polymers (polyethylene butane and polyethylene-b-propylene) and ethylene copolymers (ethylene-acrylonitrile and ethylene-vinyl acetate), the most widely used being ethylene-vinyl acetate (EVA), (Tinsley et al., 2007). Comb polymers

such as meth-acrylic acid and maleic anhydride are also effective wax crystal modifiers (Kelland, 2009).

Further details in the use of wax inhibitors for this purpose are given in the literature review in Chapter 2. Apart from saving on the heating cost necessary to overcome gelation, the application of wax inhibitors offers several benefits, including the safety of the pipeline. In severe conditions of wax precipitation, high pump pressures are necessary to restart the pipeline and these will lead to pipe rupture and fatigue especially if corrosion presents. This is the context of this research.

## 1.2 Case study context: Libyan waxy crude oils

Until 2011, before the political unrest, Libya was Africa's second-largest oil producer behind Nigeria with proven reserves of 29 billion barrels and a producing capacity of 1.5 million barrels per day (Najah and Moudri, 2006). Its oilfields are situated in several onshore sedimentary basins, Ghadames and Murzuk on the east, and Sirte, Cyraneica and Kufra on the west and an offshore oil field, El-Bouri, as shown in Figure. 1.3. These fields, a multitude in the Sirte basin (see Figure 1.4), are connected with a network of pipelines, 6000 km long pumping oil to seven terminals along the coast, Marsa el Harega, Zueitina, Marsa el Brega, Ras Lanuf, Es-Sider, Zawiya and Mellitah for export to the international market.



**Figure 1.3:** Libya oil fields, pipelines and terminals. (Libya National Oil Corporation).





**Figure 1.4:** Libya multitude of oil fields in the Sirte basin (Libya National Oil Corporation).

This case study considers one particular waxy crude, Abu attifel. Its high wax content of 29 wt.% and a pour point of 40°C (see properties in Table 1.1) makes it representative of waxy crude oils in general. Abu-attifel crude oil field is located 400Km south-east of Benghazi and has been in production since 1972, delivering 111,791 BPD, through a 30inch pipeline at a distance of about 133Km to field 103A and then through a 40inch pipeline at a distance 220Km to the Zueitina terminal for export (see Figure 1.4).

### 1.2.1 Abu attifel's current operation policy

In order to maintain the crude flowing, it was heated using three gas fired heaters. These heaters, operated at the field, were situated after the gas separators. In addition, a fourth heater was available 108 km upstream to insure that the crude temperature reached the Zueitina terminal at temperature not less than 60°C.

As explained earlier, like all other waxy crude oils, Abu-attifel crude oil must be maintained hot to prevent wax precipitation and ensure effective pumping. This is however, costly and an alternative, which dispenses of heating will be highly desirable. This research addresses precisely this, examining the use of (i) blending with a light crude oil with very low wax content and (ii) chemical wax inhibitors to prevent or reduce the propensity of strong

waxy gels forming upon cooling which frequently occurs as a result of accidental shutdown (loss of heating).

**Table 1.1:** Characteristic Properties of Abu-attifel crude oil.

Property	Abu-attifel crude oil crude oil
Specific gravity@15.6°C	0.8229
API gravity	40.43
Wax content, (Wt. %)	29
Pour point, °C	+39
WAT1 & WAT2, °C	68.14 & 39
Sulfur content, (Wt. %)	0.03
Asphaltene, (Wt. %)	0.17
Pumping temp, °C	85

### 1.3 Rheology: Principal focus of this Research

Clearly, at the heart of this research is flow-ability when temperature reduces near and below the wax appearance temperature. Rheology is thus the principal focus of this research. Without going into details at this stage of the thesis, upon a severe drop in temperature, the waxy crude oil transforms from a liquid to a gel as a result of the wax crystallising. Thus, there is a need in this research to probe the *yielding* of such a structured “soft solid” in order to extract the restart pumping pressure. Several variables will play a part, principally the temperature, the cooling rate that has led to that particular temperature and the stress loading rate. The stress loading rate embodies the time effect as the gradual elastic deformation, creep and eventual breaking of this solid (see Figure 1.5) will depend on the rate at which the applied stress is increased.

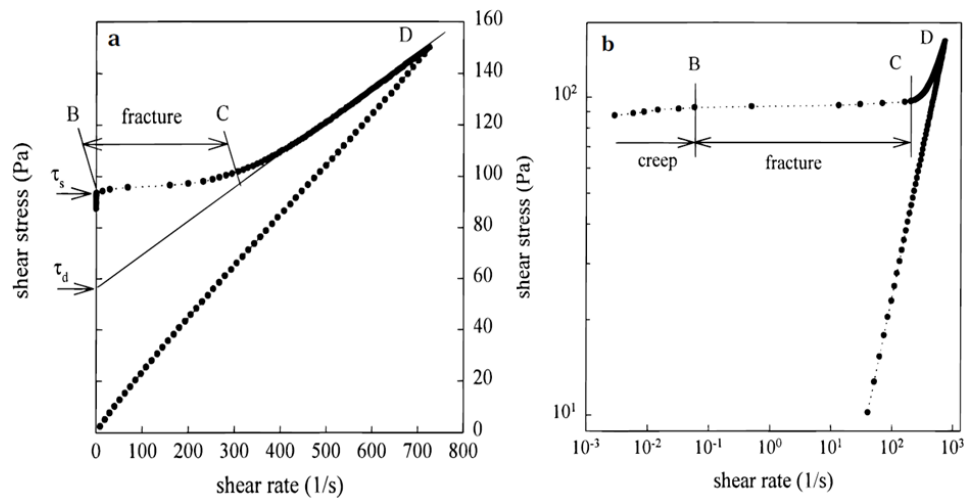


**Figure 1.5:** Deformation-flow curve of waxy crude oil gels (Chang and Boger, 1998).

Necessarily, the rheometric technique to be used has to be not only accurate and with good resolution, it must also be appropriate and mimic the actual restart pipeline situation. The application of wax inhibitors to the waxy crude oils will act to change the structure of this soft solids thus changing the yield stress, hopefully considerably so that the gelling situation if it occurs will be considerably weaker and much less costly to overcome to restart the pipeline.

#### 1.4 Aim and Objectives of the Research

Having introduced the subject of the research, the aim must be to measure the effectiveness of (i) the blending with a light crude oil with very low wax content and (ii) the addition of chemical wax inhibitors at facilitating the yielding of waxy crude oils that are cooled below their wax appearance temperature. To achieve this aim, a series of objectives are set in sight:

1. A critical review of prior work in this area to guide novel work and an appropriate selection of wax inhibitors.
2. The measurement of the wax content and wax appearance temperature of the Abu-attifel crude oil waxy crude as a function of cooling rate, the key variable controlling the formation of wax crystals.

3. The microscopic observation of wax formation upon cooling to probe the “solid” nature of the material, i.e. the size and numbers of crystals formed as function of temperature and cooling rate.
4. A thorough rheological study of the cooled waxy crude oils, at different temperatures, cooling rates and stress loading rates.
5. The effect of (i) blending Abu-attifel crude oil with a light crude oil with very low wax content and (ii) adding various wax inhibitors on all the above work-packages.
6. Assessment of the benefit of using solutions under (5) through restart pump pressure predictions using the measured rheological data.

In this research, a feasibility study was first performed to narrow down the choice of the many light crude oils and chemical inhibitors available to arrive at the following:

- a) Sirtica crude oil as a low paraffin wax content (6.4 wt.%) waxy crude oil. This oil is classified as an Intermediate crude oil produced by Arabian Gulf Oil Company, according to U.S. Bureau of Mines method of classification. It has a characterization factor of 12.0, an API of 39.3 and a very low pour point of -9 °C in comparison with Abu-attifel crude oil +39 °C. The very low pour point of Sirtica crude oil makes it a good candidate additive to reduce the restarting pressure of Abu-attifel crude oil. This particular solution was considered in the research to assess the blending required and associated cost in comparison with chemicals inhibitors.
- b) Treatment with a wax crystal detergent labelled here Chimec RO 671A, supplied by Chemic Rome Italy. It is a blend of polymeric compounds in water or glycol solution and contains about 15-25% of Mono-ethylene glycol. It has pour point of -10 °C and a viscosity at room temperature of 650-800 cp.
- c) Treatment with a wax crystal modifier, PPD-JOUF (C10), supplied by JOUF Chemical (Benghazi, Libya), essentially a polymeric in aromatic solvent. Table 1.2, Lists the concentrations of the inhibitors to be tested.

**Table 1.2:** Specifications & concentrations of wax inhibitors used.

Wax Inhibitors	Concentrations tested
Sirtica crude oil	20% vol.
Chimec R0671A	500 and 1000 PPM
PPD 110C	1000 and 2000 PPM

As the problem effectively deals with finding a solution to the restart of gelled pipeline, the rheological study was split accordingly into 3 stages:

- (i) Normal full production, i.e. high shear rate pumping whilst cold (dynamic cooling), typically in the range of shear rates 10-50 s<sup>-1</sup>.
- (ii) Decelerating production (again dynamic cooling) which starts immediately the pump stops, situation deemed to be not zero but near zero shear rate, here taken as 1 s<sup>-1</sup>.
- (iii) Ceased production, when the flow ceases, that is when the shear rate is zero.

Clearly stage (i) and (ii) concern a pure shear flow and the parameter of concern is the apparent viscosity as it controls pressure thus power. The research question is then “*Would the addition of a light crude oil, a pour point depressant or a wax inhibitor reduce apparent viscosity?*”

As for stage (iii), the research question does not concern a pure shear flow but the yielding of a gelled waxy crude oil and it is “*Would the addition of a light crude oil, a pour point depressant or a wax inhibitor reduce the yield stress?*”, the yield stress being the equivalent of the restart pressure from the simple force balance in a pipeline  $\Delta p \pi R^2 = 2\pi R L \tau_{rst}$  where  $\Delta p$  is the restart pressure,  $\tau_{rst}$  the yield stress to be measured and R the radius of the pipeline.

## 1.5 Structure of the thesis

This thesis is structured in the classical manner. This introduction that gave an overview of the problem and a statement of aim and objectives followed by a critical literature review chapter to guide novel work and the identification of suitable wax inhibitors. Chapter 3 will describe the experimental method used including differential scanning calorimetry to measure wax content and wax appearance temperature, microscopy to

measure the morphology of the crystalline structure formed for various temperatures and cooling rates and rheology. By rheology, it is meant the entire deformation flow behaviour from the application of almost zero stress until total breakage of crystalline structure and ensuing viscous flow. Chapter 4 will describe critically the results of these measurements and compare these with prior work. Chapter 4 will include a theoretical section that enables the prediction of restart pressure in actual pipelines using the rheological data measured. Chapter 5 and 6 will present the conclusions reached and recommendations for follow-up work.

## **CHAPTER 2: LITERATURE REVIEW**

### **2.1 Introduction**

In chapter one, the subject of this research work was introduced and explained, the importance of waxy crude oils and associated technical challenges in handling such oils were presented together with the aim and objectives of this research. One of the objectives set was to carry out a critical review of prior work in the field to identify voids in the knowledge gained and guide the present research. This chapter presents such a review focusing mainly on rheology as it is central to this research. The following important research issues will be considered:

- Rheology in general and in relation to waxy crude oils
- Rheology fundamental concepts and definitions
- Rheological parameters of waxy crude oils
- Viscoelastic behaviour of waxy crude oil gels
- Yielding of gelled waxy crude oil
- Effect of cooling (Static, dynamic) on yielding process
- Factors affecting the structure and yielding of gelled waxy oils
- Crystallisation and morphological structure of waxy crude oils
- Methods applied to mitigate wax problems
- Chemical additives effects on flow properties of waxy crude oils.

### **2.2 Wax and waxy crude oils**

Petroleum wax commonly encountered in crude oils may be categorized (Newberry, 1982; Hamouda et al., 1993; Singh et al., 2000) into two distinct types depending on the size of the crystals formed, macro and micro crystalline. Macrocrystalline wax is composed of straight chain low molecular weight n-alkanes also called paraffins (n-alkanes) with chain length varying from C<sub>16</sub> to C<sub>50</sub> which crystallise as needles or platelets (Figure 2.2.1). With regard to concentration, 2 to 4% by weight only of these paraffin waxes is sufficient to cause gelling (Holder and winkler, 1965; Rønningsen et al., 1991; Paso et al., 2005). However, under reservoir conditions where the temperature is high (70-150°C; 50-100 MPa), the paraffin in the oil is fully

dissolved. Microcrystalline or amorphous wax contains high proportion of high molecular weight iso-alkanes also called iso-paraffins, cycloalkanes and naphthenes with chain length varying from  $C_{30}$  to  $C_{60}$ . Due to their large molecular weight and the number of isomer permutations possible, microcrystalline paraffin waxes normally precipitate as small amorphous particles and do not exhibit distinct crystallisation regime (Figure 2.2.2).

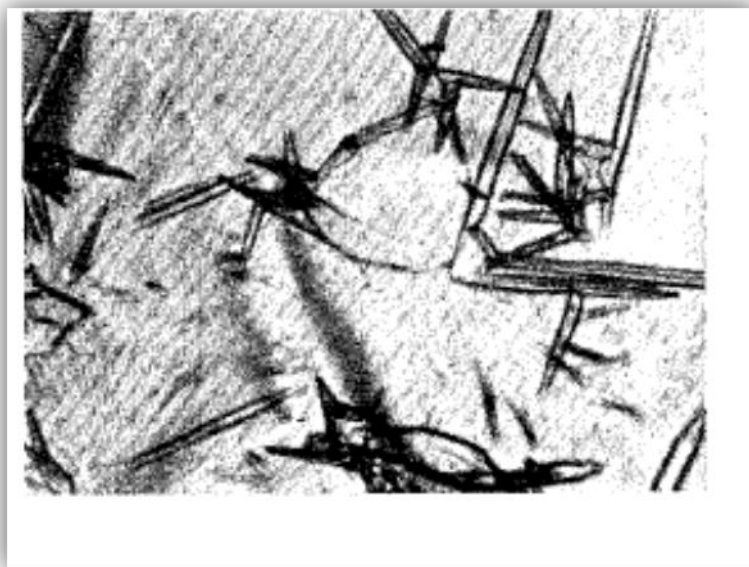


**Figure 2.2.1:** Paraffins wax crystallising showing needles crystals (Edwards, 1957).

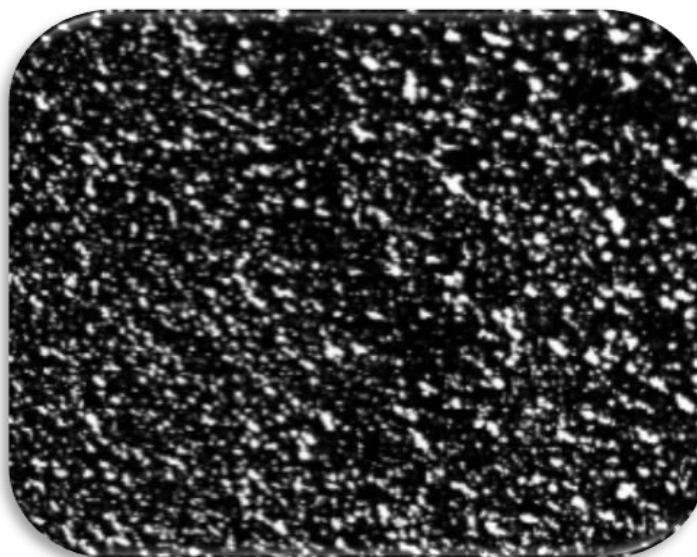


**Figure 2.2.2:** General view of Abu-attifel crude oil crystals Average crystal size  $34.4\mu m^2$ .



### 2.3 Paraffin Wax crystallisation

With regard to crystallization of paraffin wax, it occurs through several stages, starting at temperature below the wax appearance temperature (defined later) when the short range intermolecular attractive forces become greater than the energy of molecular motion (Sign et al, 2003). Strong contact and attraction forces then develop and the crystals bind together to form lamellar sub-crystal with thicknesses 1.5-3nm, roughly the length of a linear C<sub>20</sub> paraffin and lamellar distances between crystals of 30-100nm (Sign et al., 2003). The sub-crystals grow then in size to form a sheet-like shape, aggregating into a network throughout the oil (Chang et al., 2000). Such formation has been viewed through microscopy by various researchers for example Holder and Winkler (1965a, b) and Kane et al., (2003). As in all crystallization processes, these observations have confirmed the 3 stages that occur which are: Nucleation, Growth and Agglomeration (Holder et al., 1965a, 1965b; Radlinski et al., 1996; Dirand et al., 1998; Chang et al, 2000; Singh et al., 2003).

As with all crystallization processes, the crystals size and number will vary with cooling rate, with crystals growing in size when the cooling rate is small (Figure 2.3.1). Large cooling rates form in comparison smaller size crystals (Figure 2.3.1). In both cases, the gel structure that forms, resembles a sponge that traps oil between the crystals (Visintin et al. 2005; Betancourt et al., 2007; Morozov, et al., 2016). It is this interlocking of the oil that gives the gel appearance. Left un-remedied, the gel will harden and block the pipeline. Clearly, unless the trapped oil is released, no viscous flow is possible hence the need to apply large stresses to break the gel as it is explained later in the result chapter. The study of crystal formation can be approached in two ways, directly through microscopic observations as just described or indirectly by measuring the rheological properties of the gels formed as reviewed later. Both approaches are used in this research.

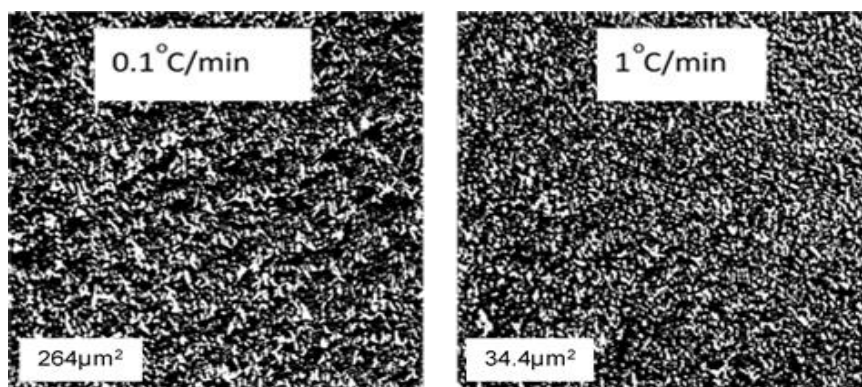


**Figure 2.3.1:** Effect of cooling rate on Ave. crystal size and density for Abu-attifel crude oil at 30°C.

## 2.4 Crystallization

Crystallization is one of the oldest unit operations known to mankind, today crystalline products can be found in every aspect of life crystals that are bound by flat faces intersecting at well-defined angles are characteristic of the substance and give the crop a reproducible appearance. (Beckmann, 2013)

The regular appearance is due to the long-range order of the building blocks of the crystal. This arrangement maximizes the attractive interactions between the building blocks and thus minimizes the energetic state. The long-range order of it is building blocks makes the crystalline state distinct from the gaseous and liquid as well as the amorphous solid state. The long-range order is also the main cause of a number of well-defined properties of the crystals, therefore the crystal properties are tailored through manipulating the crystallisation process parameters (Beckmann, 2013) which consists of the following stages:

### 2.4.1 Nucleation

First step before crystals can develop there must exist in the solution a number of minute solid bodies, nuclei or seeds that act as centres of crystallization. As well-known and consolidated in the inorganic chemistry area, nucleation is a stochastic process that requires a super cooling (or supersaturation; when the concentration of solute molecules are above the solubility curve of the solvent) to start it up (Mullin, 2001). Therefore, during the cooling, it is required that the fluid reaches a certain temperature below saturation, i.e., a metastable state,

to initiate the crystal nucleation process. The difference between the saturation temperature and the crystallization temperature is called degree of super cooling (Andrade et al, 2017). Therefore, crystals precipitation begins at a temperature that is below the solid-liquid equilibrium temperature, which is a thermodynamic property (Ji H-Y et al, 2004).

In general, Nucleation may occur by its own (primary nucleation) which might occurs as homogeneous or heterogeneous by foreign particles. However, it may be induced artificially under the influence of some external stimulus or crystals present in a supersaturated system (secondary nucleation) according to the scheme in Figure 2.4.1.

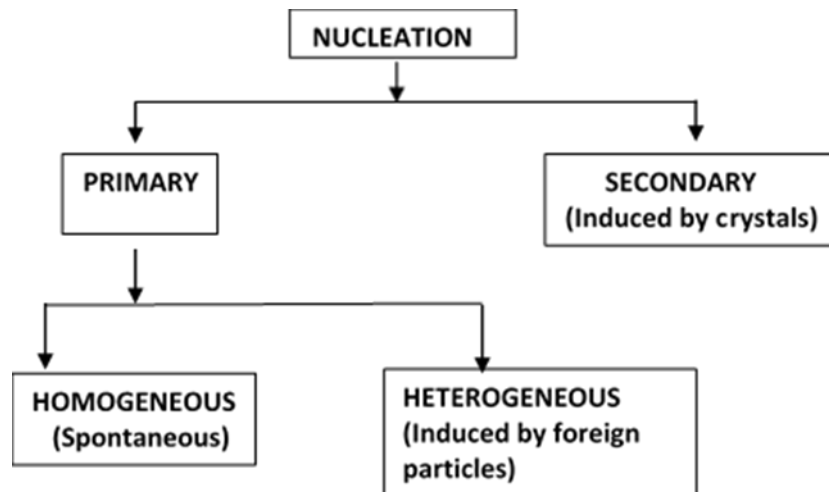


**Figure 2.4.1:** Nucleation scheme.

The nucleation process was envisaged as the development in the solution of a molecular cluster, as a disordered quasi-liquid, which after attaining critical size suddenly 'clicks' into crystalline form. As a result of this high-speed rearrangement, the surface of the newly formed crystalline particle may be expected to contain large numbers of imperfections that would encourage further rapid crystalline growth. (Garten and Head, 1963, 1966). Agitation is frequently used to induce crystallization. Most agitated solutions nucleate spontaneously at lower degrees of super cooling than quiescent ones. However, the influence of agitation on the nucleation process is probably very complex. It is generally agreed that mechanical disturbances can enhance

nucleation, but it has been shown by Mullin and Raven (1962) that an increase in the intensity of agitation does not always lead to an increase in nucleation.

### **I. Heterogeneous nucleation**

The rate of nucleation of a solution or melt can be affected considerably by the presence of mere traces of impurities in the system. However, an impurity that acts as a nucleation inhibitor in one case may not necessarily be effective in another; indeed it may even act as an accelerator. No general rule applies and each case must be considered separately.

Many reported cases of spontaneous (homogeneous) nucleation are found on careful examination to have been induced in some way. Indeed, it is generally accepted that true homogeneous nucleation is not a common event. For example, a super cooled system can be seeded unknowingly by the presence of atmospheric dust which may contain 'active' particles (hetero nuclei).

### **II. Secondary nucleation**

A supersaturated solution nucleates much more readily, i.e. at a lower supersaturation, when crystals of the solute are already present or deliberately added. The term secondary nucleation is used here for this particular pattern of behaviour to distinguish it from so-called primary nucleation (no crystals initially present) (Mullin, 2001)

### **III. Seeding**

Crystallization can be induced through seeding a supersaturated solution with small particles of the material to be crystallized. Deliberate seeding is frequently employed in industrial crystallization to effect a control over the product size and size distribution.

Atmospheric dust frequently contains particles of the crystalline product itself, especially in industrial plants or in laboratories where quantities of the material have been handled. Seed crystals, however, do not necessarily have to consist of the material being crystallized in order to be effective; iso-morphous substances will frequently induce crystallization.

#### **2.4.2 Crystal growth**

As soon as stable nuclei, i.e. particles larger than the critical size, have been formed in a supersaturated or super-cooled system, they begin to grow into crystals of visible size. Many proposed theories that explain the mechanisms

of crystal growth are available among them the surface energy theories which are based on the postulation that the shape of a growing crystal assumes is that which has a minimum surface energy. If a crystal is allowed to grow in a supersaturated medium, it should develop into an 'equilibrium' shape, i.e. the development of the various faces should be in such a manner as to ensure that the whole crystal has a minimum total surface free energy for a given volume. A liquid droplet is very different from a crystalline particle; in the former the constituent atoms or molecules are randomly dispersed, whereas in the latter they are regularly located in a lattice structure.

The diffusion theories presume that matter is deposited continuously on a crystal face at a rate proportional to the difference in concentration between the point of deposition and the bulk of the solution. The mathematical analysis of the operation is similar to that used for other diffusional and mass transfer processes. (Mullin, 2001)

#### **2.4.3 Agglomeration**

The term agglomerates is understood to include both the formation of loosely bound aggregates that easily disintegrate and the agglomerates that are tightly bound by solid bridges and that only disintegrate under brute force. For agglomeration to occur, two particles have to collide and the attractive forces between the two particles have to exceed the force resulting from the inertia of the particles to disintegrate again. The particles hit, tumble and either disintegrate or agglomerate. A low charge will often support agglomeration, while a higher surface charge often hinders agglomeration by hindering the first contacts.

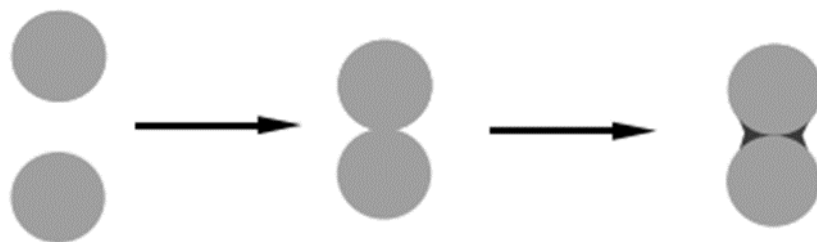


**Figure 2.4.2:** Formation of solid bridges between particles. (Beckmann, 2013).

Depending on the size of the primary particles of the agglomerates, different force regimes are necessary. While intermolecular forces suffice to bind very small particles in agglomerates, liquid or solid bridges are necessary to bind larger particles. For the formation of solid bridges between particles, a supersaturation is necessary. This can occur during growth – the higher the supersaturation, the more likely the cementation – as well as during drying by depositing residual amounts of solid (Figure 2.4.2).

## **2.5 Rheology of Waxy crude oils**

Rheology is recognized as a field of scientific research critical particularly to the chemical process industries (Ranalli G, 1995) where complex materials are handled (suspensions, colloids, polymer melts, soft solids, etc.). Indeed, many chemical engineering businesses are centered around rheology, the manufacture of food stuff (soups, yogurts, cheese, butter, chocolates, jams, processed meats), home and personal products (detergents, soaps, shampoos, creams, make-up, cleaning fluids), pharmaceuticals, paints, inks, adhesives and other coating pastes and the processing of polymers.

In such industries, the determination of the flow behavior of materials is an important tool in both the design and operation of the process units such as pipelines, pumps, heat exchangers and mixing vessels as well as the design of the materials themselves.

Rheology is applicable to all materials, from gases to solids. Fluid rheology is used to describe the consistency of different products, normally by the two components - viscosity and elasticity. Viscosity describes the resistance to flow or the “thickness” of a fluid whereas elasticity describes how a material deforms. Both viscosity and elasticity reflect material structure. Waxy crude oils are particularly complex in that at high temperature they flow like liquids but at low temperatures the wax they contain precipitates and turn them into gels which are soft solids. Remarkably and thankfully, crude oil in its original reservoir conditions is hot and under pressure so its extraction is relatively simple. It simply oozes out of the ground when a pipe is drilled deep into the reservoir. The problem is that on exit of the reservoir, it must be

maintained hot, above the wax precipitation temperature (WAT or  $T_{WA}$ ) so that it can be pumped far afield to its destination. Nature has it that oil fields are generally in remote areas (deserts, seas or glaciers) so very long pipelines are necessary, some several thousand miles long (6000km). Necessarily, these waxy oils must be heated to  $T_{WA}$  and above whilst being pumped or dosed with special chemicals; wax inhibitors that prevent the wax from precipitating.

In situations where accidentally, power and heating are lost, waxy crude oils gel as a result of wax precipitation. This precipitation of wax causes a rapid increase in viscosity. The increase of viscosity shifts the behavior of the crude oil from Newtonian to non-Newtonian flow as will be explained below. In order to reduce the energy consumption (for heating the oil and pumping it) and ensuring safety of the pipeline operation (no blockage or stresses), a thorough understanding of the rheological characteristics of the waxy crude oil being exploited is indispensable. This puts into context the broad aim of the present research

### 2.5.1 Fundamental concepts and definition

Prior to approaching the fundamental concepts of rheology, there are some important properties of waxy crude oils that help demarcate flow-deformation situations. These are:

- i. API gravity: It is a measure of the density of the crude oil and is related to specific gravity as follows: 
$$API = \frac{141.5}{Sp.gravity} - 131.5 \quad (2.5.1)$$

Generally, API gravity decreases with increasing material molecular weight, however, the presence of asphaltenes lowers API Gravity of the crude. This parameter is most often used to describe the ability of the crude oil in producing low boiling hydrocarbons in trade negotiations or biddings.

- ii. Cloud point: This is a property introduced in the early years of the oil industry and a crude determination of wax appearance temperature – the temperature is reduced and the sample visually assessed for when a cloud appears. Clearly it is a very limited technique which could only handle clear oils.

- iii. Wax appearance temperature (WAT): This is the modern alternative to the cloud point. As mentioned earlier, it is defined as the temperature at which the dissolved wax starts to precipitate out of the solvent oil and is determined by measuring the heat flow curve, using DSC calorimetry or Cross Polarised Microscopy to view the wax actually forming, as described in the Experimental Chapter. Clearly below this critical temperature, more of the wax precipitate reducing the ability of the crude oil to flow and leading eventually to the formation of a gel, a solid like structure.
- iv. Pour Point temperature (PPT): This is the lowest temperature below which the crude oil cease to flow. It is a crude assessment of flow out of a heated jar of the oil tilted horizontally from its initial vertical position. The temperature is increased gradually until flow in the tilted jar is observed (ASTM D5853-95 and D 97). In the early years of oil discovery, it was a property used to differentiate between various oils. Clearly, it is an indicator of wax gel formation but not as sophisticated as the heat flow curve determined from a DSC calorimeter which gives a precise measurement of wax appearance temperature for example or modern rheometry at controlled cooling rate which can determine the gel point as it will be discussed later.

As for the basic definitions of rheological variables, these are:

- i. Shear stress ( $\tau$ ): This is the stress that causes successive parallel layers of a material body to move, in their own planes (i.e., the plane of shear), relative to each other, and considered as analogous to pumping pressure.
- ii. Shear Rate ( $\dot{\gamma}$ ): This is the rate at which a progressive shearing deformation is applied to the material, and considered analogous to flow rate.
- iii. Apparent Viscosity ( $\eta = \tau/\dot{\gamma}$ ): This is the ratio of the shear stress to the shear rate, expressing the resistance to flow. For a Newtonian fluid, such as water, a lubricating oil or generally a fluid with very low molecular weight, the apparent viscosity is independent of shear rate and is known as the Newtonian viscosity ( $\mu$ ). Fluids with high molecular



weights such as polymer solutions, melts and complex fluids composed of small particles such as colloids will exhibit viscosities that changes depending on the magnitude of shear rate – hence the labelling of *apparent* viscosity with non-Newtonian fluids.

Having introduced the basic variables and explained the concept of apparent viscosity, the classification of viscous (time independent, inelastic) non-Newtonian fluids can be illustrated as shown in the flow curves of Figure 2.5.1.

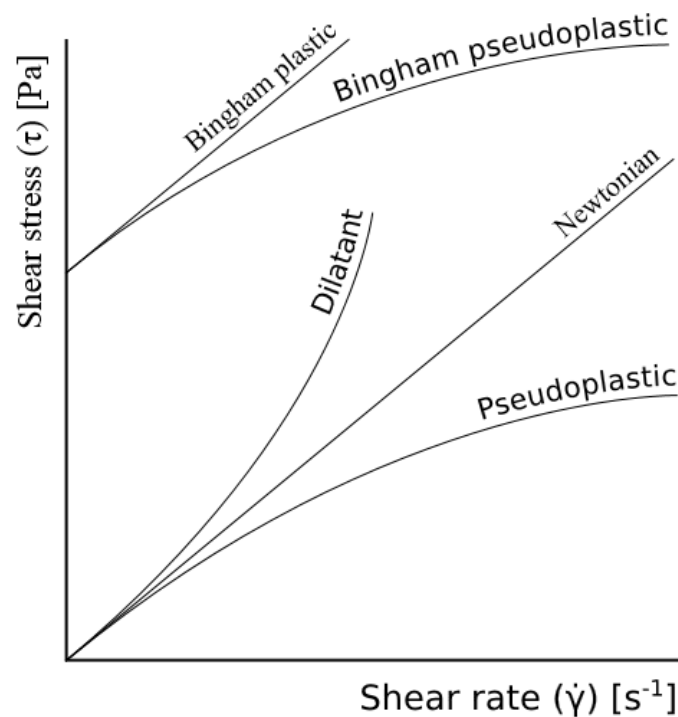


**Figure 2.5.1:** Common rheological viscous flow curve.

The following are four types of purely viscous behaviour as shown in Figure 2.5.1:

- i. *Newtonian*: As explained earlier, those that obey Newton's law of viscosity ( $\tau = \mu\dot{\gamma}$ ) and for which viscosity is affected only by the state of the fluid, that is its temperature and pressure but not the extent of shearing.

- ii. Pseudo-plastic or Shear Thinning: Fluids whose apparent viscosity decreases with increasing shear rate. This behaviour is very common and is observed with many fluids such as paints, adhesives, polymer melts, etc. It is an intuitive behaviour in that the structure of such materials gradually breaks down as the shear is increased thus reducing their resistance to flow. The most common equation that describes such behaviour is the Power Law model,  $\tau = K|\dot{\gamma}|^n, n < 1$ . Clearly such a model is an over simplification of real behaviour and implies unrealistic apparent viscosity values at extreme shear rates, infinity at zero shear rate and zero at infinite shear rates. Actual materials never obey such extreme behaviours, rather they will exhibit limiting values ( $\mu_0, \mu_\infty$ ) of apparent viscosities (plateaux) (Figure 2.5.2), hence a number of variant models to describe such behaviour.
- iii. Dilatant or Shear Thickening: As shown in Figure 2.5.3, such a behaviour is the opposite of pseudo-plasticity, that is the material appears to increase in viscosity as the applied shear rates is increased. Such peculiar behaviour is found with few materials, highly concentrated suspensions for example. Theoretically the same Power Law model holds,  $\tau = K|\dot{\gamma}|^n$  but with  $n > 1$ . Dilatancy is the subject of much research with some researchers arguing it is a common predicted feature for all shear thinning fluids at high shear rates (Woodcock, 1987).
- iv. Bingham Plastic: Bingham plastic fluids are known to have a definite yield stress value ( $\tau_y$ ) which must be exceeded before flow starts. Above the yield stress, a Bingham fluid flows like a Newtonian fluid with an apparent viscosity independent of shear rate and called “plastic viscosity” and a corresponding model is:  $(\tau = \tau_y + \mu_a \dot{\gamma})$ . There are several variants of this model, for example  $(\tau = \tau_y + K|\dot{\gamma}|^n), n < 1$ , which expresses yielding followed by shear thinning. Clearly, waxy crude oils which transform into gels, which are essentially soft solid, should be expected to exhibit yield stresses before flowing in a viscous manner after the gel is broken.

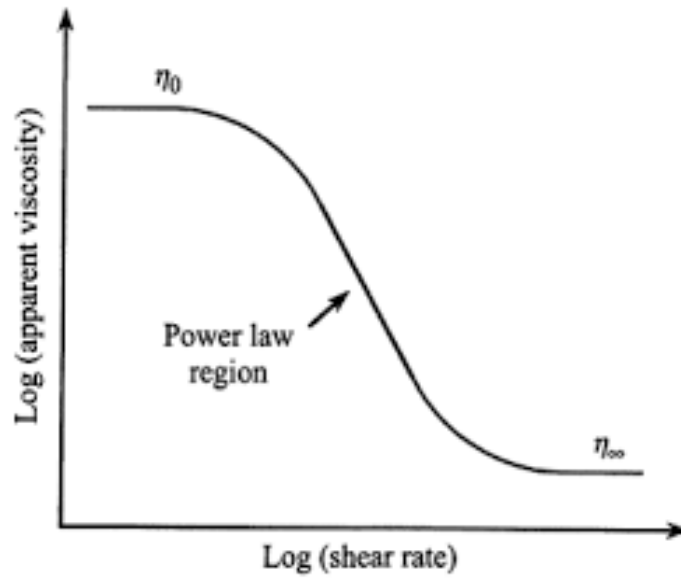


**Figure 2.5.2:** Apparent viscosity plateaux (Stickel and Powell, 2005).

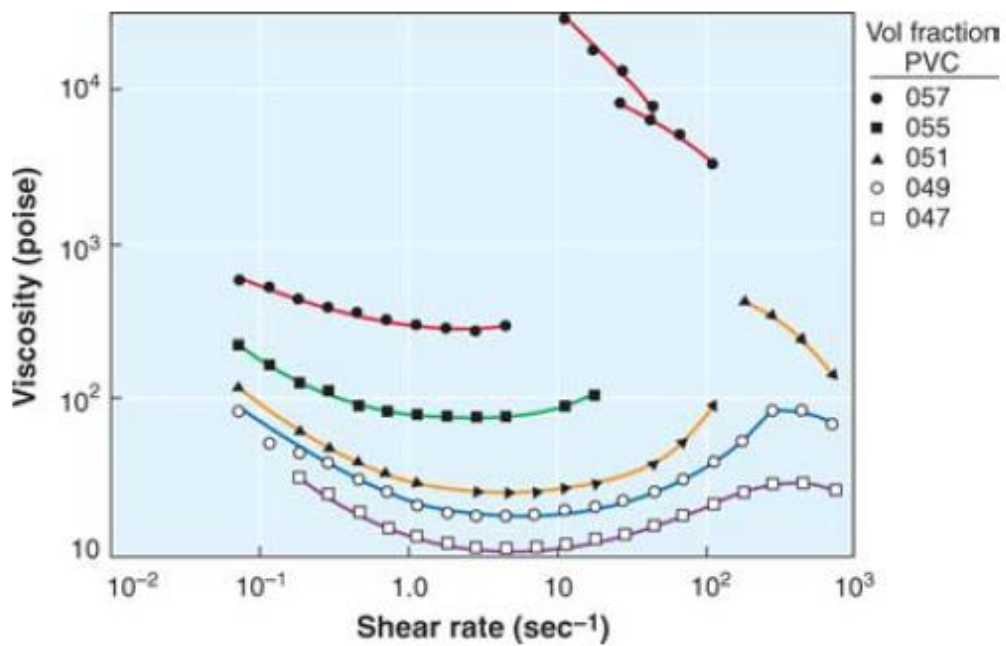


**Figure 2.5.3:** Dilatancy of  $1.25\mu\text{m}$  PVC particles in dioctyl phthalate (Stickel and Powell, 2005).

The above classification as explained assumed the behavior to be strictly time independent. There are however materials whose structure for example can be broken down in time at a set shear rate. These are known as time-dependent viscous fluids and are classified as:

- i. **Thixotropic:** fluids whose viscosity varies as a function of time at constant shear rate. Thixotropy usually occurs in circumstances where the liquid is shear-thinning. Barnes (1997) gave an extensive review of thixotropy, its origin and progress in understanding its features. Mewis and Wagner (2009) reviewed progress made in the modelling of thixotropy. Waxy crude oils are particularly thixotropic as shall be demonstrated and such behaviour results with the material not returning to its original state after it has been sheared as shown for Abu-attifel crude oil in Figure 2.5.4. Thus the decrease in viscosity with time as well as with shear rate, the up-and down flow curves form a hysteresis loop (thixotropic loop). Thixotropy in waxy crude oils and structured colloids (gels) in general is intimately linked with microstructure, how it forms and changes upon shearing and in time depends on the particular material. Thixotropic behaviour makes it difficult to obtain reproducible measurement of yield stresses (Cheng, 1986; Barnes et al., 1989; Visintin et al., 2005; Magda et al., 2009).
- ii. **Rheoplectic:** Similarly, with dilatancy, such fluids show an increase in viscosity but with time at fixed shear rate. Rheopexy, as would be expected, usually occurs in circumstances where the liquid is shear-thickening (Barnes et al 1989).

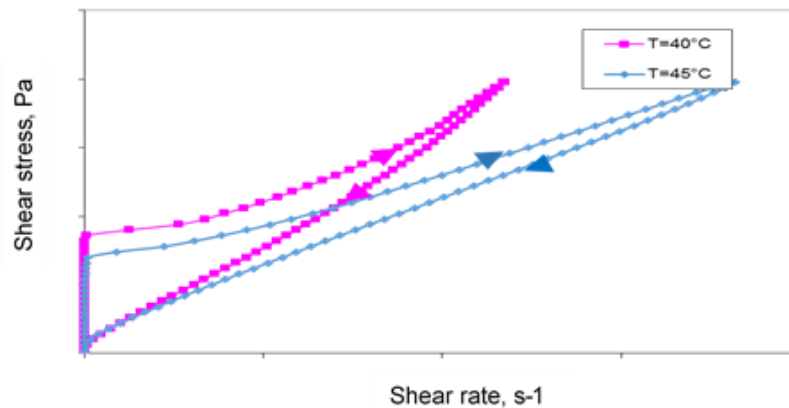


**Figure 2.5.4:** Flow curve for Abu-attifel crude oil untreated, shear stress vs shear rate at cooling rate of 1°C/min.

Finally, and to complete the general classification of non-Newtonian fluids, elastic behaviour must be considered. This is particularly important with polymer melts and indeed with waxy crude oils near and below their wax appearance temperature.

As can be seen in Figure 2.5.1, flow curves of model fluids with reference to Newtonian fluids is presented. It shows shear thinning, shear thickening and yield stress non-Newtonian fluids. Waxy crude oils namely Abu-attifel crude oil are complex in their structure and do not follow such simple classification. Waxy crude oils are complex materials which exhibit viscoelasticity, viscoplasticity and thixotropy (Ronningsen, 1992; Kan et al., 2004; Visintin et al., 2005; Visintin et al., 2008; Adeyanju and Oyekunle, 2012). Their yield stress and viscosity are time-dependent (see Figure 2.5.8 and Figure 2.5.9). At present, there is no comprehensive constitutive equation valid for all kinds of waxy oils (Shabestari et al, 2016). Models such as Casson model (Kirsanov and Remizov, 1999), Bingham model (Fasano et al., 2004), Herschel–Buckley model (Ghanaei and Mowla, 2010), and Richardson model (Dimitriou and McKinley, 2014) have been found to fit the rheological data for certain waxy oils provided that they are modified appropriately.

**Table 2.5.1:** Relationship of apparent viscosity with type of material behaviour.

Type of behaviour	Description	Examples
Time and shear independent viscosity  Generalized Newtonian fluids	<ul style="list-style-type: none"> <li>Viscosity is independent of shear rate and of duration of shearing.</li> <li>Shear stress dependent on shear rate.</li> </ul>	<ul style="list-style-type: none"> <li>Water [Keleşoğlu et al. (2012)]</li> <li>Low contents of wax crude oils [Ilyin et al. (2016), Ghannam et al. (2012), Benziane et al. (2012)]</li> <li>wax crude oils at high temperature [mendes et al. (2015), Chang et al. (1998), Wardhaugh and Boger (1991), Zhang et al. (2013)]</li> </ul>
Thixotropic  Rheopexy	<ul style="list-style-type: none"> <li>Apparent viscosity decrease with duration of shear rate.</li> <li>Apparent viscosity increases with duration of shear rate.</li> </ul>	<ul style="list-style-type: none"> <li>Drilling muds [Houwen and Geehan (1986), Alderman et al, (1988)]</li> <li>paints</li> <li>Waxy crude oil @ <math>T &lt; T_{WAT}</math> [Ronningsen (1992) and Kane et al. (2004)]</li> <li>Print ink [Emre and Halloran (2013)]</li> </ul>

		<ul style="list-style-type: none"> <li>gypsum paste [González et al. (2013)]</li> </ul>
Shear thickening (Dilatant)  Shear thinning (pseudoplastic)	<ul style="list-style-type: none"> <li>Apparent viscosity increases with increased shear rate.</li> <li>Apparent viscosity decrease with increased shear rate.</li> </ul>	<ul style="list-style-type: none"> <li>Suspension of corn starch in water [Alfonso et al. (2012)]</li> <li>Crude oil [mendes et al. (2015), Chang et al. (1998), Wardhaugh and Boger (1991), Zhang et al. (2013)]</li> <li>latex paint [Onur et al. (2011)]</li> <li>Silicone oils [Shenghai et al. (2012)]</li> </ul>

### 2.5.2 Application of Rheology to pipeflow

As stated of introduction of this thesis, Rheology is flow and or flow are the face of the same coin. As experimentally shown and explained here, the rheological properties of waxy crude oils represented by Abu-attifel crude oil is determined through direct measurements of yield stress ( $\tau_f$ ) using Viscometry and oscillatory technique, the value of ( $\tau_f$ ) which is equivalent to  $\tau_w$  in the following section and can be directly applied to the force balance equation acting on a section of a fluid in the pipeline. With reference to Figure 2.5.5, a stress  $\tau_w$ , acting at the wall balancing the pressure drop  $\Delta P$ . Since the flow is steady, the net force on this element must be zero so by applying the momentum equation, we obtain:

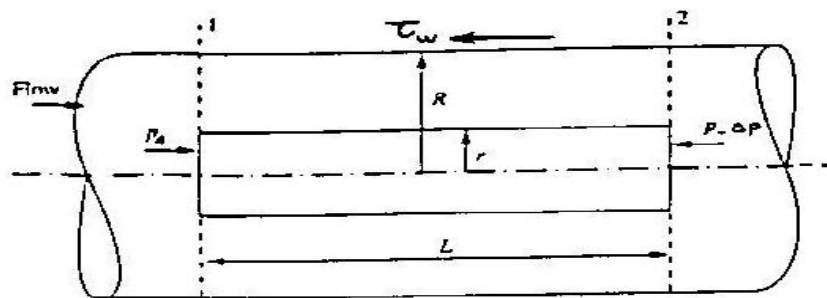


**Figure 2.5.5:** Force Balance on a section of fluid in a pipe.

$$PA - (P - \Delta P) A - \tau_w A = 0$$

For a circular conduit,  $A = \pi r^2$ , and the area over which the shear stress acts  $A = 2\pi r L$

The equation becomes

$$P\pi r^2 - (P - \Delta P) \pi r^2 - 2\pi r L \tau_w = 0$$

$$\Delta P \pi r^2 = 2\pi r L \tau_w$$

$$\tau_w = \frac{\Delta P}{2L} \cdot r \quad (2.5.2)$$

Equation (2.5.2) can be extended across the whole radius of the pipe

$$\tau_w = \tau_R = \frac{\Delta P \cdot R}{2L}$$

This can be written as

$$\frac{\Delta P}{L} = \frac{4\tau_w}{D} \quad (2.5.3)$$

At this point we need to introduce a constitutive equation describing the rheology of the fluid. For example, if the fluid is Newtonian the equation is:

$$\tau = \mu \gamma = \mu \left( -\frac{dv_r}{dr} \right) \quad (2.5.4)$$

Where  $v_r$  is the local velocity at position  $r$

If the fluid was a Bingham plastic, the model equation will be:

$$\tau = \tau_y + \eta_p \gamma \quad (2.5.5)$$

We now combine the above equations (2.5.2&2.5.4) to obtain for the Newtonian fluid:

$$-dv_r = \frac{1}{\mu} \frac{\Delta P}{2L} r \cdot dr \quad (2.5.6)$$

The velocity profile can then be integrated across the pipe diameter to obtain:

$$-\int_{v(r)}^{v(R)} dv_r = \frac{1}{\mu} \frac{\Delta P}{2L} \int_r^R r \cdot dr$$

$$[v]_r^R = \frac{1}{\mu} \frac{\Delta P}{2L} \left[ \frac{r^2}{2} \right]_r^R$$

Boundary conditions  $v_r=0$  at  $r=R$

$$0 - (-v_r) = \frac{1}{\mu} \frac{\Delta P}{4L} (R^2 - r^2)$$

The velocity distributions becomes now

$$v_r = \frac{1}{\mu} \frac{\Delta P}{4L} R^2 \left[ 1 - \left( \frac{r}{R} \right)^2 \right] \quad (2.5.7)$$

This velocity profile is parabolic as shown in figure 2.5.6

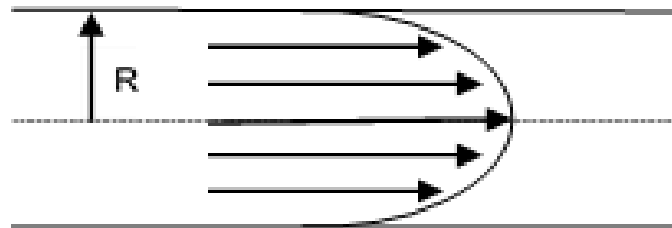


**Figure 2.5.6:** Velocity distribution in the form of a parabola.

The correlation for flow rate-pressure drop which is equivalent to a correlation flow rate- wall shear stress can be obtained by considering flow through a differential tube element (see Figure 2.5.7)



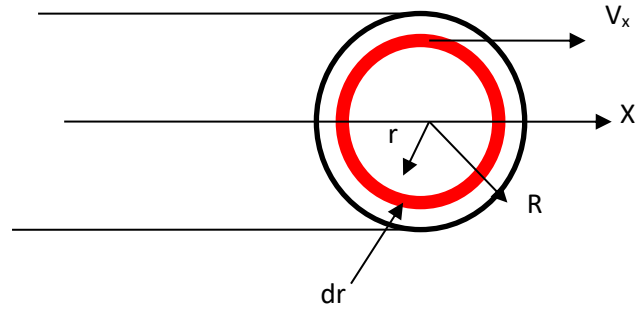


**Figure 2.5.7:** Annulus of flow in a pipe.

Since  $v_r$  is constant on this ring the volume rate of flow,  $Q$

$$dQ = v_r (2\pi r) dr$$

Hence

$$\int dQ = 2\pi \int_0^R v_r dr$$

From velocity profile eq. (2.5.7)

$$v_r = \frac{1}{\mu} \frac{\Delta P}{4L} R^2 \left[ 1 - \left( \frac{r}{R} \right)^2 \right]$$

$$\therefore Q = \frac{2\pi \Delta P R^2}{4L\mu} \int_0^R \left( r - \frac{r^3}{R^2} \right) dr$$

$$= \frac{2\pi \Delta P R^2}{4L\mu} \left[ \frac{r^2}{2} - \frac{r^4}{4R^2} \right]_0^R$$

$$= \frac{2\pi \Delta P R^2}{4L\mu} \cdot \frac{R^2}{4}$$

$$Q = \frac{\pi \Delta P R^4}{8L\mu} \quad \text{or}$$

$$Q = \frac{1}{\mu} \frac{\Delta P}{128L} \pi D^4 \quad (2.5.8)$$

Similarly with a Bingham fluid, we obtain after integration, a flowrate-pressure drop or flowrate-yield stress correlation

$$Q = \pi R^3 \tau_w \left[ 1 - \frac{4}{3} (\tau_0 / \tau_w) + \frac{1}{3} (\tau_0 / \tau_w)^4 \right] / 4\mu_p \quad (2.5.9)$$

We can extend the argument further by considering other rheological constitutive equations (Power model, Casson model etc....). The results of some known models are presented in Table 2.5.2 (Benkreira 1990). Clearly, any model could be treated in similar way and the results do not have to be expressed analytically. It may be that the model is complicated but a computed correlation between flowrate and pressure drop, i.e. flow rate and wall-stress can always be found.

The crux of the matter is that the rheology must be established and it can only be done experimentally. Only when the relevant model is found can the correct relationship between flow rate and pressure drop be established.

**Table 2.5.2:** Analytical solutions to pipe flow equations using viscometric models. (Benkreira 1990)

Model	Equations
Power Law	$\tau = \kappa \dot{\gamma}^n$ $Q = (\tau_w / \kappa)^{\frac{1}{n}} \pi R^3 n / (3n + 1)$ $\tau_w = \kappa [4Q(3n + 1) / (\pi R^3 4n)]^n$
Casson	$\tau^{1/2} - \tau_0^{1/2} = (\mu_c \dot{\gamma})^{1/2}$ $Q = \pi R^3 \tau_w \left[ 1 + \frac{3}{4} (\tau_0 / \tau_w) - \frac{16}{7} (\tau_0 / \tau_w)^{1/2} - \frac{1}{21} (\tau_0 / \tau_w)^4 \right] / 4\mu_c$ $\tau_w = (4Q\mu_c / \pi R^3) - \frac{3}{4} \tau_0 + \frac{16}{7} (\tau_0 \tau_w)^{1/2} + (\tau_0^4 / 21 \tau_w^3)$

### **2.5.3 Yielding of Waxy crude oil gels**

Waxy crude oils as explained early are complex mixtures of solvent oil and waxes (paraffinic hydrocarbons). When hot and totally dissolved in the solvent oil, waxy crude oil are essentially viscous fluids as shall be seen. However, when temperature drops (the issue in this research), the wax precipitates out in the solvent oil to eventually crystallise and form a network. The gelled oil is mainly composed of a structured material, soft solid like and with a complex rheology, intimately related to the state of the structure, i.e. to temperature, cooling rate and past deformation history. Crucially, time also is embodied in these effects and must be brought in the rheological measurements if a complete evaluation is sought.

#### **2.5.3.1 Critical or “Yield” stresses**

As an applied research, this study is driven by industrial considerations, here predicting the pumping pressure to restart pipelines holding gelled waxy crude oil following shutdown and subsequent cooling. Thus yielding refers to the gradual breakdown of the gel as it would happen when pumping is restarted. The question to be answered is what is the minimum restart pressure to use and at which rate the pressure should be increased to this minimum pressure to restart the pipeline as quickly as possible?

Theoretically, the concept of yield stress is controversial (see Barnes and Walters (1985) *The Yield Stress Myth*) and is attributed to the limitation of rheological instruments to measuring flow, i.e. shear rate below a certain value, typically  $0.001 \text{ s}^{-1}$ . Waxy crude oils are examples of such materials that show no such flow at significant shear stresses (larger than 100 Pa) as shown in the Results Chapter. Such definition of yield stress, based on a threshold of sufficiently low shear rate, may be controversial in rheological terms but the gel strength of waxy crude oils that ensues below the wax appearance temperature is an engineering reality that costs the oil industry billions of dollars as a result of prolonged shutdown of pipelines or, as in many cases, not being able to restart the operation altogether.

Following this relaxation of the concept, Wardhaugh and Boger (1991) and Chang et al. (1998) characterized through a series of rheological tests (constant stress, oscillatory and creep) the yielding of a waxy crude oil as

being composed of three deformation regions, elastic-creep-fracture as shown in Figure 1.5 and Figure 2.5.8. They identified the end of the elastic and creep regions by an elastic and a static yield stress,  $\tau_e$  and  $\tau_s$  respectively.

Both the elastic-limit and static yield stresses are dependent on the strength of the interlocking network of wax crystals in the oils before the structure is disturbed, while the dynamic yield stress is related to the concentration and size of the wax particles in the oils after the structure is completely destroyed. Engineers are most interested in the static yield stress  $\tau_s$ , the stress value when the fracture occurs, as this stress value effectively determines the pump capacity required to initiate flow and ensure pipeline restart.

Surprisingly they did not identify the end of the fracture region. This is a critical stress as it will be demonstrated in the present study and indeed the most important yield stress in relation to restart rather than the elastic or static stress. Their so called 3-stress model is composed of these two stresses,  $\tau_e$  and  $\tau_s$  plus  $\tau_D$ , the elastic yield stress represents the region where the stress applied is proportional to the produce strain while the static yield represent the end of creep region and the beginning of gel fracture before flow commences. However, dynamic stress, is an imaginary stress found by extrapolation of the viscous part of the flow curve to zero shear rate. Due to the poor resolution of the instruments used in their rheological measurements, these workers were unable to measure  $\tau_e$  which they determined indirectly through oscillatory and creep tests, not control stress. Furthermore, the fact that they measured a shear rate at the end of creep makes their labelling the end of the creep region as a yield stress questionable.

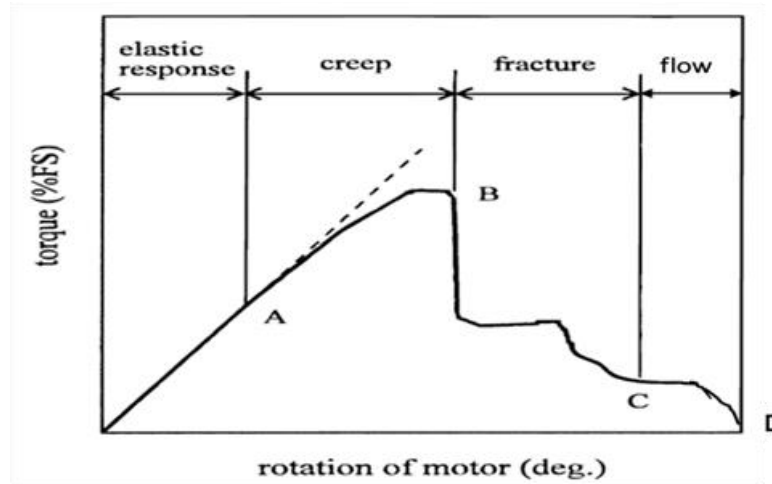


**Figure 2.5.8:** Yielding of waxy crude oil (Wardhaugh and Boger, 1991).

Recently, Fakroun (2017) followed their approach, using an advanced rheometer (Anton Paar MCR 301) capable of measuring flow at very low shear rates and was able to measure the entire deformation flow curve showing it to be quite complex. In particular, the so called elastic region may even not exist as a flow was measured as clearly seen in Figure 2.5.9 albeit, a very small and not continuous.

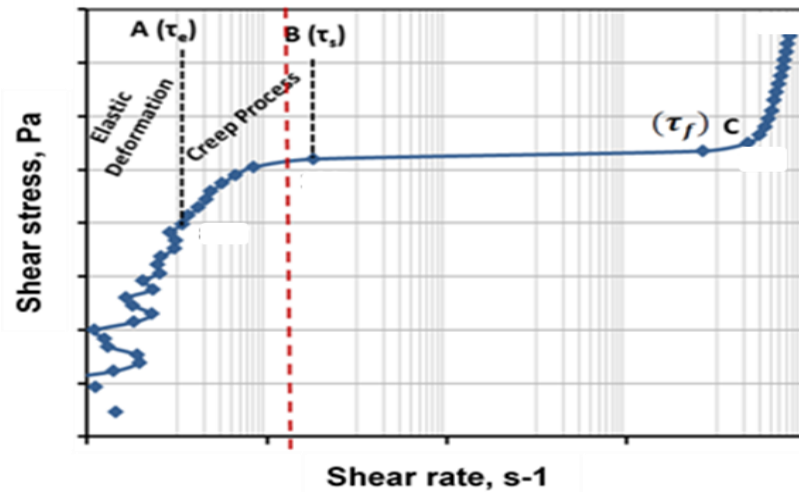


**Figure 2.5.9:** Zoom into the controlled stress data for BPO at 15°C, cooling rate 0.5°C/min, stress sweep 0 -150 Pa at rate 30Pa/min (Fakroun, 2017).

An important contribution made by Fakroun (2017) to the understanding of waxy crude oil rheology is his identification and accurate measurement of the fracture yield stress,  $\tau_f$ . Again a criticism of this, is the fact that as with the static stress it is obtained at a measurable shear rate. The conclusion drawn

from these important studies is that these so called yield stresses would be best defined as limiting stresses, demarcating changes in the structure of the gelled waxy crude oil. This is one important contribution of the present research in that it removes the contentious issue of yield stress, which strictly implies no flow but a reversible elastic deformation. In between the initial work of Boger and his associates in the 1990's until the work of Fakroun in 2017, these so-called 3 yield stresses  $\tau_e$  and  $\tau_s$  plus  $\tau_D$  were accepted as the norm to describe the yielding of waxy crude oils with many researches simply following on such an approach but focusing on obtaining more reproducible data using a range of rheometric techniques (further details to follow). As explained earlier, gels are structured materials which form after cooling below the wax appearance temperature. The gel structures being formed as a result of crystallization of the wax depend crucially on cooling rates, temperatures and probably other parameters not accounted for. It is thus highly likely that the gels formed on each occasion (at fixed temperature and cooling rate and after being properly conditioned) are not strictly the same. It is thus not surprising that discrepancies occur even with the same oil at the same temperature and cooling rate, particularly when different modes of rheometric techniques are used. For this reason, below is a review of techniques used for measuring these so called yield stresses.

#### **2.5.3.2 “Yield” stresses measurement techniques**

A strong interest in yield stress fluids has led to developments of a variety of experimental methods and techniques for measuring yield stress (Nguyen and Boger, 1992). Whilst each method has its own merits and limitations, and although some techniques may be more popular than the others therefore, no single method has been universally accepted as the standard for measuring yield stress. Since yield stress measurements are extremely difficult to interpret, it is not unusual to find variations in the results obtained from different methods with the same material prepared and tested in the same laboratory e.g., Zhu et al. (2001); Uhlherr et al. (2005); Barnes (1999)]. Such variability is often attributed to the differences in the principles employed by different techniques, the definition of the yield stress adopted and the time scale of the measurements involved (Nguyen and Boger, 1992;

Barnes, 1999). The variable nature of yield stress measurements has led to a suggestion that an absolute yield stress is an elusive property and any agreement of results from different techniques is accidental (Barnes, 1999).

Direct measurements generally rely on some independent assessment of the yield stress as the yield stress measured under near static condition, is termed "static or true" yield value or rheometric (using a rheometer). In addition to the terminology problem, since most viscoplastic fluids are structured materials where the rheology is strongly dependent on past shear history, it has been found that the yield stress can be very sensitive to the duration of time of measurement (Cheng 1986). Direct measurements fall in two groups; vane, slotted plate, penetrometer and inclined plane techniques are the first group, the second group uses a controlled stress rheometer in controlled stress mode, oscillatory mode or creep mode and are more prevalent (discussed further below). In addition to these methods, pressure drop measurements in pipes have been used determine yield stress as the pressure required to commence flow, viewed visually or through the measurement of pressure (Davenport and Somper (1971), Verschuur et al. (1971), Wardhaugh and Boger (1991), Rønningsen (1991), Rønningsen (1992), Chang et al. (1998), Thomason (2000), Karan and Ratulowski. (2000), Borghi et al. (2003), Lee et al. (2007), Amhamed (2009) and Fakroun (2017). Such methods however ignore such effects as nonlinear pressure distribution, pipe compressibility, porosity of wax structure and wax contraction effects. Generally, the yield stress measured in controlled stress rheometry is higher than the one obtained from the pipeline technique.

**Table 2.5.3:** Various techniques for measuring the yield stress.

Yield stress technique	Used by:
<ul style="list-style-type: none"> <li>▪ Vane</li> <li>▪ Slotted plate</li> <li>▪ Penetrometer</li> <li>▪ Inclined plane</li> </ul>	<ul style="list-style-type: none"> <li>▪ Nguyen and Boger (1983, 1985), Coussot et al. (1995), Zhu et al. 2001) and Uhlherr et al. (2002)</li> </ul>
<ul style="list-style-type: none"> <li>▪ Controlled stress</li> <li>▪ Oscillatory stress</li> <li>▪ Creep</li> </ul>	<ul style="list-style-type: none"> <li>▪ Wardhaugh and Boger (1991), Rønningsen (1992), Chang et al. (1998), Henaut et al. (1999), Borghi et al. (2003), Lee et al. (2007), Ekweribe (2008), Mohamed (2003), Amhamed (2009), Abdelrahim (2011), and Fakroun(2017).</li> </ul>
<ul style="list-style-type: none"> <li>▪ Capillary U-tubes</li> </ul>	<ul style="list-style-type: none"> <li>▪ Gill and Russell (1954) and Davenport and Russell (1960)</li> </ul>
<ul style="list-style-type: none"> <li>▪ Lab-scale model pipelines</li> </ul>	<ul style="list-style-type: none"> <li>▪ Rønningsen (1992), Carniani et al. (1996), Borghi et al. (2003), Lee et al. (2007), Amhamed (2009), and Fakroun (2017).</li> </ul>
<ul style="list-style-type: none"> <li>▪ Large pilot pipeline</li> </ul>	<ul style="list-style-type: none"> <li>▪ Davenport and Somper (1971) and Veschuur et al. (1971).</li> </ul>

**Controlled stress technique:** The application of a constant shear stress to a sample of gelled waxy crude oil in a cone and plate or plate-plate geometry provides an experimental condition which is similar to the pipeline itself, in that most pipeline systems, which operate using centrifugal pumps, apply a controlled pressure drop, rather than a fixed rate of flow. From an experimental point of view, it is much easier to measure a very small displacement at a fixed torque than it is to control an equivalent small rate of rotation and measure the resultant torque. Controlled stress rheometers therefore make measurements that are not possible with other instruments, for example, the measurement of a zero shear viscosity at extremely low shear rates at the order of  $10^{-7} \text{ s}^{-1}$  (Barnes and Walters, 1985). Many researchers used this technique - see listing in Table 2.5.2 above and examples of works by Schramm (1994), Kane et al., (2004), Venkatesan et al., (2005), Ghannam et al., (2012). This technique was most recently reviewed by Malkin et al. (2017) who emphasised the important point that the yielding of waxy crude oils is not the destruction of a structure at one definite yield stress but a transition extending over a stress range and occurring in time. This precisely what is demonstrated in this work using control stress rheometry.



Oscillatory technique: This technique is designed to measure not only yielding but also the viscoelasticity of waxy crude oil gels through the application of a sinusoidal shear deformation and the measurement of the corresponding stress response (see Figure 2.5.10 and 2.5.11).

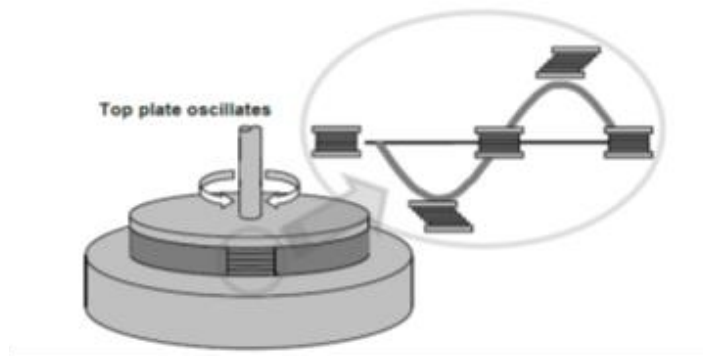


**Figure 2.5.10:** Schematic of atypical oscillatory rheometer setup.

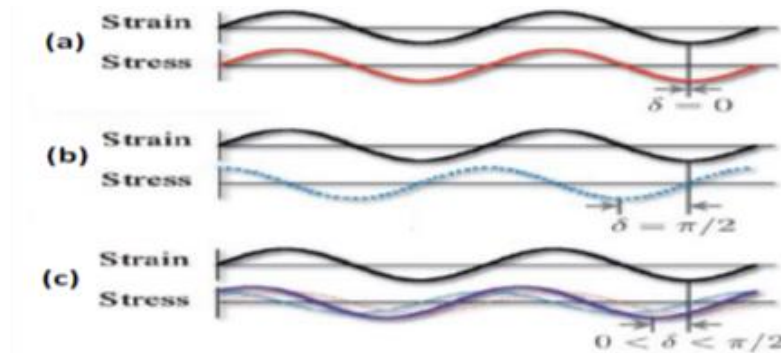


**Figure 2.5.11:** Applied strain and stress response on oscillatory shear flow.

The governing equations in this situation are (Mezger, T.G., 2006):

$$\gamma = \gamma_0 \sin(\omega t + \delta), \quad \tau = \tau_0 \sin(\omega t + \delta) \equiv \tau_0 \sin(\omega t) \cos(\delta) + \tau_0 \sin(\delta) \cos(\omega t)$$

The complex modulus  $G^* = \tau_0 / \gamma_0$  decomposes into an elastic  $G' = (\tau_0 / \gamma_0) \cos(\delta)$  and viscous modulus  $G'' = (\tau_0 / \gamma_0) \sin(\delta)$  according to equation:

$$\tau = \gamma_0 [G' \sin(\omega t) + G'' \cos(\omega t)] \quad (2.5.10)$$

A loss factor,  $\tan(\delta) = \frac{G''}{G'}$ , is used to assess the relative magnitude of these two moduli with  $G'=0$  and  $G''=0$  signifying purely elastic and viscous deformation respectively.

In this technique, the measurements are conducted initially in the linear viscoelastic range (LVR) at very small stress and frequencies that do not break the gel structure, giving  $G'$  and  $G''$  that are independent of strain amplitude. Yielding is then detected when the viscoelastic region ceases to be linear as shown in Figure 2.5.12a, b to become gradually less elastic and more viscous with the viscous modulus  $G''$  becoming much higher than the elastic modulus  $G'$ . To obtain such deformation profile, in this research, the measurements are carried out at fixed frequency whilst increasing the amplitude of oscillation (stress) slowly. The experimental oscillatory frequency ( $f$ ) is often chosen from 0.1 to 1 Hz as established in the early work of Boger and colleagues (Chang et al., 1988) and followed since.

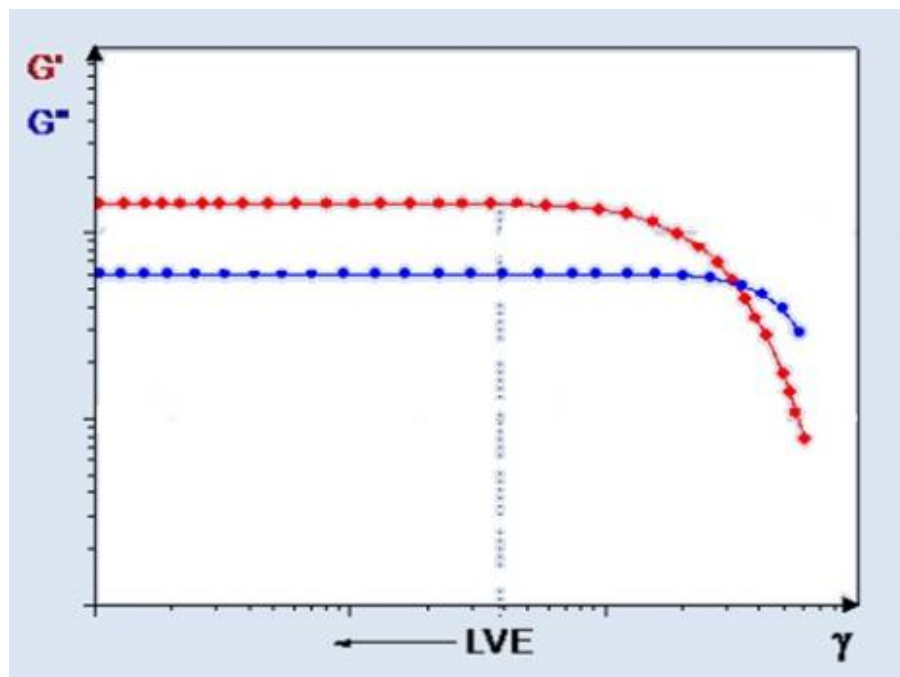


**Figure 2.5.12a:** Yielding in oscillatory flow: General Features.

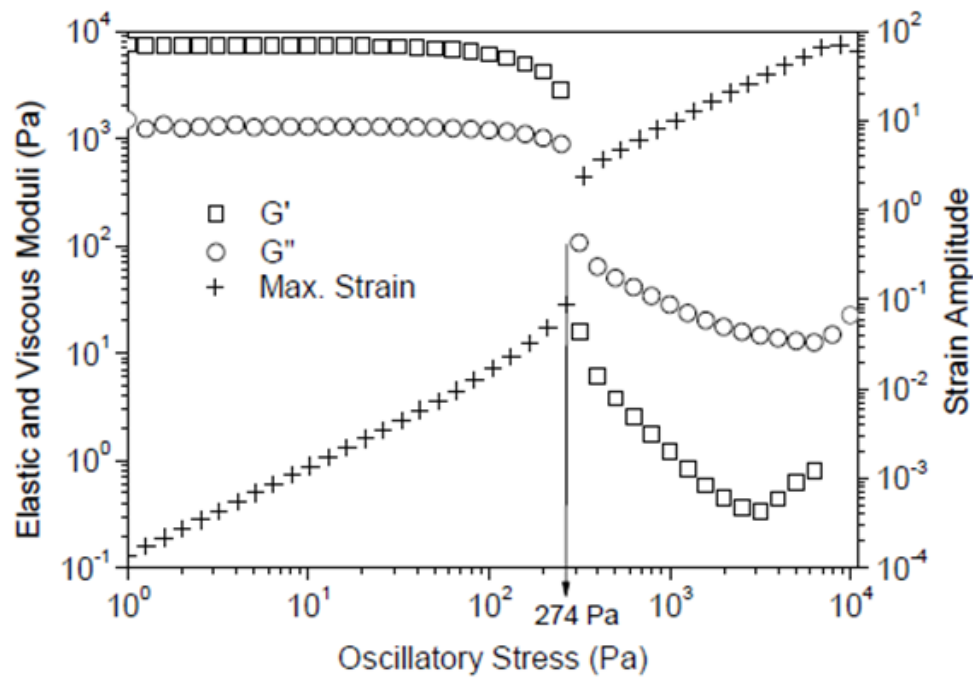


**Figure 2.5.12b:** Oscillatory test at 10Hz of a waxy crude oil gel (Mendez, 2015).

Creep technique: This consists of applying a stress, measuring the corresponding deformation as expressed by the strain rate, then removing the stress and observing the recovery of the strain. A series of such tests are used in a range of shear stresses resulting in one of two possibilities: (i) if the applied stress is below a minimum yield stress limit, no flow will be observed and (ii) if the applied stress is higher than yield stress, the material will start flowing within some time, depending on the material properties, exposure temperature, time and applied stress magnitude (see Figure 2.5.13). In the elastic region (i.e. below a certain critical stress), a total recovery will be observed. Yielding is deemed to start, when the recovery is no longer complete. Although used in studying the rheology of waxy crude oil gels, creep tests are not practical for determining waxy oils yielding due to the time it takes to get to a good approximated value (see for example the early work of Chang et al., 1998 and that of Oh et. al., 2009).

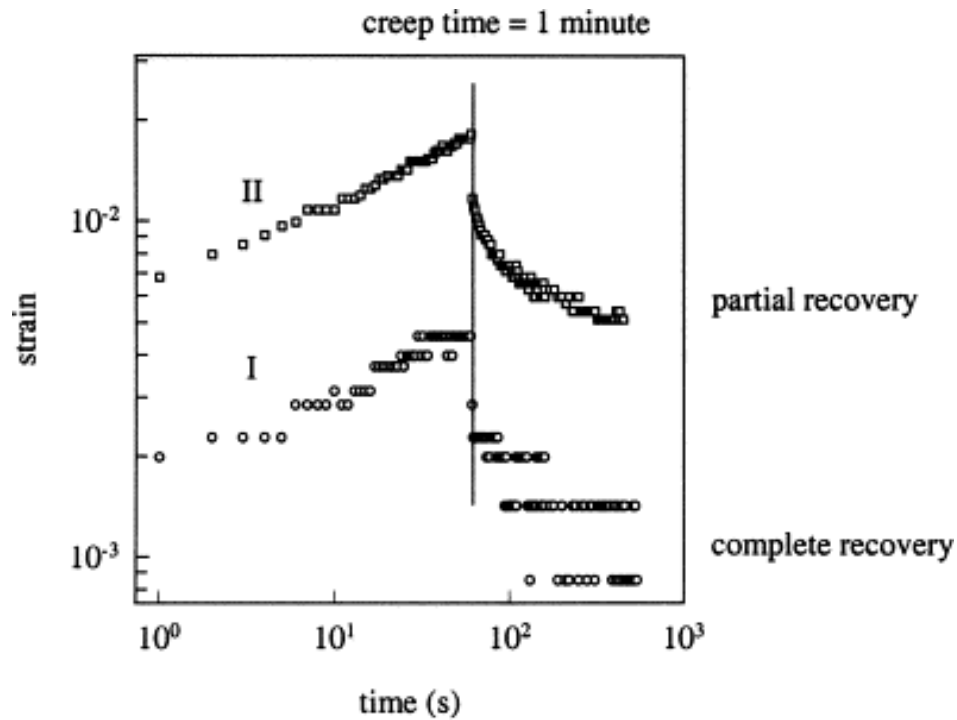


**Figure 2.5.13:** Yielding in creep flow (Chang et al., 1988).

### 2.5.3.3 Importance of Cooling on yield stress

Clearly, for waxy crude oils to gel they must be subjected to cooling to allow the wax to precipitate out and form a crystal network. As gel formation is a crystallisation process, cooling is most critical to the strength of the gels that are formed, i.e. to the yield stress. In actual pipeline operation, cooling can occur whilst the oil is static (quiescent cooling) or flowing (dynamic cooling). Under quiescent cooling, the yield stress of waxy crude oil gels has been reported (Venkatesan et al, 2005; Zhao et al, 2012; Lin et al, 2011; Sun et al, 2014; Elsayed and El-shiekh, 2010) to decrease with increasing cooling rate and increase with decreasing cooling rate as found in this research, see results chapter. This is because slow cooling allows crystal wax to grow and to be mobile thus being able to organize into network. Large cooling rate freezes growth with small crystals being formed (see Figure 2.4.1), unable to connect in a strong network. In dynamic cooling, flow will hinder the formation of crystal network and can indeed destroy some of the crystal agglomerates ((Lorge et al 1997); Venkatesan et al. (2005)).

Thus the structural property of waxy crude oil gels is affected by all factors relating to the cooling process, temperature, cooling rate and shear stress/rate applied during cooling.

Temperature effect: Rheological experimental of results (Chang et al., 2000; Kané et al., 2004; Visintin et al., 2005; Lin et al., 2008 and present research) showed that the storage modulus  $G'$ , loss modulus  $G''$  and yield stress  $\tau_0$  of waxy crude oils increased with lowering the test temperature due to the increasing amount of crystallised paraffins, meaning that the structure strength of the crude oils increased with decreasing test temperature.

Static cooling effect: Under static conditions, most of the researches (Chang et al., 2000; Kané et al., 2004; Venkatesan et al., 2005; Visintin et al., 2005; Lin et al., 2008) found that the gelation temperature, shear modulus and  $\tau_0$  decreased with the increase of cooling rate. Microscopic observations (Webber, 2001; Visintin et al., 2005; Lin et al., 2008) showed that the crystal size became smaller when the cooling rate increased, which was in accordance with the rheological results. However, Russell (Russell and Chapman, 1971) and Cawkwell (Cawkwell and Charles, 1989) found that rapid cooling produced stronger gels under static condition. This discrepancy is perhaps induced by the presence of other impurities in the crude oils. Under shearing conditions, the gelation temperature, shear modulus and yield stress were lower at a slower cooling rate (Venkatesan et al., 2002; Venkatesan et al., 2005).

Dynamic cooling effect: When the wax–oil sample is cooled under an applied (constant) shear stress, a slower cooling rate implies a slower rate of crystal formation and longer time duration of the sample being under the shear. Therefore, the structure formed under a certain shearing condition is weakened at a lower cooling rate. Coutinho et al. (Coutinho et al., 2003) also found the hardening of wax deposits with the increase of aging time in the absence of temperature-composition gradients and they attributed this phenomenon to Ostwald ripening of the paraffin crystals, a mechanism by which the large crystals grew at the expenses of the melting of smaller crystals of higher energy. (Lorge et al 1997)

From the ongoing review of previous work done in this area, the strong relationship between microstructure of the gelled wax and other rheological properties and yielding characteristic of waxy crude oils. Therefore, among our objectives in this research is to acquire more data on the microstructure property and the process of network development including the strength degree of the interlock of the gelled wax crystals network, aiming at precisely estimating the required restarting pressure and assigning the proper scenario to be applied to imitate the flow of waxy crude oil.

In this research, both static and dynamic cooling will be investigated. Also, experiments with very low cool rates ( $0.1\sim1\text{ }^{\circ}\text{C}/\text{min}$ ) will be conducted as these produced in principal the strongest gels possible as far as yield stresses are concerned.

The effect of shear stress/rate applied during cooling process on the structure of waxy crude oils was systematically investigated to modulate the flow conditions in the pipeline. Rheological results obtained (Webber, 2001; Kané et al., 2004; Venkatesan et al., 2005) showed that shearing during cooling process affected the microscopic structure development of waxy crude oils: with the increase of shear stress/rate, the gelation temperature of waxy crude oils decreased and the modulus showed loss modulus dominant response, i.e.,  $G'' > G'$ . According to microscopic observation of the morphology of paraffin crystals (Kané et al., 2003), the formation of extended, large lamella crystals was allowed under static condition, making a colloidal gel, which embodied the oil itself. The gel had high shear modulus, high gelation temperature and high yield stress, possibly due to the side-by-side interactions of lamella crystals. Under shearing condition, however, the lateral growth of the individual crystals was constricted and a lot of small disc crystals were formed (Kané et al, 2003), which made the formation of a continuous network structure difficult. Therefore, the structure strength of waxy crude oils decreases with the increase of shear stress/rate applied during cooling.

Finally, the strength of waxy crude oil gels in relation to cooling is said in the literature to be attributed to cohesive or adhesive forces (Verschuur et al., 1971; Venkatesan, 2004). This is a misconception as these concepts describe different states of forces. Upon rapid cooling, as described earlier,

wax crystallises into very small crystals. At the pipe wall, these crystals offer a very large interfacial area of adhesion crystals-wall, thus the concept of adhesive strength, here being large although the gel itself is not strong! Conversely, at low cooling rates, the wax crystals are large and form a strong network as just described. Cohesive strength is here appropriate to describe this type of state.

#### **2.5.3.4 Scaling Models of Yield Stress**

As explained above, rheological data have served to explain the yielding of waxy crude oil gels and construct models (Chang & Boger 1998). Also microscopic observations have been used to support these models for example the determination of the gel temperature (Singh et al., 2000; Zhang et al., 2011; Yang et al., 2013a). In addition, scaling models, widely used to describe the microstructures of colloidal gels (Shih et al., 2000; Cipelletti et al., 2000; Solomon and Spicer, 2010) have also been used (Visintin et al., 2005; Weeber, 2001; da Silva, 2004).

The basic concept of the scaling model for polymer gels is to relate the elastic properties of a gel to its network structure. The scaling model was extended by (Shih et al, 1990) to colloidal gels by considering the structure of the gel network as a collection of flocks, which are fractal objects closely packed through the sample. Using oils with different wax concentration (5-20 wt.%), Yang Fei et al. (2013b) found the gels that form to be similar to colloidal gels, transiting from a strong-link regime to a weak-link regime with an increase of precipitated wax percent ( $\phi_w$ ). The transition takes place for all of the model waxy oils studied. In the strong-link region,  $G'_E$  increases while  $\gamma_E$  decreases with an increasing  $\phi_w$  and the microstructure of the gelled crude oils is porous and loose due to the small value of  $\phi_w$ . In the weak link region, both  $G'_E$  and  $\gamma_E$  increase with increasing  $\phi_w$  and the microstructure of the gelled crude oils is relatively compact because of the high value of  $\phi_w$ . The fractal dimension  $D$  increases with increasing  $\phi_w$  indicating the continuous development of the microstructure of the gelled crude oils with increasing  $\phi_w$  (Yang et al, 2013a). Figure 2.5.14a, b shows such typical behavior.

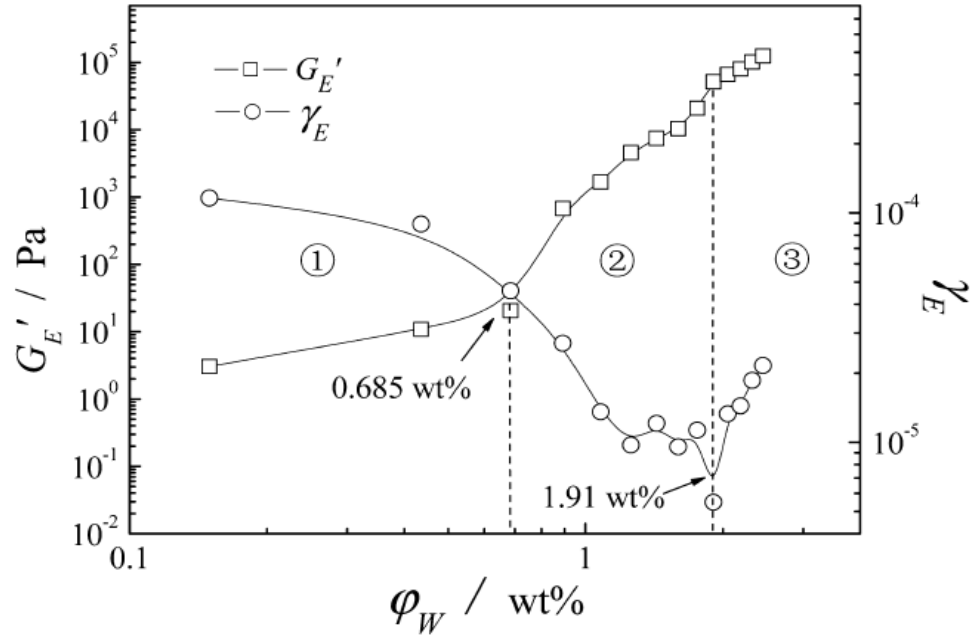


**Figure 2.5.14a:** Variations of  $G'_E$  and  $\gamma_E$  of 5 wt % gelled model waxy oil with concentration of precipitated wax crystals  $\phi_W$  (Yang et al, 2013b).

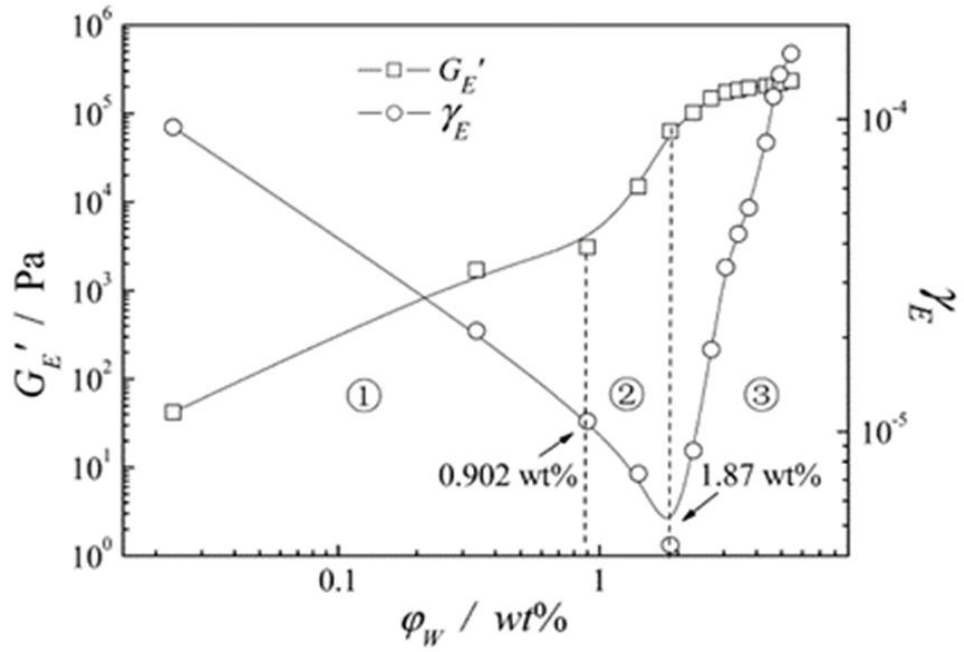


**Figure 2.5.14b:** Variations of  $G'_E$  and  $\gamma_E$  of 10 wt % gelled model waxy oil with concentration of precipitated wax crystals  $\phi_W$ . (Yang et al. 2013b).



## 2.6 Hindered gelling with solvents or chemical wax Inhibitors

As stated in the introductory chapter, the aim of this research is to develop solutions to mitigate against wax formation. There are several methods to approach this and Figure 2.6.1 summarizes the various possibilities.

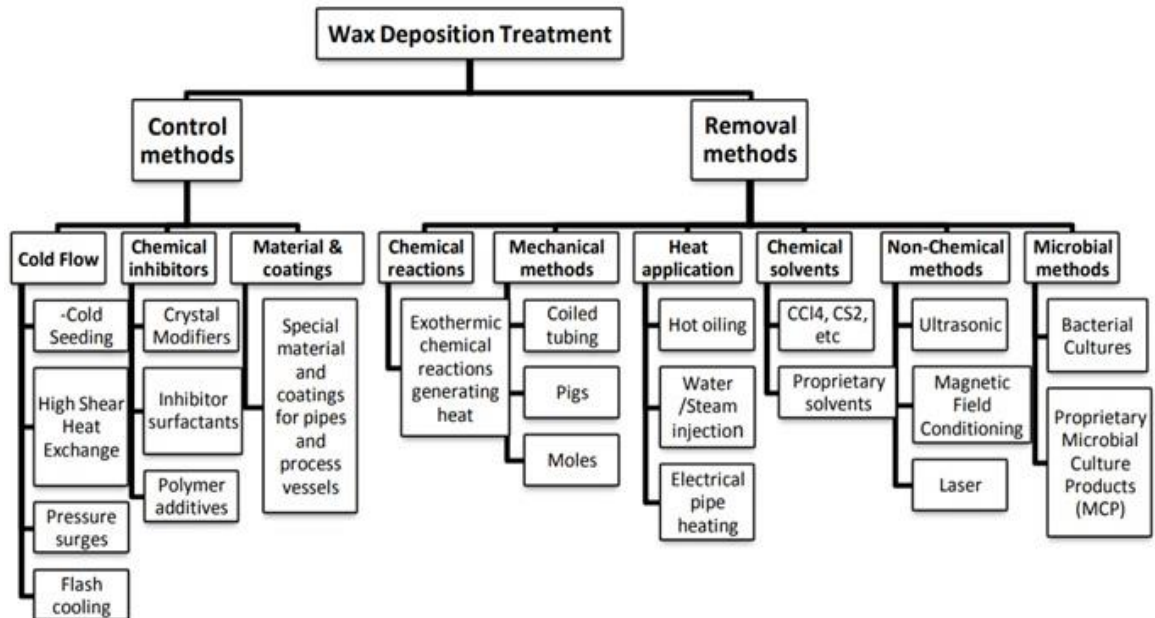


**Figure 2.6.1:** Treatment methods for wax deposition problems (Frenier et al., 2010).

This research is particularly concerned with blending a high content wax oil with a light very low wax content crude oil or using solvents, gas condensates, or chemical wax inhibitors that hinder gel (crystallization) formation.<sup>49</sup>

### 2.6.1 Wax Inhibitors types & wax inhibition mechanisms

As stated earlier, wax inhibitors are from two broad categories (Pederson and Rønningsen, 2003):

- wax crystals detergents or dispersants which are surface active agents that hinder the wax crystals that form from assembling into a gel network. Typical dispersants include alkyl sulfonates and fatty amine ethoxylates (Kelland, 2009).
- wax crystal modifiers, polymers dissolved in solvent, which insert themselves between the crystals formed thus hindering their assembly

into a gel network. These crystal modifiers intend to reduce pour point and or viscosity are also known as pour point depressants (PPD) because they reduce viscosity. Typical polymers used as crystal modifiers are ethylene polymers (polyethylene butane and polyethylene-b-propylene) and ethylene copolymers (ethylene-acrylonitrile and ethylene-vinyl acetate), the most widely used being ethylene-vinyl acetate (EVA), (Tinsley et al., 2007) as it reduces viscosity significantly (Machado et al., 2001). Comb polymers such as meth-acrylic acid and maleic anhydride are also effective wax crystal modifiers (Kelland, 2009). These comb polymers have paraffin like chain that co-crystallise with the crude oil wax crystals and polar chain that hinder co-crystallisation. Figure 2.6.2 shows the structures of some of these wax crystal modifiers.

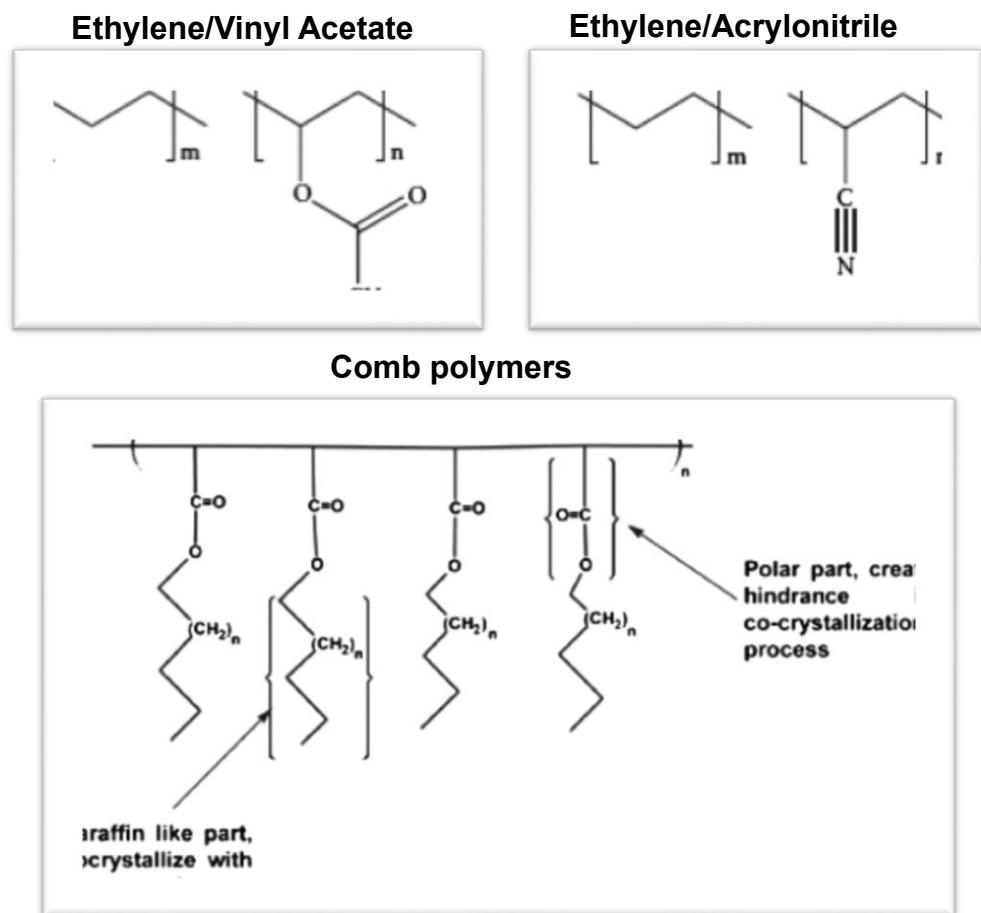


**Figure 2.6.2:** Typical wax inhibitors (Kelland, 2009).

*Nucleation:* Here the inhibitors self-assemble into micelle-like aggregates exhibiting a crystalline core and soluble hairy brushes surrounding the core, thus creating a larger number of subcritical size wax nuclei (poly nucleation). The partially shielded nuclei reduce super-saturation, thus reducing crystal growth rates, and facilitating the formation of larger number of smaller wax crystals. Such structures are weak and of very small yield stress as shall be measured later.

*Adsorption and co-crystallisation:* At temperature below the wax appearance temperature, wax inhibitors may co-crystallise with wax molecule or be adsorbed on growing surfaces of precipitated wax crystals thus disturbing crystal growth. Also, the non-polar groups of the inhibitors may incorporate into the lattice of the waxes crystal cells, while polar group extend outside the facet. Previous researchers (Zhang et al., 2008; Duffy et al., 2004; Wu et al., 2005) suggest that the function of additive is to hinder growth rate on crystal facets while facilitating the spiral growth mechanism in the perpendicular direction of the facet therefore shifting the morphology from plate-like to weaker spherulitic like structures.

*Solubilisation:* At temperature slightly higher than the wax appearance temperature, the inhibitors interact with soluble wax in the oil due to van der Waals attraction forces and hence, interact with paraffin chains. According to the research of Khidr (2007), solubilisation is a key function of copolymer crystal modifiers.

## **2.6.2 Hindered gelling with chemical wax inhibitors**

*Addition of low-wax low-pour-point fluids:* An example often referred to is the effect of blend Gullfaks Southing (Norway) high-pour point waxy oils with low-wax, low-pour-point fluids, co-producing from different reservoirs and in pipeline networks with multiple sources (Rønningsen et al. 2012). As shown in Figure 1.1, this effect is highly nonlinear; even a small volume fraction of low-wax fluid may have a tremendous lowering effect on pour point and yield stress, which has to be taken into account when planning production and transport systems.

Addition of chemical polymer wax crystals modifiers: Achievements with regard to the flow improvement and wax inhibition of waxy oils using traditional polymeric wax crystal modifiers, is reviewed by (Bing Wei, 2015) with the following conclusions made:

- The performance of wax crystal modifiers is strongly dependent on the capacity of polymer to co-crystallize with wax. In other words, performance is related not only to the structure of the polymer but also to the composition of the wax and in a complex manner. For example, EVA 30 which contains 30wt% of vinyl acetate was found for the particular oil treated to be more efficient than EVA 20, 40, and 80. There thus appears to be in this case an optimum vinyl acetate and an insight into the chemical interaction between the wax in the oil and the inhibiting chains of the additive.
- The efficiency of polymer wax crystal modifiers increases with the length of the side chains.
- Wax crystal modifiers are usually used in combination with solvents to further improve wax inhibition efficiency for example addition of trichloroethylene xylene (TEX) with ethylene copolymers and comb polymers as studied by Elhaddad et al., 2015.

Addition of natural polymer wax crystals modifiers: As expected of these crystals modifiers polymers, some of them will exist naturally. Such polymers are extracted from Jatropha plant seed oil (Giri et al., 2018) and have been tested with Sudanese waxy crude oil Heglig with high pour point and wax appearance temperature, 33°C and 60°C respectively at concentration of 5%v/v. These natural PPD were found to reduce Heglig crude pour point substantially, from 33°C to 15°C suggesting a good potential for further investigation with other waxy crude oils.

Optimal addition and limit of effectiveness: Clearly, by the fact that the mechanisms described for wax inhibition are chemical in nature, affecting bonds and chains, there is a need for optimizing the effect since excess PPD may have adverse effect. [As it will be shown in this research, increasing the concentration of a PPD from 1000 ppm to 2000 ppm had adversely increased the rheological parameter of yield stress.] Further insight in the structure of

these PPD show they are composed of two parts, an oleaginophilic part that co-crystallizes with wax forming components and a polar component that limits the degree of co-crystallization. PPDs with these properties are very selective and not very effective for every crude oil (Gang et al., 2015). In addition to this, the longer molecular chain, larger molecular weight and high thermal stability of some of the PPDs make them hard to decompose in petroleum refining process. So there is the necessity to see new small molecular compounds as clean flow improvers. Also, the use of PPD at low temperature tends to narrow the choice of acceptable PPDs because the choice of PPD is strongly influenced by the origin of crude oil, oil production fields and properties of crude oil. These combined attributes make the selection of PPD more difficult but the research findings say that this challenge can be overcome by correct PPD selection. Similarly, the dosage of PPD needed for the laboratory test will not be the representative and will always be higher than that is necessary for field use. Treating waxy crudes offers a solution to high pour point problems. However, in chemical additive treatment for reducing the pour point many waxy crudes - among them Abu-attifel crude oil - show only a limited response to PPD posing a major uncertainty. Additionally, the mechanism of pour point reduction, while often hypothesized, is not clearly understood and is to some extent controversial. As a different crude oil or model is adopted in each study, it is difficult to get a unified theory to explain the experiment results (P. Sivakumar et al., 2018).

These aspects put in perspective the challenge of the research undertaken here to arrive at optimal solutions. Similar challenges are documented from previous work such that of Wang et al., (2003) who found that most of commercial wax inhibitors he tested could decrease the deposition of low molecular weight paraffins (C34 and below), while having little effect on the wax deposition for high molecular weight paraffins (C35–C44). In many cases, although the total amount of wax formed on the cold plate was reduced, the absolute amount of deposition for high molecular wax was actually increased. Deposition from decane solutions of model paraffins such as n-C<sub>24</sub>H<sub>50</sub> (C24), and n-C<sub>36</sub>H<sub>74</sub> (C36), as well as a mixture of n-alkanes (C21 to C44) was examined with and without chemical wax deposition inhibitors.

The author stated that, the net effect of many commercial inhibitors is to make even harder wax under the similar test conditions.

### **2.6.3 Hindered gelling with solvents (light crude oils, gas condensate and gas).**

Dilution is one of the oldest and effective methods to reduce oil viscosity and help in the crude mobility through pipelines (Gateau et al., 2004). The classical diluents used for this method are condensates, light hydrocarbon naphtha, light crude oil and some organic solvents (Bassane et al., 2016 and Rønningsen et al., 2001). The resulting viscosity of the mixture depends on the dilution rate and the respective viscosities and densities of the crude oil and diluents (Gateau et al., 2004). In this research, heavy naphtha in the boiling range of 175-195 °C is blended with Abu-attifel crude oil and blend performance is determined.

*Dilution with solvents and gas condensate:* Here the dilution consists of the addition of lighter liquid hydrocarbons to heavy oil, typically condensates from natural gas production, but lighter crude oils are also used. This is an effective option to reduce oil viscosity and facilitate its mobility in the pipeline since a ratio of 20–30% of solvent is often enough to avoid high-pressure drops or the need for high temperatures (Dehaghani, 2016). Also, diluting the crude may facilitate certain operations such as dehydration and desalting. Such technology is the most widely used solution where condensates or lighter crude oil is available to transport heavy and extra-heavy oils by pipeline. However, it requires substantial investments in pumping and pipelines, the need to separate at some point the solvent, process it and subsequently return it to the oil production site. Moreover, the dilution option has some challenges since any change in oil composition may affect the required oil/solvent ratio. Then, it is important to predetermine the ratio of solvent to heavy oil since simple mixing rules do not directly apply. Special attention has to be paid to asphaltenes and paraffins stability, since condensate or light oil addition may cause asphaltenes precipitation in pipelines (Zahan et al., 2004). An example of such dilution can be found in the research by Dehaghani et al., (2016) of two Iranian heavy crude oils with heptane, methanol, toluene, gas condensate and naphtha at different temperatures. Dilution with toluene, naphtha or

heptane, resulted in viscosity reduction; however, the effect became less significant at higher concentrations of diluent. Dilution with methanol on the other hand resulted in higher viscosity because of the formation of hydrogen bonds. Gas condensate had a greater impact on heavier oil, reducing viscosity; however, at higher temperatures its effect was reduced.

*Dilution with light crude oil:* This is an interesting proposition, particularly in countries and area with such availability and was investigated by Ghannam et al., 2017 using Canadian heavy and light crude oils in a 90%/10% proportion. This caused a strong reduction in the heavy crude oil viscosity from 10 Pa.s to 1.2 Pa.s at 25 °C. An even higher viscosity reduction from 10 Pa.s to 0.375 Pa.s at 25 °C can be achieved in the presence of 20% light crude oil. The yield stress of the heavy crude oil reached 0.7 Pa at a room temperature of 25 °C and it decreased to 0.4 Pa at 65 °C. Also, the presence of the light crude oil increases the solubility of heavy paraffin and lowers the paraffin content, which result in eliminating the thixotropic behavior of the heavy crude oil.

*Dilution with non-reacting gas injected in a production wells*

As with the dilution with light crude oil, this approach is most feasible in countries and area with such availability and was investigated by Elhaddad et al., 2015 in three oil wells in Libya with gas injected at a pressure of 83.3 bar and a temperature of 65 °C (greater than the pour point temperature) during the gas-lift operation. Field observations confirmed that by applying these techniques, production was kept clean and no wax was formed. However, no data were provided to quantify this

*Dilution with non-reacting gas injected in the pipeline:* This is clearly a simpler operation and an easier alternative to injecting into a well. Sulaiman et al., 2017 investigated such a method using nitrogen gas to waxy crude oil that had stopped flowing in a pipe, immediately prior to gelation. For both instantaneous restart and gradual restart of the experimental flow loop, it was observed that there was a reduction in restart pressure, typically 10-18% depending on temperature. The restart pressure required under gradual restart approach was observed to be higher compared to instantaneous restart approach. It was also found that the restart pressure decreased as the gas-to-oil volume ratio increased due to an increased slippage effect.

## 2.7 Conclusion

Basic information regarding waxy crude oils characteristics are presented, which distinguish it from other ordinary crudes, as mentioned in the introduction of this chapter, wax crystallisation are the source of peculiarity in managing waxy crude oil transportation and storage, some related technical terms which are commonly used in describing the characteristics of waxy crude oils such as Wax appearance temperature and pour point, in addition to some rheological terms and flow models are introduced, however, waxy crude oil do not necessary have to follow one of the introduced models, due to it is unique characteristics under some specific flow conditions, among most rheological properties is the yield stress concept which is reviewed in respect of most recently fundamental understanding of the yielding process and yield stress measurement techniques.

As explained in this part, the problems encountered with waxy crude oils during pumping are related to cooling of the crude under the wax appearance temperature, the method of cooling, whether without shearing (static), or with shearing (dynamic) and the rate of cooling which play a major effect on the magnitude of yield stress and it is relation to the a mount of wax being precipitated under certain conditions, once the magnitude of wax precipitated are accurately determined, then it is used for selecting the most appropriate and economic mitigation method, among reviewed and presented methods in the cited literature , more focuses on dilution with lighter crude and the chemical additives methods to hinder the gelling of waxy crude oils is investigated as can be seen in the following experimental chapter.



## CHAPTER 3: EXPERIMENTAL METHOD

### 3.1 Introduction

This work is an extensive research concerned with studying the flow behaviour of waxy crude oils. The structure of waxy crude oil and its properties are to be investigated thermally, visually and dynamically. Following the introduction chapter, aims and objectives and the update knowledge as established in the literature review, the experimental methodology is now presented. It describes a series of work objectives building towards being able to address the principal aim – that of being able to predict the re-start pressure of gelled pipelines in real situations, and to understand the effect of chemical additives on crude microstructure and crude oil rheological characteristics which in turn assess the restarting pressure requirements. This chapter comprises four sections, starting with an introduction followed by the materials used, then a description of the equipment and experimental procedure which describe the techniques used to evaluate the samples, finally this chapter is concluded by a description of the samples preparation and conditioning to ascertain that the measurements are well defined.

This research is dependent on data obtained from experiments which are carefully planned and designed to achieve as precisely as possible (within experimental errors) an accurate determination of restart and pumping pressures of waxy crude oils. Therefore, objectives of the experimental method are thus (in the order the work was carried out):

- I. Preparation and conditioning of crude oil samples: It is essential for meaningful data to be obtained with structural materials such as waxy crude oil gels that any prior history of the crude oil samples be erased. To that effect, the samples were heated and shear mixed, well above the wax appearance temperature, to ensure all the wax was thoroughly dissolved in the solvent oil and any remnant of prior structure formation was destroyed. Upon cooling of such conditioned samples, the structures that are formed are then uniquely defined.

- II. Accurate determination of the wax appearance temperature ( $T_{WA}$ ) of these conditioned samples using differential scanning calorimetry (DSC) which measures heat flow at various temperatures and cooling rates. The measurement will cover in addition to untreated crude oil samples, samples treated with various concentrations of wax inhibitors and aiming at finding and understanding the working mechanisms of these additives on microstructural changes.
- III. Microscopic observation of gel structure including crystal size and morphology using a cross polar microscope (CPM). The microscopy, being a sophisticated method, is implemented in studying the crystal, clusters interconnection structure and distribution aiming at understanding the relation governing different parameters (temperature, cooling rate, chemical type and concentration).
- IV. Rheological measurements of the different conditioned samples cooled in situ (on the rheometer plate- further details below) down to a temperature, in a range near and below  $T_{WA}$  and for a range of cooling rate to determine as precisely as possible (within experimental errors) the deformation and subsequent yielding, creeping, fracture and finally viscous flow of these elasto-plasto-viscous gels. High resolution is obtained through the usage of a state of the art rheometer CVO 100 Bohlin that enables a series of rheological techniques to be used to compare finding:
  - a. Controlled Continuous Stress (shear stress ramping)
  - b. Controlled Oscillatory Stress (amplitude sweep at fixed frequency).

Critically, these techniques enable to bring out the important time effect such that the yield stresses (there are many as shall will be established), gel temperatures, elastic and viscous moduli measured are fully assessed in relation to temperature, cooling rate and stress loading with respect to time.

### **3.2 Waxy crude oil and wax inhibitors used**

As explained in the introductory chapter, this research is of industrial relevance applicable to a real crude oil namely Abu-attifel crude oil of Libya, a paraffinic waxy crude oil. This oil is most appropriate for research studies also

as it has a high wax content of 29 wt. %, representative of the range of waxy crude oils commonly found. Because of the high wax content, at production site, the crude is thermally treated using gas heaters in order to reduce the wax deposition problems during shipping; eight gas heaters are distributed along the pipelines. To put in perspective, the fuel cost, the total quantity of the dry gas which used to heat the whole system at this oil field is very large indeed - 19 million ft<sup>3</sup> per day. In a project to reduce cost, this field is now subject to selecting chemical treatment in addition to the heating option, therefore, on one hand, this research will greatly contribute to provide a sufficient valuable information related to the rheology data that will be needed in the selection of the proper chemicals and secure safe and economical piping and transportation of the crude. On the other hand, the methodology followed in this research will pave the road for evaluating produced treatment chemicals instead of the current method which depends on the measurement of pour point and viscosity only.

The crude was characterised by measuring the physical properties according to standard methods as shown in Table 3.2.1. As these standards are commonly used, their description can be found in <https://compass.astm.org/Standards/>. The DSC measurements will however be described as they are particularly critical in the context of this work- they determine the wax appearance temperature and the wax content.

**Table 3.2.1:** Physical properties of Abu-attifel crude oil.

Test method	Property	Abu-attifel crude oil
<b>ASTM D 5002</b>	Specific gravity@15.6°C	0.8229
<b>CALCULATION</b>	API gravity	40.43
<b>UOP 46</b>	Wax content, (wt. %)	29
<b>ASTM 5853</b>	Pour point, °C	39
<b>DSC</b>	WAT, °C	68.14 & 39
<b>ASTM D 4006 42</b>	Sulfur content, (wt. %)	0.030
<b>API 43</b>	Asphaltenes, (wt. %)	0.17
<b>ASTM D 4006</b>	Water content, (wt. %)	0.3
Pumping Temperature, °C		85

As for the wax inhibitors used in this study (inhibitor meant in a general sense), in principal the choice is from three broad categories (Pederson and Rønningsen, 2003):

- a) Blending with a crude oil of a much lower wax content, means simply reducing the wax content hence, the formation of strong gel.
- b) Treating the crude oil with wax crystals detergents or dispersants which are surface active agents that hinder the wax crystals that form from assembling into a gel network. Typical dispersants include alkyl sulfonates and fatty amine ethoxylates (Kelland, 2009).
- c) Treating the crude oil with wax crystal modifiers, polymers dissolved in solvent, which insert themselves between the crystals formed thus hindering their assembly into a gel network. These crystal modifiers are also known as pour point depressants (PPD) because they reduce viscosity. Typical polymers used as crystal modifiers are ethylene polymers (polyethylene butane and polyethylene-b-propylene) and ethylene copolymers (ethylene-acrylonitrile and ethylene-vinyl acetate), the most widely used being ethylene-vinyl acetate (EVA), (Tinsley et al., 2007). Comb polymers such as meth-acrylic acid and maleic anhydride are also effective wax crystal modifiers (Kelland, 2009).

In this research, a feasibility study was first performed to narrow down the choice of the many inhibitors available to arrive at one of each from the above category:

- d) Sirtica crude oil as a low paraffin wax content (6.4%) waxy crude oil. This oil is classified as an Intermediate crude oil produced by Arabian Gulf Oil Company, according to U.S. Bureau of Mines method of classification. It has a characterization factor of 12.0, an API of 36.46 and a very low pour point of -9 °C in comparison with Abu-attifel crude oil +39°C. The very low pour point of Sirtica crude oil makes it a good candidate additive to reduce the restarting pressure of Abu-attifel crude oil. This particular wax inhibition solution was considered in the research to assess the blending required and associated cost in comparison with chemicals inhibitors.
- e) Treatment with a wax crystal detergent labelled here Chimec RO 671A, supplied by Chemic Rome Italy. It is a blend of polymeric compounds in water or glycol solution and contains about 15-25% of Mono-ethylene

glycol. It has pour point of -10 °C and a viscosity at room temperature of 650-800 cp.

- f) Treatment with a wax crystal modifier, PPD-JOUF(110 C), supplied by JOUF Chemical (Benghazi, Libya), essentially a polymeric in aromatic solvent, Table 3.2.2 gives the specifications and concentrations of the inhibitors tested.

**Table 3.2.2:** Specifications & concentrations of wax inhibitors used.

<b>Wax Inhibitors</b>	<b>Concentration</b>
<b>Sirtica crude oil</b>	20% VOL.
<b>Chimec R0671A</b>	500 and 1000 PPM
<b>PPD 110 C</b>	1000 and 2000 PPM

### 3.3 Samples preparation and conditioning

Waxy crude oils are materials that change structure depending on temperature, particularly near and below their wax appearance temperature. In order for meaningful experiments to be carried out a reference state had to be set for all samples prior to measurements. This reference is one where the samples are deemed to have no memories of past structure and was achieved by shear mixing at a temperature well above the 39 °C wax appearance temperature of Abu-attifel crude oil. The conditioning procedure was as follows:

1. The oil from the field arrived at the laboratory in 10 of 1Lit drums.
2. Each drum was heated at 85°C, maintained at that temperature whilst stirred for 3 hrs. The drum top cover was such that once the stirrer was inserted, it was maintained sealed (see Figure 3.3.1).
3. Upon completion of this first conditioning, the drum contents were transferred to a series of 50mL aluminium bottles, sealed immediately after, and stored at room temperature ( $\approx 20^{\circ}\text{C}$ ).
4. Prior to any experiment (DSC, microscopy and rheology), such preconditioned samples were mixed at impeller speed of 100rpm for 30 mins in a hot water bath maintained at 75°C. The wax inhibitor was then

added at the tested concentration and with a further 30 minutes of mixing at 100rpm impeller speed in the 75°C water bath.

5. Step 4 completed the conditioning with the sample to be measured now thoroughly mixed and kept hot in the water bath at 75°C ready to be transferred to say the rheometer plate itself preheated to 75°C and to be programmed for subsequent cooling from this reference temperature well above the 39 °C wax **appearance** temperature of Abu-attifel crude oil.



**Figure 3.3.1:** Oil samples conditioning rig and holding pots.

### 3.4 Differential scanning calorimetry (DSC)

Here the purpose of the differential scanning calorimetry is to measure the heat flow as the waxy crude oil is subject to a set cooling rate and determine from the heat curve the wax appearance temperature  $T_{WA}$  and the wax fraction precipitated at any temperature below  $T_{WA}$ . A state of the art DSC was used for this purpose, the Thermal Analysis DSC Q20 from TA Instruments (see Figure 3.4.1) which can operate over a very large range of temperatures (-180°C to 725 °C) with a temperature and calorimetric accuracy of  $\pm 0.1^\circ\text{C}$  and  $\pm 0.05\%$ . In these experiments, the lowest temperature set was  $-20^\circ\text{C}$  using dry nitrogen gas purged through the DSC cells. The highest temperature set was  $75^\circ\text{C}$ , the conditioning sample temperature. The instrument uses a very small amount of sample (4-8mg) and operates with a 50-position auto sampler and Platinum software convenient for automated off-work hours runs. Three cooling rates were tested (1, 5 and  $15^\circ\text{C}/\text{min}$ ) and two

parallel runs were carried to check the repeatability of the results. Figure 3.4.2a&b give a typical flow curve that was obtained to explain the depiction of the wax appearance temperature  $T_{WA}$ .

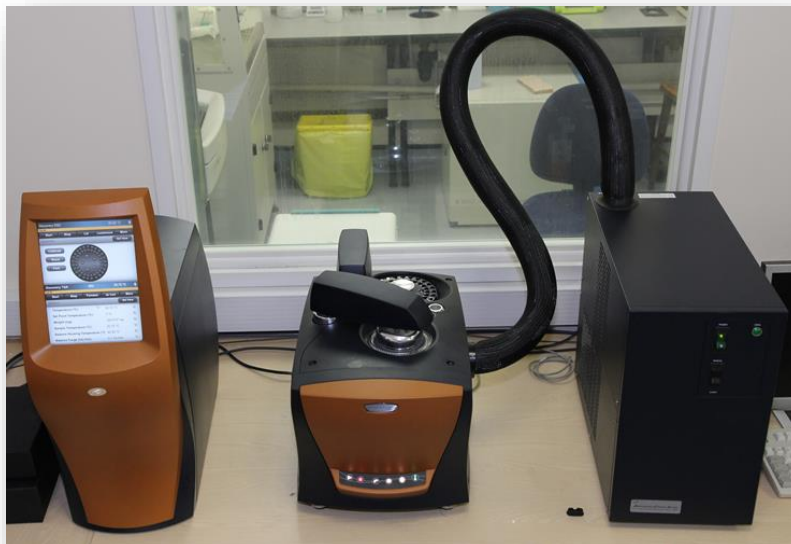


**Figure 3.4.1:** Photograph of the the Thermal Analysis DSC Q20.

As can be seen in the heat flow curve Figure 3.4.2a, a small amount of waxes precipitates at the WAT, then at the beginning stage of cooling, the heat flow was kept almost constant to form a baseline. At point A, the heat flow started to deviate from the baseline because of wax precipitation. The latent heat released in wax precipitation (change of phase from liquid to solid) began to increase, so did the heat flow needed in the cooling. The temperature at point A, was determined as (WAT). The wax precipitation amount was zero from 80°C to WAT. Below WAT, the heat flow increased rapidly until it reached a peak (point B), after this point, the heat flow declined to point C at -20°C. Taking the temperature drop  $\Delta T$  as an integrating unit, the area between the heat flow curve ABC and the extended baseline was integrated to calculate the total heat capacity of wax crystallization divided by the average crystal enthalpy of wax  $\Delta H$ , here taken as 210 J/g (HY. et al., 2003). The total percentage of wax content (X) within dt; [WAT or WPT - (-20°C)] was obtained as shown in the following equation:

$$X \text{ (Wax) \%} = \frac{\int_{-20}^{\text{WPT}} [(q_t - q_0)/c] dt}{\Delta H} \times 100 \% \quad (3.1)$$

Where  $q_0$  is the heat flow of the baseline in  $\text{W g}^{-1}$ ,  $q_t$  is the measured heat flow at a specific temperature in  $\text{W g}^{-1}$ , and  $c$  is the cooling rate in  $^{\circ}\text{C min}^{-1}$ .

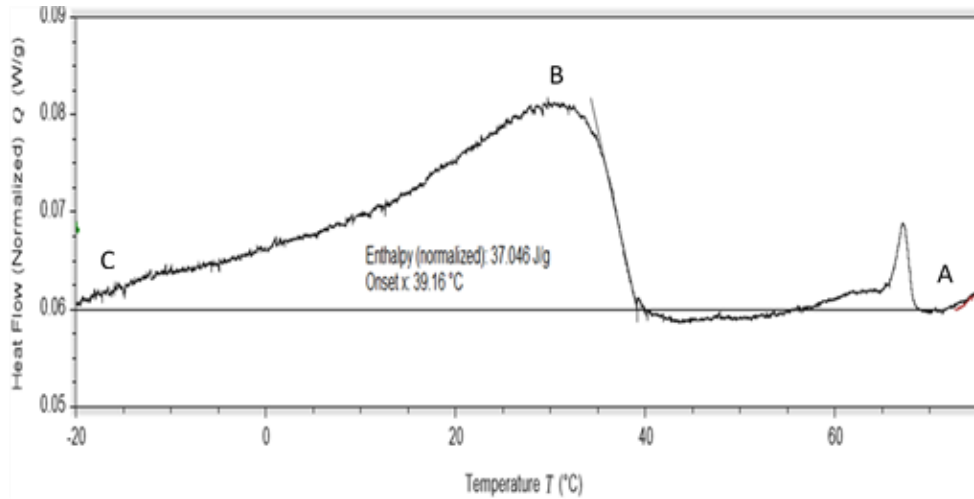


**Figure 3.4.2a:** Typical DSC heat curves measured for Abu-attifel untreated crude oil at cooling rate of  $15^{\circ}\text{C/min}$ .

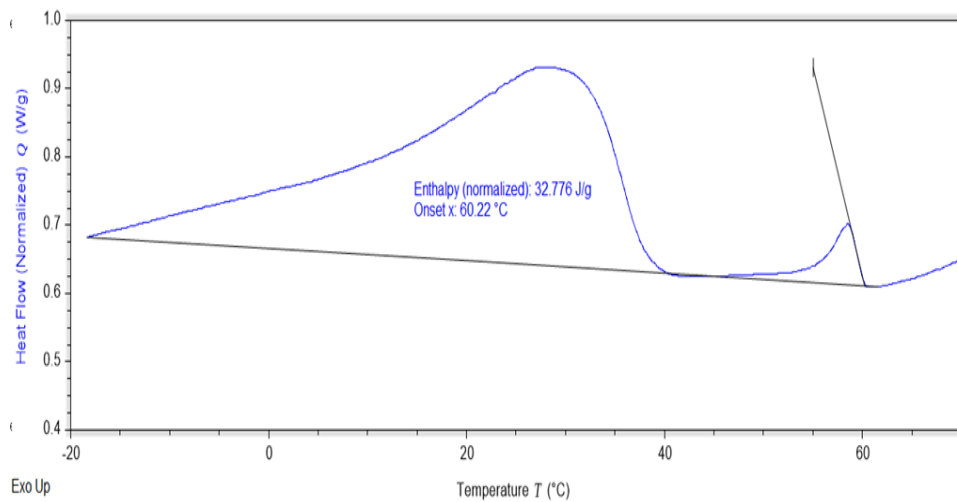


**Figure 3.4.2b:** Typical DSC heat curves measured for Abu-attifel crude oil .treated with ROA500 PPM at cooling rate of  $15^{\circ}\text{C/min}$ .



### 3.5 Wax composition determination

As for characterising the crude and blends compositions, gas chromatography was used. Here the Varian Gas Chromatograph (CP3800) with a flame ionization detector was used (Figure 3.5.1)



**Figure 3.5.1:** Varian Gas Chromatograph (CP3800).

The chromatograph capillary column was type CP-5, 30 m long, 0.32 mm internal diameter and 0.25  $\mu\text{m}$  film thickness. First the sample was dissolved in carbon disulphide ( $\text{CS}_2$ ), then a sample of this solution injected in the column using an auto-sampler at a rate 1.2 ml/min, with the column injector and detector temperatures set at 250°C and 300°C, respectively. The analysis was performed under a helium atmosphere with the temperature of the injected sample increased at 12°C/min and held for 5 min to insure all the sample is analysed at the highest temperature. Such method identifies and quantifies the distribution of n-alkanes.

### 3.6 Microscopy

The probing of the waxy oil as the wax precipitates and crystallises provide valuable information of the structure formed, the size of the crystals and their numbers. Also, when the wax inhibitors are added, changes in the integrity of the wax network will be detected. Remember that the wax inhibitors action is to prevent the crystals formed from interconnecting into compact, strong gels. Here the samples tested were viewed as they cooled at a set cooling rate from their conditioned temperature of 75°C using a Cross Polarised Microscope (Axioskop 40 CPM, Zeiss Co, Germany) as shown in Figure 3.6.1.

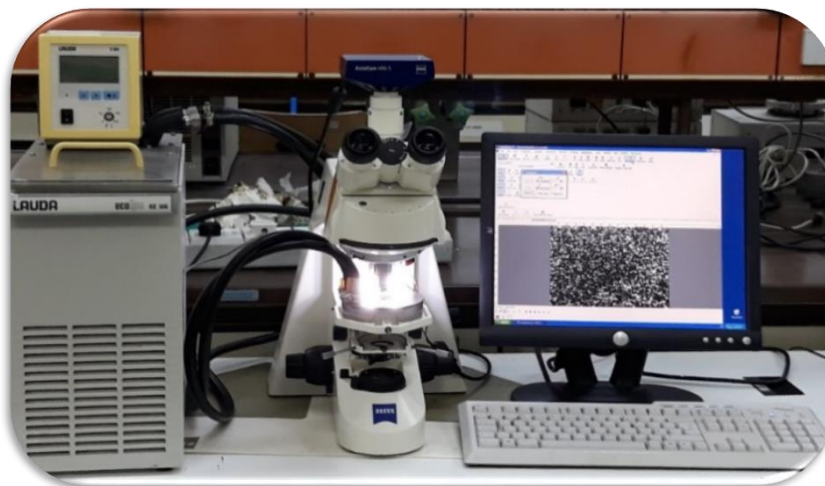


**Figure 3.6.1:** Axioskop 40 Cross-Polarised Microscope.

The associated instruments of the microscope unit were as follows:

- i. A hot stage microscope connected to a heating-cooling unit that can operate in the 10-200°C temperature range accurate to  $\pm 0.1^\circ\text{C}$  and capable of delivering heating-cooling rate in the range 0.01-10°C/min.
- ii. Reflected light source to identify crystals and co-crystals.
- iii. A high-resolution camera, 12-bit, single chip charge coupled device (CCD) with primary colour filtration (Axio-cam, MRC 5 Zeiss, Tv2/3" c, 0.63x, 1069-414) to obtain pictures series of the gel structures as they develop at high resolution (1.45 million pixels) using the associated computer software AxioVision.
- iv. Image analysis of the structures with AxioVision software giving measured values of lengths, areas and angles and object parameters such as size, circumference, and numbers.

For the measurements, the samples were first maintained at their 75°C conditioning temperature for 30 min then loaded on the thermal cell of the microscope and the set cooling rate imposed. Images of the gel structures as they formed were then collected and processed by image analysis as described above. Typical photographs of structures viewed are shown in Figure 3.6 with the crystals in white against a black background. Interestingly as already see in the comparative Figure 3.6.2 the hindering effect on crystal network formation when a wax inhibitor is used (further details in the Results chapter).

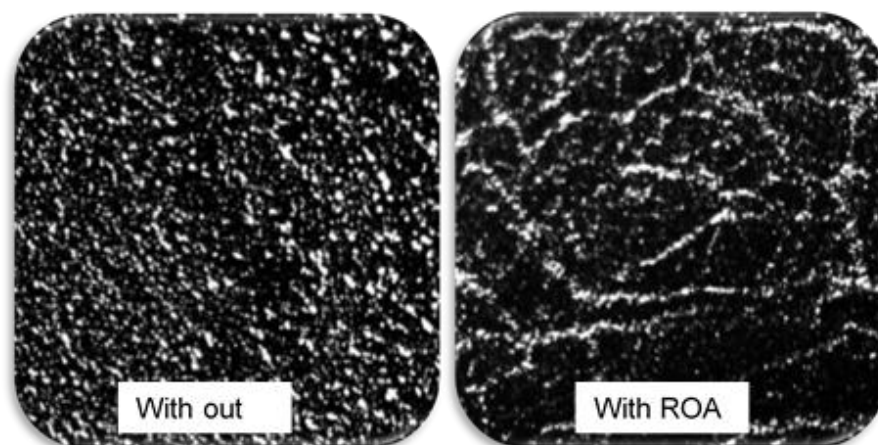


**Figure 3.6.2:** Abu-attifel crude oil gel structure without and with a wax inhibitor ROA (1000 ppm, 22°C).

### 3.7 Rheometry

As explained in the introduction, the aim of the research is to alter the rheology of the waxy crude oil when wax inhibitors are added so as to reduce their tendency to gel thus facilitating their pumping, particularly restart after cooling during shutdown. The rheological work must thus be comprehensive, comparing the crude oil with and without the wax inhibitors. As, waxy crude oils are elasto-plasto-viscous, they will exhibit complex deformation, shearing elastically first, then creeping, fracturing and finally flowing. Such deformation occurs over a small range of shear stresses. The objective of the rheological experiments is to measure such deformation in order to be able to predict flow. An appropriate rheometer and rheometric techniques that can capture precisely such deformation are thus essential. Here, two rheometers were used, the Anton Paar SVM 3000 and the Bohlin CVO 100 (Malvern).

#### 3.7.1 Anton Paar SVM 3000

The SVM 3000 is a rotational viscometer in which a tube is filled with sample which rotates at a constant speed. In this tube floats a measuring rotor (Figure 3.7.1).

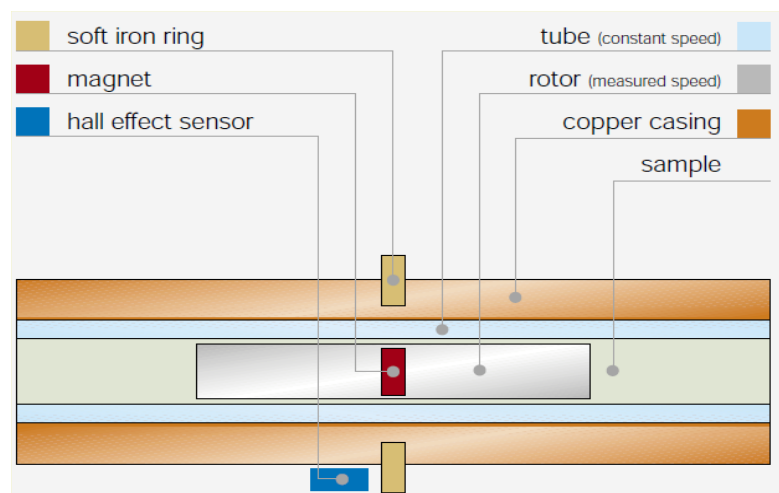


**Figure 3.7.1:** Principle of SVM 3000 rotational viscometer.

The result is a rotational viscometer which eliminates the influence of bearing friction and provide a very precise measure of viscosity. It is however incapable of measuring the elasto-plasto characteristics of the crude oil below the wax appearance temperature. A useful feature of the SVM 3000 is it has an integrated microbalance enabling also the measurement of the density of the crude oil. This viscometer was used to obtain the viscosity and the density of all conditioned samples above the wax appearance temperature at 40°C and 80°C.

### 3.7.2 Bohlin CVO 100

This rheometer (see Figure 3.7.2) is well suited for the task in hand which is the measurement of the deformation-flow properties of elasto-plasto viscous gels as it can operate in controlled stress and oscillatory shear modes with temperatures, cooling rates and stress loading rates controlled to a very good accuracy (see Table 3.7.1). It has a Peltier unit that controls the temperature to an accuracy within  $\pm 0.5^\circ\text{C}$  at programmable cooling rate in the range  $0.01^\circ\text{C}/\text{min}$  to  $5^\circ\text{C}/\text{min}$ . It accommodates a range of shear geometries (concentric cylinders, cone and plate and plate and plate). In this work, plate-plate (25mm/25mm and 50mm/50mm diameter) and cone-plate (25mm diameter and  $1^\circ$  cone angle). Upon calibration, it was found that errors in the viscosities measured with all geometries were less than 1%.



**Figure 3.7.2:** The Bohlin CVO 100 (Malvern).

**Table 3.7.1:** Specifications of the Bohlin CVO100 (Operating manual).

<b>Torque range</b>	0.5 $\mu$ Nm to 100mNm .
<b>Torque resolution</b>	1 nano Nm
<b>Position resolution</b>	0.9 micro radians
<b>Frequency range</b>	10 micro Hz to 100Hz
<b>Controlled speed range (CR mode)</b>	50 milli rad/sec to 320 rad/sec
<b>Measurable speed range (CS mode)</b>	0.1 micro rad/sec to 320 rad/sec
<b>Normal force NI measurement range*</b>	0.001 to 20N (50N option)
<b>Temperature range (dependent on controller)</b>	-150°C to 550°C
<b>Nominal operating voltage</b>	110 or 220V
<b>Size (with Peltier plate)</b>	52cm (H) x 29cm (W) x 34cm (D)
<b>Weight (with Peltier plate)</b>	27kg

\*Normal force option available

In the actual experiments, 0.5ml of the hot (75°C) conditioned samples were extracted from their sealed bottle and placed on the plate rheometer, the temperature of which had been set to (75°C) and then left for 2 minutes to ensure conditioning. A cooling rate was then programmed bringing the

temperature down to a test temperature for a set cooling rate and left for 5 minutes. The rheology was then measured at different temperatures (45, 40, 35, 30 °C) and cooling rates (0.5 and 1°C/min), using in all cases fresh conditioned samples, in constant stress mode or oscillatory mode as described below. Such tests are defined as quiescent cooling tests and intended to mimic conditions in the field where the pipeline was accidentally shut, i.e. not pumping. The same procedure was repeated but with cooling whilst the sample was sheared at 1 s<sup>-1</sup> for 1min. Such tests are defined as dynamic cooling tests and intend to mimic conditions in the field where the pipeline cooled whilst still operational, i.e. pumping but at very low throughput.

### 3.7.2.1 Controlled stress measurements:

In this hysteresis loop method, the stress is increased gradually from 0 Pa to a large stress where the crude oil is completely destroyed a fully flowing and back to 0 Pa, the stress increments tested being 25 and 100 Pa /min. Figure 3.7.3, shows a typical hysteresis loop measured.

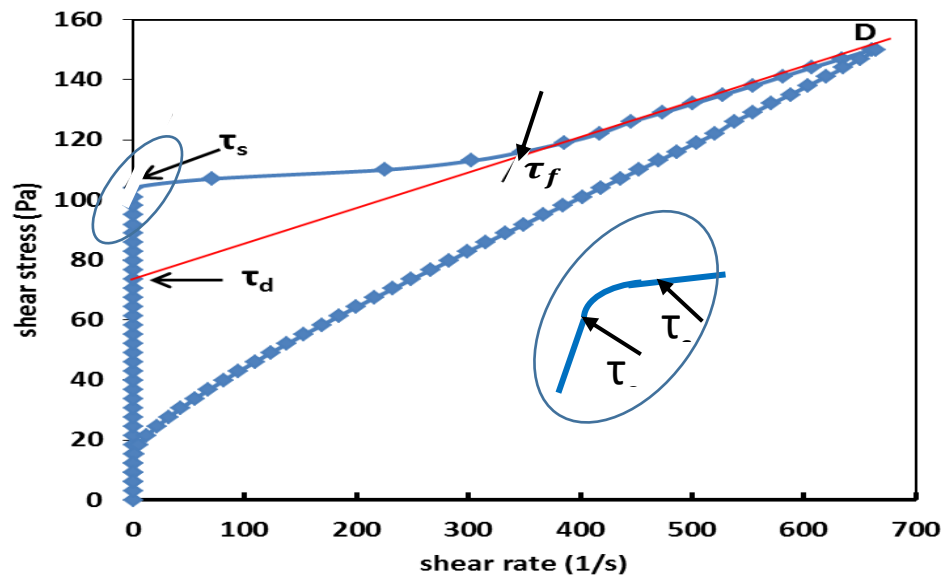


**Figure 3.7.3:** Typical controlled stress hysteresis loop of waxy crude oil.

In this Figure, the elastic-plastic-viscous deformation is seen to develop in stages, exhibiting initially an apparent elastic yield stress  $\tau_e$ . The wax then creeps before fracturing at a second “yield” stress,  $\tau_s$ , the static yield stress.

Above this stress, the fracture progresses rapidly until the gel structure is completely destroyed at a third “yield” stress,  $\tau_f$ , the fracture yield stress.

Above this stress the viscous regime commence, where now the wax crystals are dissociated in the solvent oils, the mixture now behaving as a colloids with an imaginary fourth yield stress,  $\tau_D$ , the dynamic yield stress, obtained by extrapolation of the viscous branch of the flow curve.

The objective of testing the behavior so described at various stress loading rate is to investigate the important effect of time which is very relevant to restart (the rate at which the pressure is increased from 0 to the optimal restart pressure as predicted from the relevant “yield stress” out of these four yield stresses- further details in Results Chapter 4). The conditions tested without and with the wax inhibitors are shown in Table 3.7.2.

**Table 3.7.2:** Controlled Stress & Oscillatory Stress measurements testing conditions.(Initial temperature 75°C, oscillatory frequency 0.5 Hz)

Parameters	Tested Temperatures °C	Static cooling rate, °C/min	Control Stress tests: Stress loading rate, Pa/min
Abu-attifel crude oil untreated	30, 35, 40 and 45	0.5 and 1	25 and 100
Abu-attifel crude oil + 500ppm ROA	30, 35, 40 and 45	0.5 and 1	25 and 100
Abu-attifel crude oil + 1000ppm ROA	30, 35, 40 and 45	0.5 and 1	25 and 100
Abu attifel+ 1000ppm PPD	30, 35, 40 and 45	0.5 and 1	25 and 100
Abu attifel+ 2000ppm PPD	30, 35, 40 and 45	0.5 and 1	25 and 100
Abu-attifel crude oil + Sirtica oil	30, 35, 40 and 45	0.5 and 1	25 and 100

The constant shear stress technique approach was also used to determine the gel point by carrying out measurements in a range of temperature from the conditioned state of 75°C to 35°C at a cooling rate of 0.5 °C/min and 1°C/min

with a small stress of 0.3 Pa (deemed to represent a threshold of gel strength) imposed during this cooling. The variation of shear rate thus was monitored as the temperature dropped gave the gel point when the shear rate became zero. Table 3.7.3 gives the range of conditions measured in this protocol. It is important not to confuse between the wax appearance temperature, the temperature when wax first precipitates and the gel point, the temperature when the precipitated wax formed a structure, a network of wax. Thus in these experiments, the tested temperature must be below the wax appearance temperature (39°C), found by repeat experiments to be actually below 39°C.

**Table 3.7.3:** Gel point determination using set Shear Stress (initial temperature 75°C, shear stress 0.3Pa).

Parameters	Tested Temperatures °C	Dynamic cooling rate, °C/min
Abu-attifel crude oil untreated	35	0.5,1
Abu-attifel crude oil + 500ppm ROA	35	0.5,1
Abu-attifel crude oil + 1000ppm ROA	35	0.5,1
Abu attifel+ 1000ppm PPD	35	0.5,1
Abu attifel+ 2000ppm PPD	35	0.5,1
Abu-attifel crude oil + Sirtica oil	35	0.5,1

### **3.7.2.2 Oscillatory measurements (dynamic amplitude sweep):**

These are aimed at obtaining the viscoelastic properties of the gels by applying a small amplitude oscillatory sinusoidal strain varying with time,  $t$  with a frequency  $\omega$  as:

$$\gamma = \gamma_0 \sin \omega t \quad (3.2)$$

The measured stress is given by equation (3.3):

$$\tau = \tau_0 \sin (\omega t + \delta) \quad (3.3)$$

This equation is expressed as:

$$\tau = G'(\omega) \sin \omega t + G''(\omega) \cos \omega t \quad (3.4)$$



$G'$  (the storage modulus) and  $G''$  (the loss modulus) are the parameters measured as a function of frequency. They express the relative contribution of the elastic ( $G'$ ) and viscous ( $G''$ ) components of the total modulus of such waxy crude oil. A typical response is presented in Figure 3.7.4 showing initially the deformation to be elastic ( $G' > G''$ ) and linear (constant  $G'$ ). The difference in  $G'$  and  $G''$  gradually diminishes with further deformation, becoming zero, then switching over in the viscous region where  $G' < G''$ . Table 3.7.2 given above list also the tests carried with the oscillatory method which is intended to cross-check against the controlled stress tests.

The above description of the oscillatory tests was for a given temperature. When a series of such tests are carried out over a range of temperatures, the gel point can be found at the cross over of the  $G'$  and  $G''$  curves as shown in Figure 3.7.5. Such data provided a complementary check of the gel point measured using the constant shear stress technique described above.

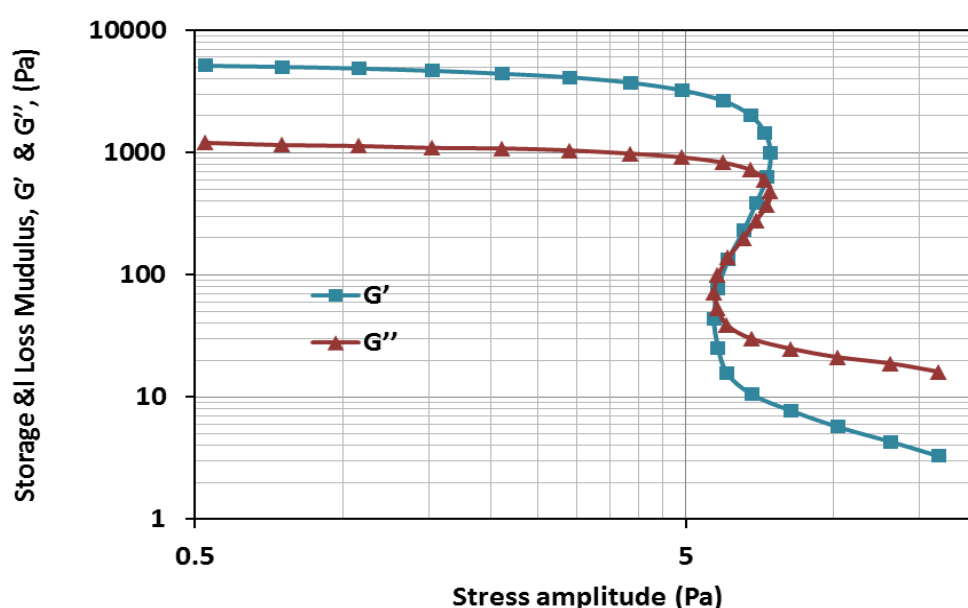


**Figure 3.7.4:** Typical Oscillatory  $G'$  and  $G''$  variation with amplitude.

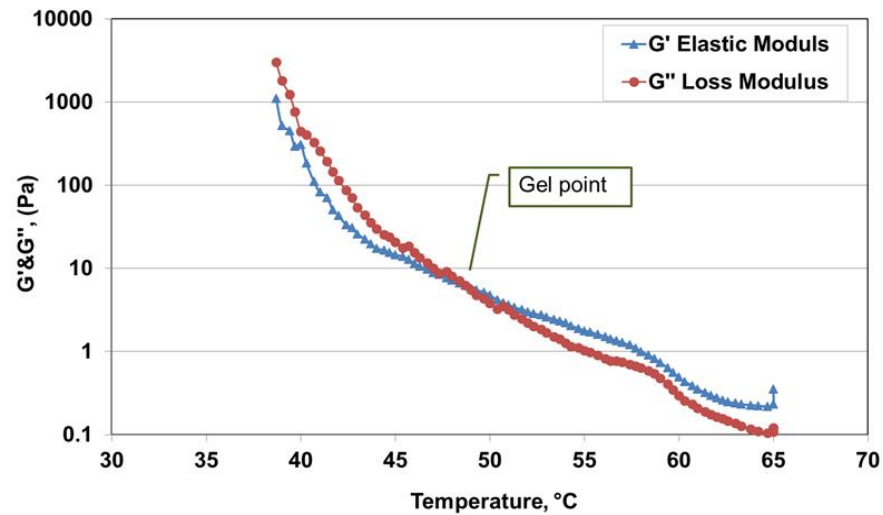


**Figure 3.7.5:** Gel point for Abu-attifel crude oil.

### **3.7.2.3 Control shear rate measurements:**

It is clear from the description of the deformation flow behaviour of Figure 3.7.3 given above that waxy crude oils above the wax temperature or above a certain stress will flow in a viscous manner. Thus to complete the characterisation, measurement in controlled shear rate mode were undertaken at temperature sweep from 85°C down to 30°C to cover wide range of temperature below and above the wax appearance temperature. This state was deemed to mimic the colloid regime just before gelation or after complete fracture where the wax particulates are just about suspended in the solvent oil. The conditions tested to describe this situation without and with the wax inhibitors are given in Table 3.7.4 below.

**Table 3.7.4:** Controlled Shear Rate measurements testing conditions.

Parameters	cooling rate, °C/min	Control rate, s <sup>-1</sup>
Abu-attifel crude oil untreated	0.5 and 1	1, 10, 50
Abu-attifel crude oil + 500ppm ROA	0.5 and 1	1, 10, 50
Abu-attifel crude oil + 1000ppm ROA	0.5 and 1	1, 10, 50
Abu-attifel crude oil + 1000ppm PPD	0.5 and 1	1, 10, 50
Abu-attifel crude oil + 2000ppm PPD	0.5 and 1	1, 10, 50
Abu-attifel crude oil + Sirtica oil	0.5 and 1 0.5 and 1	1, 10, 50

### 3.7.3 Pour Point determination

The wax appearance temperature and the gel point are critical characteristics of waxy crude oils and the methods just described show how involved are the techniques used to determine them. A more practical characteristic that helps have confidence in these intricate properties is the pour point, a crude assessment of flow out of a heated jar of the oil tilted horizontally from its initial vertical position. A standard exists, ASTM D97– 06 (American Society), and this was followed, with temperature increased by 3°C until flow in the tilted jar is observed after 3s. The set-up used is shown in Figure 3.7.6.



**Figure 3.7.6:** Set-up for pour point measurement.

### 3.7.4 Measurement errors

Every experimental measurement carries a certain amount of uncertainty (error). The error in the DSC and CVO tests arise mainly from the limit in accuracy of the DSC and CVO instruments and actual errors during measurement. Although the DSC and CVO Rheometer used were state of the art with very good accuracy (see Table 3.7.1) care was taken to minimise the experimental errors using calibration samples (Indium for DSC and standard oils for CVO) and three repeat experiments (See Appendix H).

For the DSC measurements, important parameters such as heat flow and wax appearance measurement (WAT) were subjected to error analysis. Standard deviation ( $\sigma$ ), and % differences were calculated, according to equations 3.5-3.8. The data are tabulated and presented in Chapter 4 and Appendix F.

For the rheological measurements, important parameters such as shear rate and shear stress were subjected to error analysis. Standard deviation ( $\sigma$ ), and % differences were calculated according to equations 3.5-3.8.

For a number ( $n$ ) of measurements of the same variables are taken and the arithmetic mean or average can be calculated from the expression:

$$x_m = \frac{1}{n} \sum_{i=1}^n X_i \quad (3.5)$$

The deviation for  $d_i$  for each reading is defined by:

$$d_i = x_i - x_m \quad (3.6)$$

The standard deviation ( $\sigma$ ) can be estimated by equation:

$$(\sigma) = \sqrt{\frac{(x_1 - x_m)^2 + (x_2 - x_m)^2 + \dots + (x_n - x_m)^2}{n-1}} \quad (3.7)$$

Where  $x_1 \rightarrow x_n$  are  $n$  results and  $x_m$  is their mean

From the standard deviation, ( $\sigma$ ), the percentage difference can be estimated by dividing the standard deviation by the arithmetic mean.

$$\% \text{ percentage difference} = \frac{\text{Standard deviation}(\sigma)}{\text{arithmetic mean} (x_m)} \quad (3.8)$$

Statistical analysis of rheological measurement data were calculated, tabulated and graphically presented in Appendix B0.

## CHAPTER 4: RESULTS AND DISCUSSION

### 4.1 Introduction

In this chapter, the results of the research are presented in the perspective of the aim and objectives as set in the introduction. With the pumping of waxy crude oils such as the one considered here (Abu-attifel crude oil), three aspects are of great importance in practice when diluting such a waxy oil with a light oil (Sirtica) or dosing with pour point depressants (PPD) or wax inhibitors (WI) chemicals:

- 1) Reducing pumping pressure under normal conditions, i.e. does the diluting or dosing decrease the apparent viscosity, hence the pressure? Under normal operating condition of in excess of 100,000 barrels per day being pumped in the typical 30inch diameter pipeline, this is equivalent to a nominal shear rate of  $\dot{\gamma} = \frac{8V}{D} \cong 30 \text{ s}^{-1}$  (Hagen-poiseuille formula) Thus, investigating the effects at higher shear rates ( $10 \text{ s}^{-1}$  and  $50 \text{ s}^{-1}$ , chosen here as a good range for normal pumping) is important to assess the pumping benefits, offsetting the cost of these additives.
- 2) Preventing the formation of large “quasi-yield stress”, when sudden shut down occurs of both power and heating, the scenario dreaded in the industry but which is common in spite of strict control measures. In such a situation, the previously moving crude oil decelerates to very low shear rates, typically of  $\dot{\gamma} = 1 \text{ s}^{-1}$ , cooling in the process as a result of environmental cooling, typically in the Libyan desert of order 0.5 to 1°C/min. Under this condition, does dilution with the light crude oil or dosing with the PPD and WI helpful in preventing the rapid build-up of “quasi-yield stresses”. Here the label “quasi” is used as strictly these stresses are yield stresses which by definition are stresses to commence flow. There is flow in this condition but it is very small tending towards zero eventually. This scenario will be referred to as “dynamic cooling”,

the label dynamic meaning there is flow albeit a small one ( $\dot{\gamma} = 1 \text{ s}^{-1}$ ).

- 3) Preventing the formation of large yield stresses once the flow ceases leaving the waxy crude oil to gel under the influence of environmental cooling, typically in the Libyan desert of order 0.5 to 1°C/min as stated above. This scenario will be referred to as “static cooling”.

Thus, the results of the research are split into these 3 categories in order to understand the efficacy of light crude oil dilution and PPD/WI dosing. Clearly, these results are rheological data but in addition, microscopic observations of the structures formed, particularly during gelling, will be presented in an effort to underpin rheological data. Remember that dilution with a light oil, effectively reduced the wax concentration, dosing with PPD in principle delays gelling to lower temperatures and dosing with WI hinder the formation of wax network. Evidence of these effects will be seen in the microscopic observations?

Prior to the presentation of these rheological and microscopic observations, the chapter opens with a presentation of the full characterization of Abu-attifel crude oil, Sirtica, the PPD and the WI obtained through chromatography and differential scanning calorimetry as explained in the experimental chapter.

## **4.2 The characteristics of untreated and treated Abu-attifel crude oil**

### **4.2.1 Chromatography Analysis**

The purpose here, is to establish the presence and extent of paraffin wax in Abu-attifel crude oil and assess the effect of dilution with the light crude oil Sirtica and dosing with the PPD and WI. Figure 4.2.1 shows the carbon number distribution of Abu-attifel crude oil determined using high temperature gas chromatography (HTGC). A significant quantities of n (normal)-paraffin wax as expressed in the carbon number in the range C20-C36 is observed. These are the wax that crystallise into relatively large crystals (macro-crystalline wax) compared with the higher hydrocarbons branched paraffins which are micro-crystalline (see Figure 4.2.2). A closer computation of Figure 4.2.1 gives the C20-C36 range to

be 55.50 wt.%. Further analysis using high pressure liquid chromatography (HPLC) showed the composition as given in Table 4.2.1. With HPLC, the analysis is done with a liquid carrier so it enables to determine those components that are not stable at the high temperature gas phase chromatography and classify them as saturates, resins, aromatics and asphaltenes. This characterization is helpful particularly in relation to evaluating the importance of asphaltene when PPD and WI are added. As will be discussed later, asphaltenes function as PPD

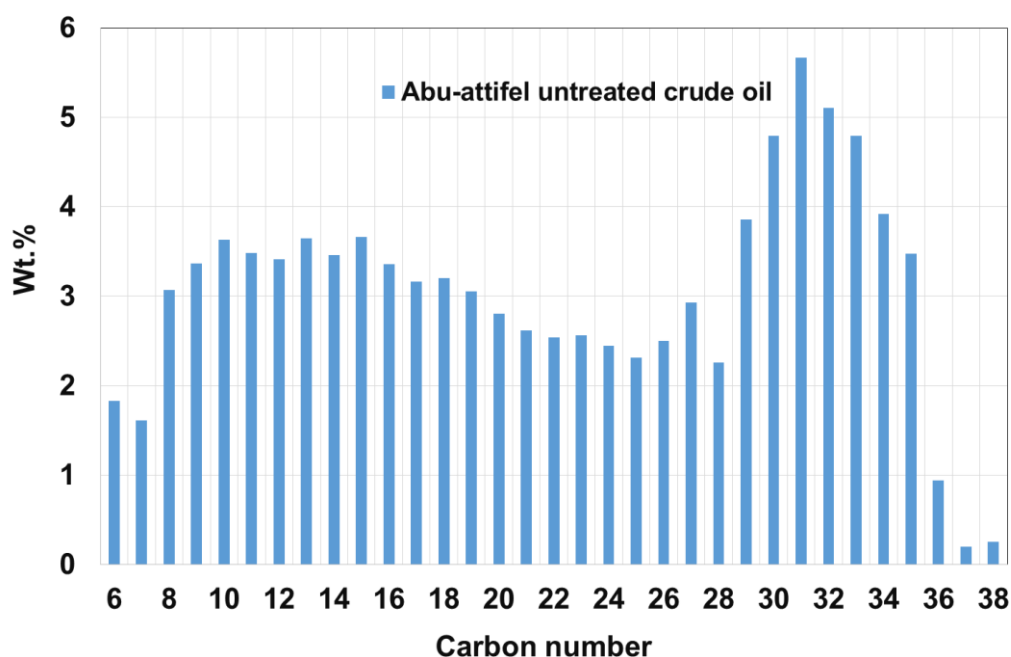


**Figure 4.2.1:** Carbon number distribution of Abu-attifel crude oil obtained with GC.

Providing nucleating sites for many more crystals, i.e. smaller crystals to form. Naturally neither HTGC nor HPLC measure the actual wax content which must be precipitated out and determine through phase transition methods, i.e. using differential calorimetry (DSC) as described later.



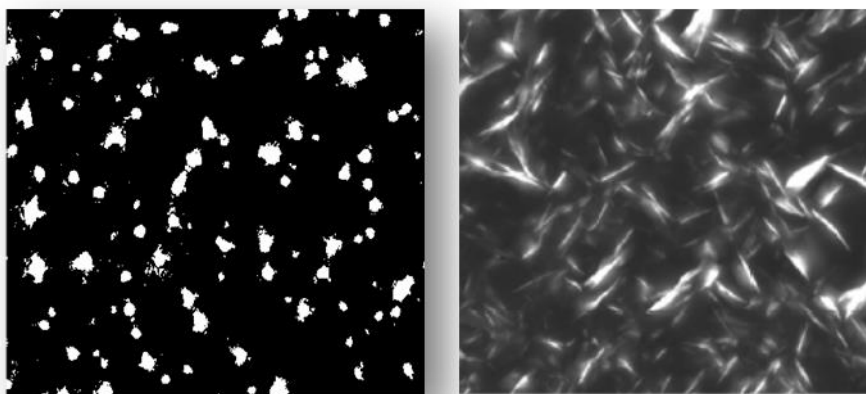


**Figure 4.2.2:** Macro and micro crystalline paraffins wax structures. (Lee et al., Energy & Fuels 2008).

**Table 4.2.1:** Result of fractionation of Abu-attifel crude oil in HPLC

Saturates (wt. %)	Resins (wt. %)	Aromatics (wt. %)	Asphaltenes (wt. %)
74.55	7.60	2.29	1.39

Turning now to the effects of dilution with the light crude oil Sirtica, as can be seen in Figure 4.2.3, the n- paraffin C20-C36 has now shifted to the left, the lower carbon number and reduced from the original 55.50 wt.% to 38.20 wt.%.

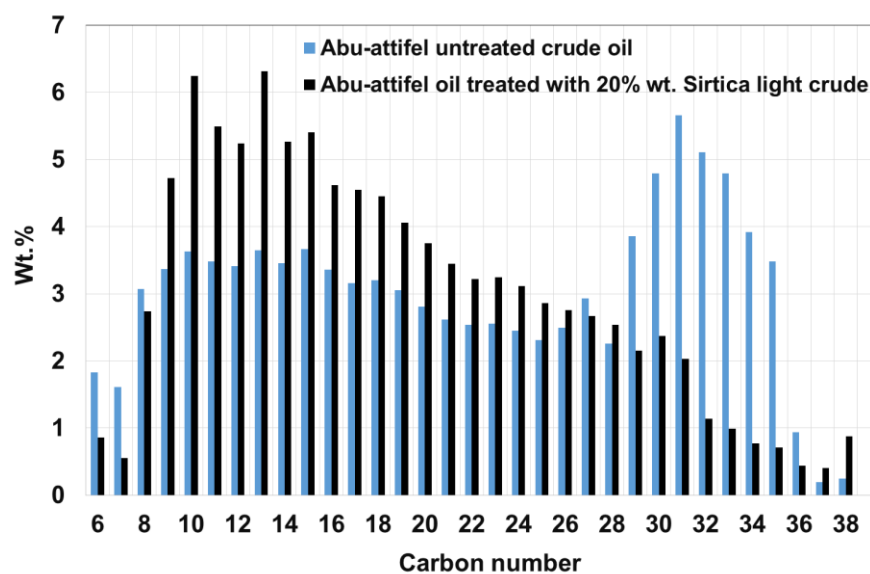


**Figure 4.2.3:** Carbon number distribution of Abu-attifel crude oil diluted with Sirtica.

A significant decrease of 17%. This dilution is to be expected on a simple mass balance as the light crude oil contains very little C20-C36. It infers a positive effect on rheology as a reduction in viscosity.

The effect of dosing with the PPD and WI on the carbon number distribution is now given as shown in Figures 4.2.4 and 4.2.5 showing too, a shifting towards lower C20-C36, particularly when the PPD and WI concentration are increased.

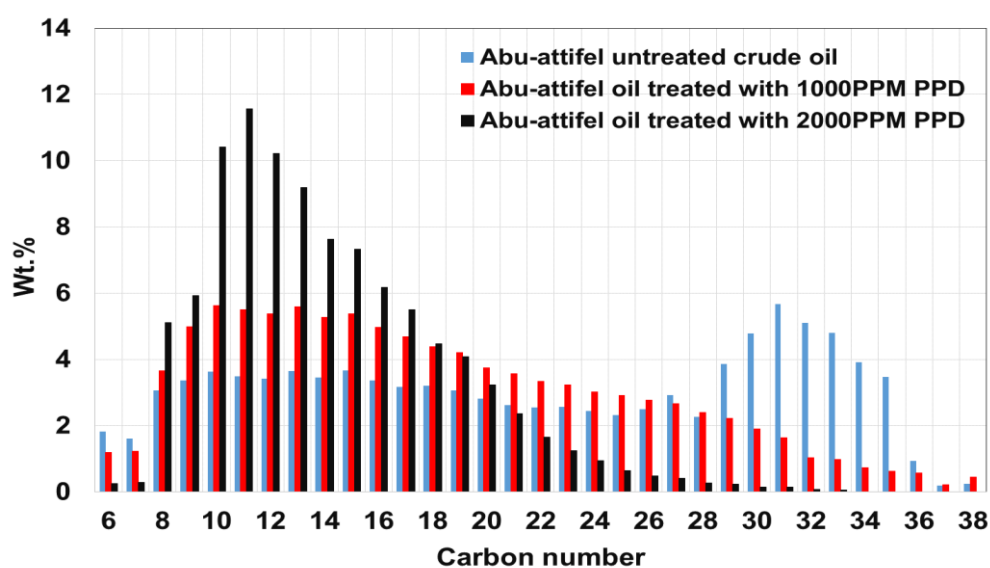


**Figure 4.2.4:** Carbon number distribution of Abu-attifel crude oil dosed with PPD.

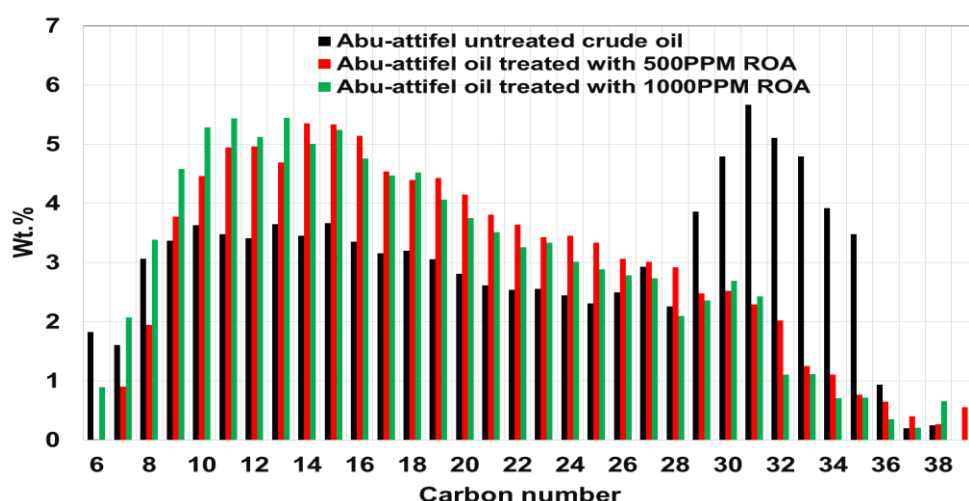


**Figure 4.2.5:** Carbon number distribution of Abu-attifel crude oil dosed with WI.

Thus already, the characterization with Sirtica, PPD and WI added is pointing towards positive effects on rheology. Further characterization results are now given measuring the actual amount of wax content and the wax appearance temperature (WAT).

#### 4.2.2 DSC Analysis

Here, essentially the temperature is lowered and the heat removed measured to pin point the onset of phase change, the wax appearance (precipitation) temperature (WAT). Accordingly, a trace as shown in Figure 4.2.6 is obtained from which the WAT is identified and the wax content (WC) calculated from a knowledge of the heat of crystallization of the pure wax. The WAT is determined from the intersection of the baseline of the trace and the tangent at the peak inflection point and the wax content by dividing the heat of crystallisation of pure wax by the heat measured for the phase change (area under the curve). Figure 4.2.6 however, shows two peaks, signifying that two species have precipitated, the first one, with the small peak, being the highest Mwt of paraffin which might be associated with the asphaltene and the second one, with the larger peak, being the rest of paraffin wax molecules. Thus, these two peaks are associated to the two corresponding WAT and wax precipitated or wax contents as shown on Table 4.2.2. Of course both WAT1 and WAT2 are of interest, since the first shows the temperature of first crystal to appear however, the second is a signed to the temperature at which crystallisation is commenced for the rest of wax molecules presented in the sample. As Table 4.2.2 shows, the dosing with the PPD and WI have lowered the WAT1 and have a minor or limited affect the WAT2 ( $<1^{\circ}\text{C}$ ), at the low cooling rate typical of the environmental conditions in Libya ( $0.5$  and  $1^{\circ}\text{C}/\text{min}$ ). It must be noted in relation to PPD, that the actual indicator of their efficacy is not their effect on WAT but on the pour point which is the lowest temperature at which the oil continues to *flow* which can only be measured rheologically as shall be shown later. On the basis of the DSC data at these low cooling rates, the first conclusion of this research is that DSC analyses alone cannot be used to evaluate the performance of PPD and WI.

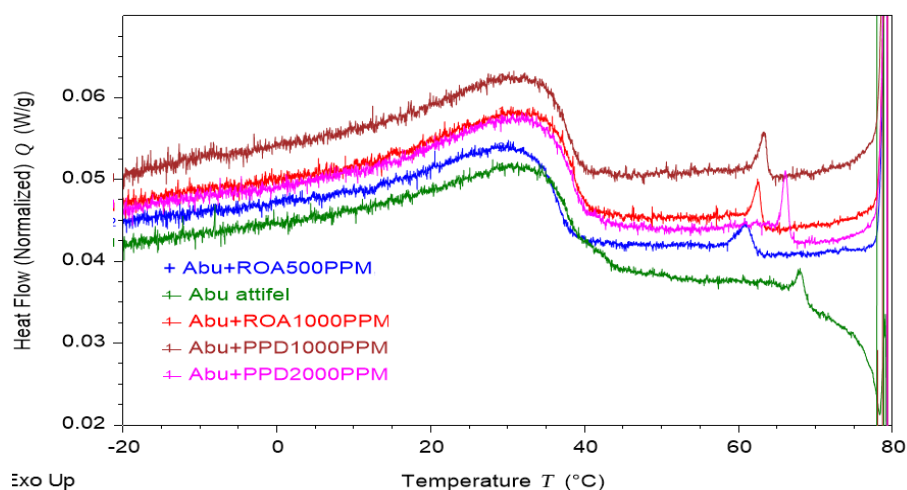


**Figure: 4.2.6:** DSC traces for treated and untreated Abu-attifel crude oil.

**Table 4.2.2:** Wax appearance temperature (WAT1 and WAT2) and wax content (WC2) of treated and untreated Abu-attifel crude oil at cooling rate of 1°C/min.

Oil	WAT1,°C	WAT2,°C	WC2, %wt.
<b>Abu-attifel untreated crude oil</b>	68.1	39.2	27-29
<b>Abu-attifel +2000 PPM PPD</b>	65.7	39.3	
<b>Abu-attifel +1000 PPM PPD</b>	63.3	39.7	
<b>Abu-attifel +1000 PPM ROA</b>	62.1	39.8	
<b>Abu-attifel +500 PPM ROA</b>	61.6	38.4	

In further attempts to find a trend between DSC data and performance of PPD and WI, experiments were carried out to assess the effect of cooling rate on WAT and wax content of these mixtures up to cooling rate of 15°C/min. Coutinho and Darindon (2005) have reported super-cooling to result with a nucleation lag in the sample and a decrease in WAT. The data are presented in Figure 4.2.7 a&b showing the variation of the two WAT with cooling rate.

Furthermore, statistical analysis for three measurement runs is carried for untreated Abu-attifel crude oil WAT which revealed only a 0.44% difference between the WAT2 measured readings at considered cooling rate (1, 5 and 15 °C/min) ,this difference is considered a minor and is considered as that cooling rate has no effect on WAT2. (see Appendix F3).

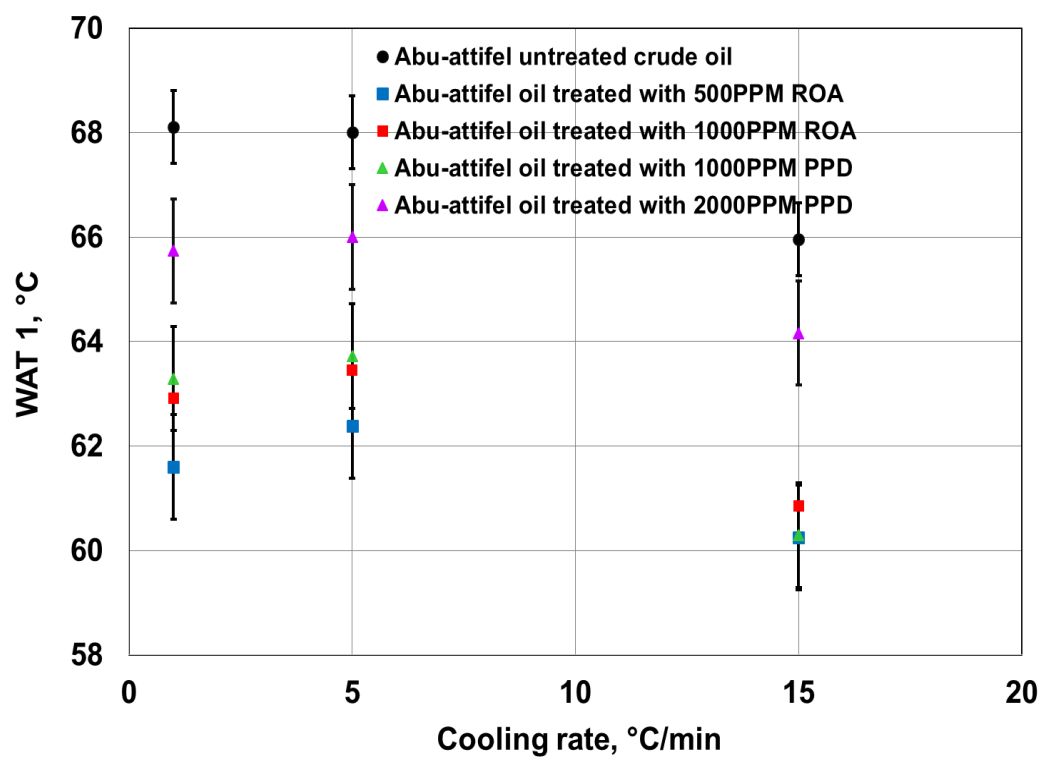


**Figure 4.2.7a:** Variation of WAT1 with cooling rates for treated and untreated Abu-attifel crude oil.

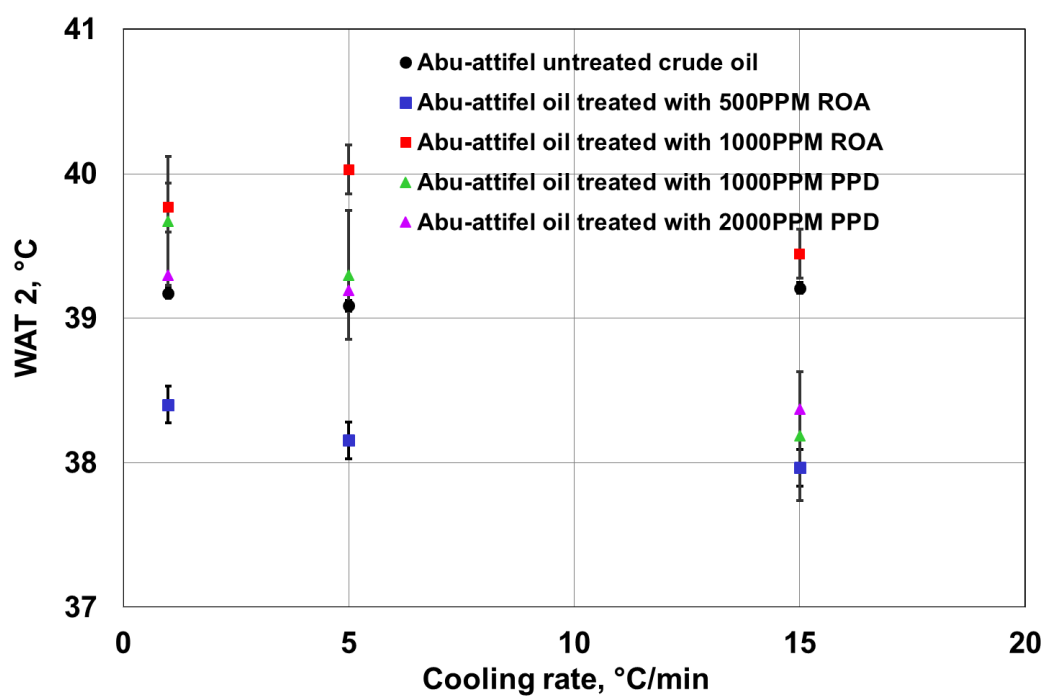


**Figure 4.2.7b:** Variation of WAT2 with cooling rates for treated and untreated Abu-attifel crude oil.

Although the variation is modest, the positive effect of the PPD and WI can be identified, particularly that of ROA500 which reduces WAT1 by 7 °C and WAT2 by nearly 2 °C. This result points to the possibility that the wax inhibitor ROA at dosage of 500 PPM could result in reduced gel strength, beneficial to lower restart pressure. This is only a tentative conclusion that will be verified later with rheological data. Appendix 1 gives all the data to help future research.

#### **4.3 Rheology of treated and untreated Abu-attifel crude oil cooled under normal operating conditions, i.e. at 10-50 s<sup>-1</sup>**

As explained earlier, these shear rate conditions are representative of normal pipeline pumping operations at the typical flow rates of 100,000 bbl per day) and larger in pipelines of 30 inches diameter, and equivalent to shear rates in the range 10-50 s<sup>-1</sup>. What is important here, is to assess the effect of dilution on the corresponding apparent viscosity with a lighter crude oil or the addition of a PPD or a WI when cooling occurs. This situation depicts the start of the problem leading to the pipeline shutting following loss of heating. Figure 4.3.2a-d present the data at 2 typical cooling rates (0.5 and 1°C) from the normal operating temperature of 80°C down to 40°C very near the WAT of the paraffin wax (39-40°C). The following effects can be observed.

##### **4.3.1 Presentation of data**

As seen from presented Figures 4.3.2a-4.3.2e viscosity of untreated Abu-attifel crude oil and treated crude has shown clear increase in viscosity as temperature were decrease from initial temperature at 85°C as temperature approached 60°C, this increase in viscosity can be explained by the wax network structure development which was continued with temperature decrease, however, the magnitude of viscosity were hindered when the crude were diluted or blended with chemicals as shown in the presented Figures.

- Abu-attifel untreated crude oil

Prior to treating Abu-attifel crude oil with (light crude dilution, dosing with PPD and WI chemical), crude rheological properties (Instantaneous Viscosity) were determined as a function of temperature, (during dynamic cooling) at shear rate of 10 s<sup>-1</sup> and

cooling rate of 1°C/min, in order to assess the effect of treatment, three runs were carried and percentage difference between runs were determined (see Appendix B0) data were graphically presented in Figure 4.3.1. As can be seen from tabulated and graphically presented data, average % difference between the measured viscosity of the three runs were below 11% at the temperature range of 85°C to 68°C, however as the temperature decreased from 68°C to 60.2°C at which the wax crystallisation progresses, the variation in the viscosity measurement become more pronounce and the average % difference between runs become greater reaching 23% and at temperature range of 60°C-40°C, the average difference between viscosity measurements reached 9%. Overall average in % difference between three measurements runs were 12% which is considered an indication of CVO Rheometer measurement accuracy for such non-Newtonian waxy crude as compared with difference of 1.5% using standard Newtonian oil (see Appendix B0).

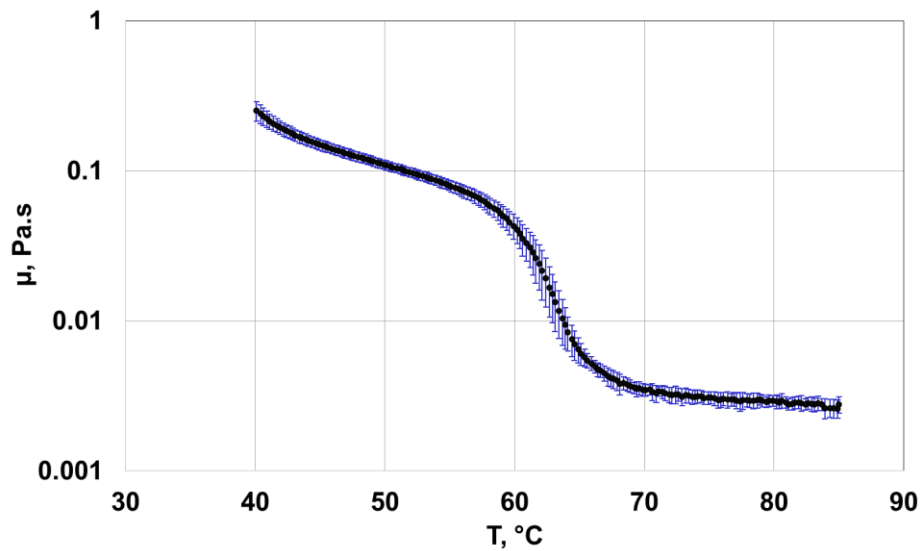


**Figure 4.3.1:** Variation of viscosity with temperatures for untreated Abu-attifel crude oil at 1°C/min.

- Dilution with Sirtica is most effective from 60°C and below as shown in Figure 4.3.2a, reducing the apparent viscosity at 40°C from 0.25 to 0.09 Pa.s, (64%) suggesting that normal pumping can be carried not only at the current 85°C but even at 40°C, hence, a huge saving in the heating cost can be accomplished.
- Dosing with wax inhibitor ROA at the low 500 PPM becomes beneficial starting at 60°C and below as shown in Figure 4.3.2b, reducing the apparent viscosity at 40°C from 0.22 to 0.11 Pa.s (50%) suggesting that like Sirtica dilution, dosing with this particular WI at 500 PPM is also effective at reducing pumping power by reducing crude oil apparent viscosity.

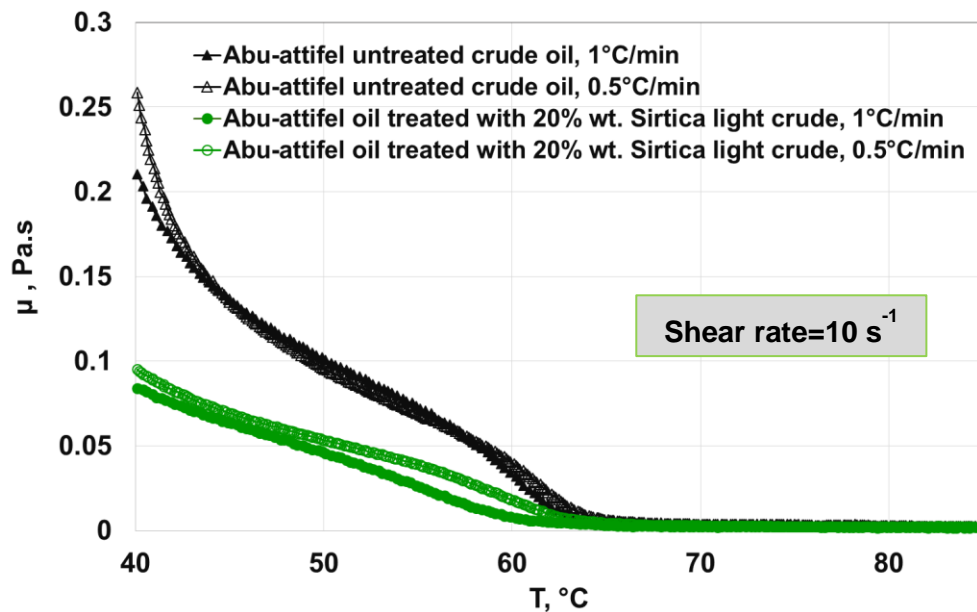


**Figure 4.3.2a:** Reduction in apparent viscosity after dilution with light crude oil Sirtica.



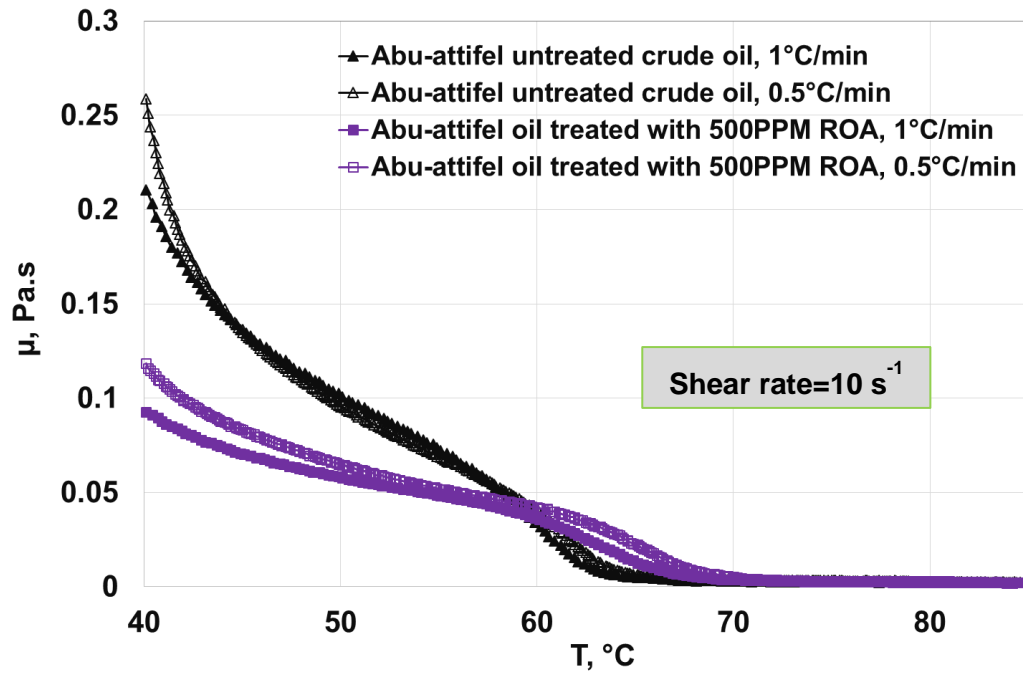


**Figure 4.3.2b:** Reduction in apparent viscosity after dosing with WI ROA at 500 PPM.

- Dosing with wax inhibitor ROA at 1000pm or twice the level added above does not lead as shown in Figure 4.3.2c to significant improvement compared with the 500 PPM level. Thus 500 PPM is an Optimum value of WI addition, helpful in that it reduces the cost by 50%.

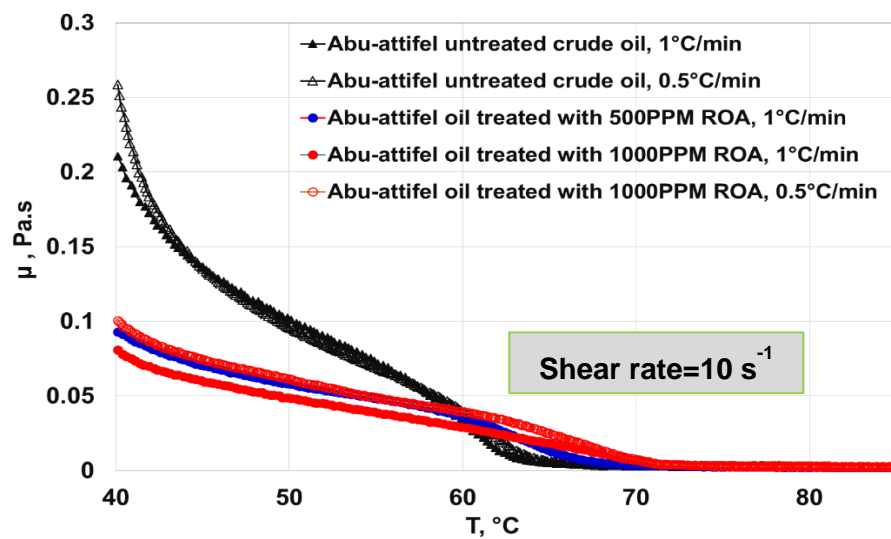


**Figure 4.3.2c:** Reduction in apparent viscosity after dosing with WI ROA at 1000 PPM.

- Dosing with pour point depressant PPD at 2000 PPM lead as shown in Figure 4.3.2d to a massive reduction in apparent viscosity from 0.28 to 0.05 Pa.s or 82% @40°C. Further cooling to 30°C shows the benefit to continue (Figure 4.3.2e and expanded scale Figure 4.3.2f) supporting the function of such additive as pour point depressants rather than wax inhibitors.

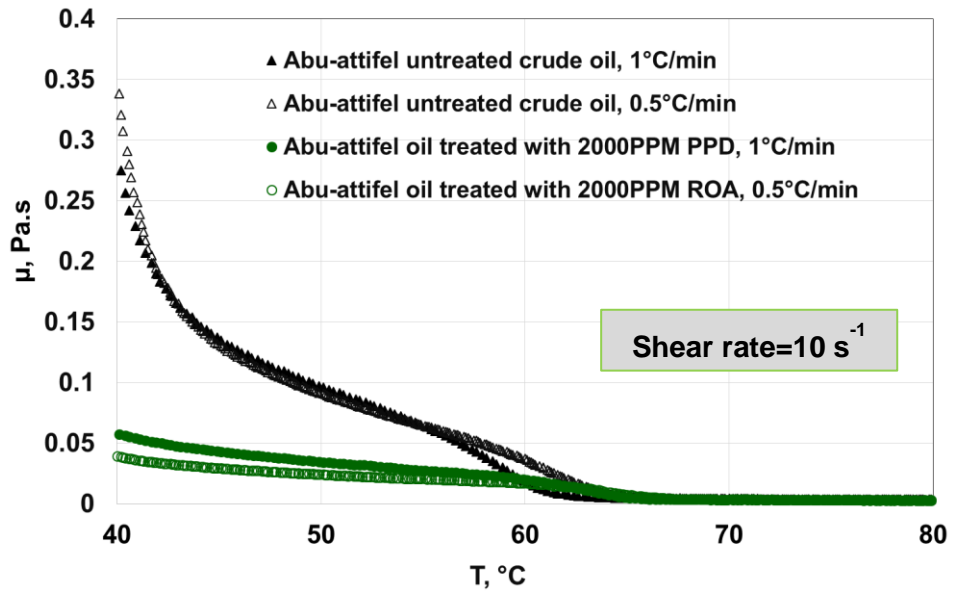


**Figure 4.3.2d:** Reduction in apparent viscosity upon dosing with PPD2000.

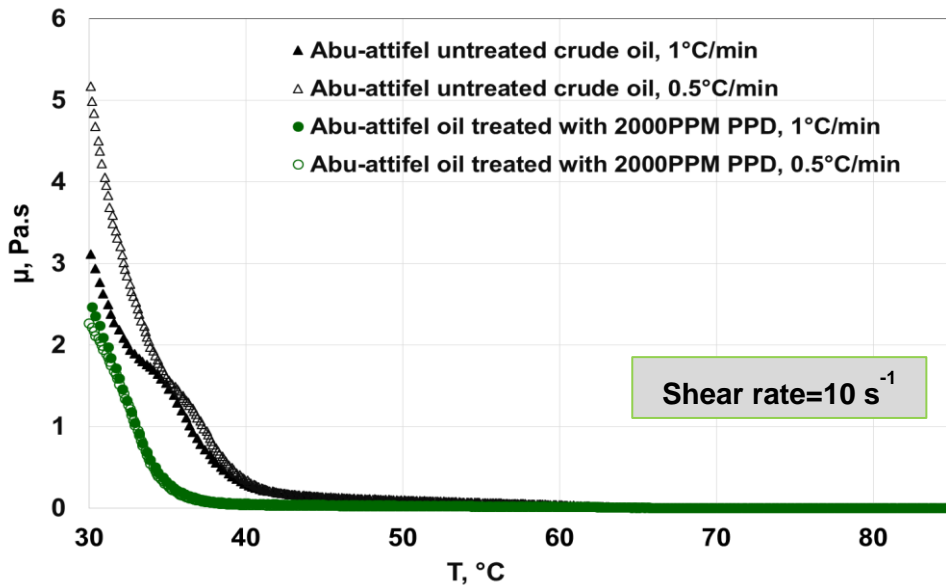


**Figure 4.3.2e:** Reduction in apparent viscosity upon dosing with PPD2000 down to 30°C.

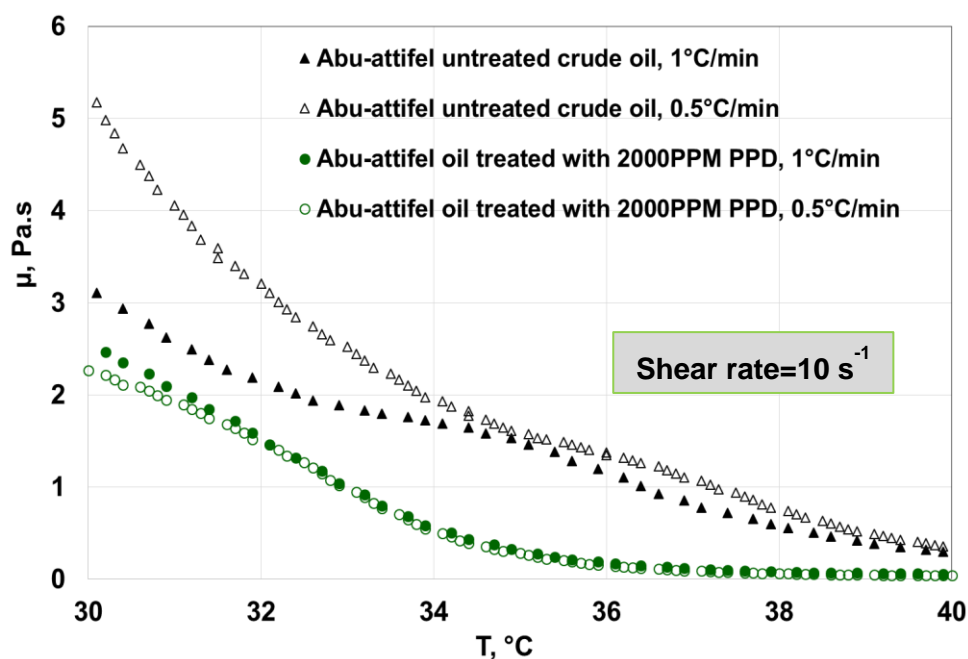


**Figure 4.3.2f:** Reduction in apparent viscosity upon dosing with PPD2000. (Expanded scale in 40-30°C region).

In order to ascertain the results observed above, the same experiments were carried, but with the measurement of apparent viscosity at a larger shear rate,  $50 \text{ s}^{-1}$  to assess if any shear thinning benefit results from operation at larger flow rates, here equivalent to time 5 increase as the above observations were at  $10 \text{ s}^{-1}$ . The observations are as follows:

- Dilution with Sirtica at the higher shear rate of  $50 \text{ s}^{-1}$  shows (Figure 4.3.2g) the same benefit as described earlier but with now the apparent viscosity reducing from  $0.083 \text{ Pa.s}$  (rather than  $0.25 \text{ Pa.s}$  @  $10 \text{ s}^{-1}$  because of shear thinning affect) down to  $0.037 \text{ Pa.s}$  (rather than  $0.09 \text{ Pa.s}$  @  $10 \text{ s}^{-1}$ ) or by 57% decrease. Thus the benefit of dilution with the light oil remains even when the flow rate is increased which is desirable.

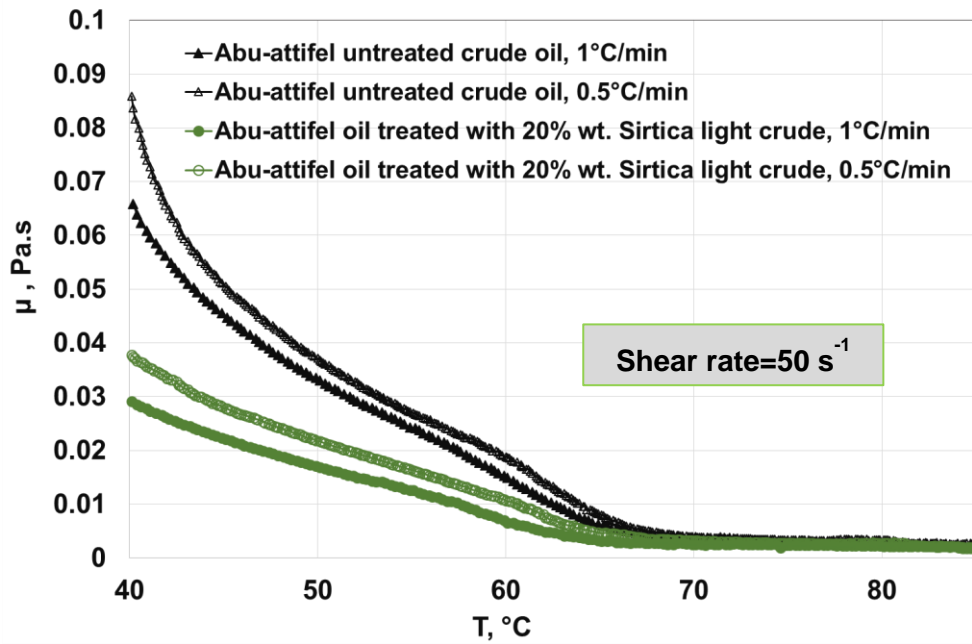


**Figure 4.3.2g:** Reduction in apparent viscosity after dilution with Sirtica light oil at the higher shear rate of  $50\text{s}^{-1}$ .

- Dosing with wax inhibitor ROA at the low 500 PPM at the higher shear rate of  $50\text{s}^{-1}$  shows (Figure 4.3.2h) the same benefit as described earlier but with now the apparent viscosity reducing from 0.083 Pa.s (rather than 0.25 Pa.s @  $10\text{s}^{-1}$  because of shear thinning) down to 0.038 Pa.s @  $50\text{s}^{-1}$  (rather than 0.11 Pa.s @  $10\text{s}^{-1}$ ) or by 54% decrease. Thus the benefit of dosing with WI remains when the flow rate is increased which is again desirable.

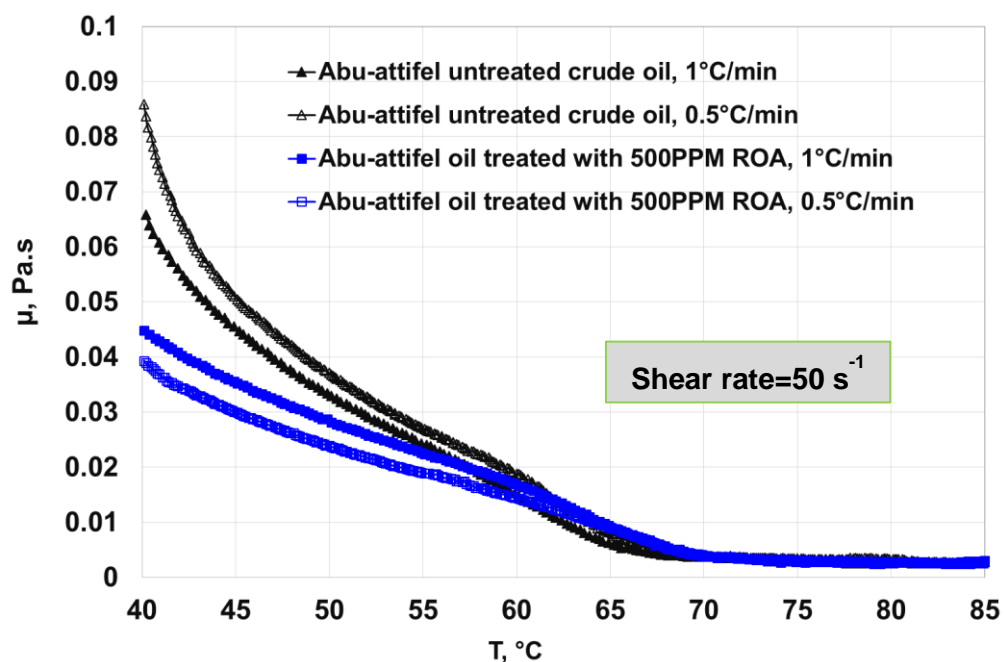


**Figure 4.3.2h:** Reduction in apparent viscosity after dosing with WI ROA at 500 PPM at the higher shear rate of  $50 \text{ s}^{-1}$ .

- Dosing with pour point depressant PPD at 2000 PPM at the higher shear rate of  $50 \text{ s}^{-1}$  shows (Figure 4.3.2i) the same benefit as described earlier but with now the apparent viscosity reducing from 0.083 Pa.s (rather than 0.25 Pa.s because of shear thinning) down to 0.015 Pa.s (rather than 0.11 Pa.s). Thus the benefit of dilution with the light oil remains when the flow rate is increased which is desirable. Performing the experiments below  $40^\circ\text{C}$  (see Figure 4.3.2j) shows again the particular the pour point depressing benefit of this particular type of additive.

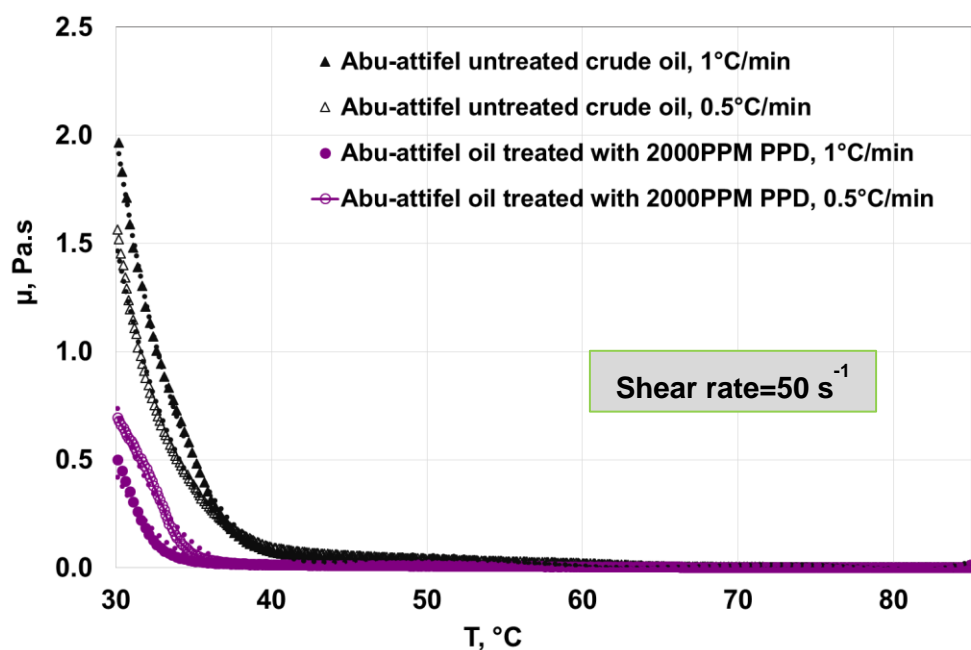


**Figure 4.3.2i:** Reduction in apparent viscosity upon dosing with 2000 PPM at the higher shear rate of  $50 \text{ s}^{-1}$ .

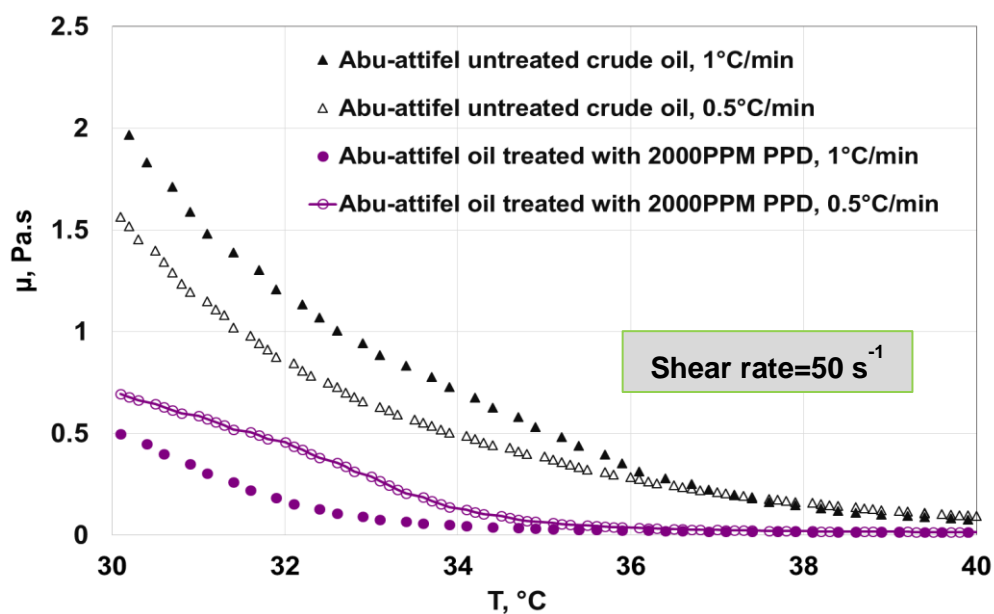


**Figure 4.3.2j:** Reduction in apparent viscosity upon dosing with 2000 PPM PPD at the higher shear rate of  $50 \text{ s}^{-1}$ . (Expanding scale in 40-30 °C range).

#### **4.3.2 Conclusion**

From the data presented, the important conclusion to be made is that dilution with a light oil or dosage with a wax inhibitor or a pour point depressant will be most beneficial to the pumping of waxy crude oils, here Abu-attifel crude oil taken as an example, as these reduce the apparent viscosity significantly, (50% and more) at temperature of close to the wax appearance temperature of the crude oil. In other words, substantial pumping power and heating savings can be made compared to the current operation at 75-80°C.

#### **4.4 Rheology of treated and untreated Abu-attifel crude oil cooling under pipeline near shut down conditions, i.e. at very low shear rate here $1 \text{ s}^{-1}$**

The purpose of these experiments, as explained earlier was to replicate the condition leading to shutdown of the pipeline. Upon power failure, flow in the pipe will decelerate towards zero flow. This is the most critical condition as in the field efforts would be made to remedy the problem immediately and increase flow rate back again. These conditions are mimicked here rheologically by cooling down the oil from its normal operating temperature of 75-80°C down to 30°C that is below the critical point which is the paraffin wax appearance temperature here 39-40°C at cooling rate typical of the environment of Abu-attifel crude oil that is 0.5-1.0 °C/min. Thus, data at this  $1 \text{ s}^{-1}$  shear rate and cooling rates of 0.5-1.0 °C/min are presented for the crude oil with and without dilution with a light oil or dosing with the wax inhibitor ROA and the pour point depressant PPD.

#### 4.4.1 Presentation of data

- Dilution with Sirtica is no longer effective, albeit a small reduction in apparent viscosity can be seen at temperature 35-40 °C and below, as shown in Figure 4.4.1a.

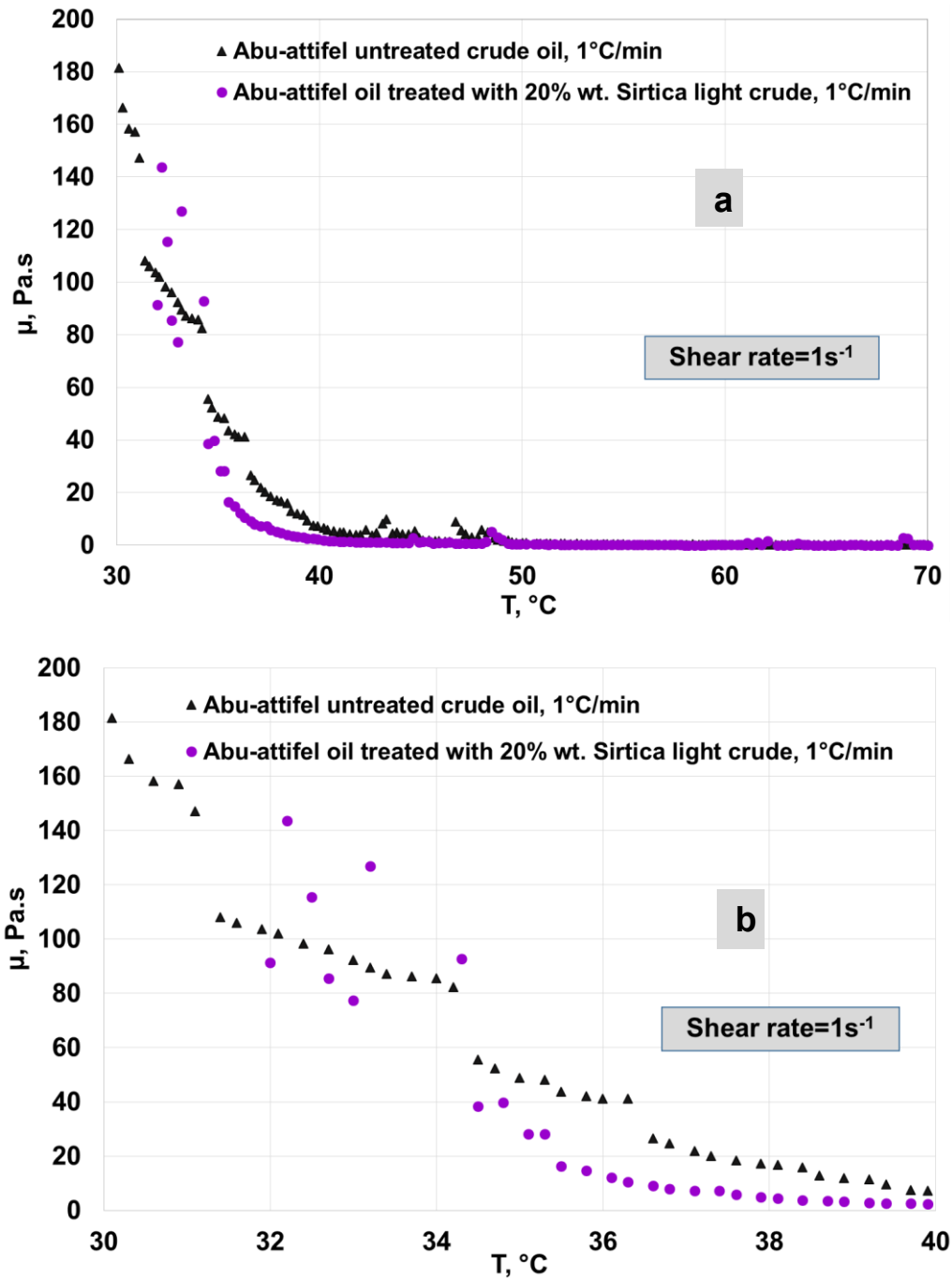


**Figure 4.4.1a:** Reduction in apparent viscosity upon dilution with Sirtica at the low shear rate of  $1 \text{ s}^{-1}$  and cooling rate of  $1^\circ\text{C}/\text{min}$  (a) 70-30 °C and (b) expanded scale in 40-30 °C range.



- Dosing with pour point depressant PPD at 1000 PPM as shown in Figure 4.4.1b remains effective in reducing the apparent viscosity, particularly below 40°C further emphasizing the unique function of pour point depressant which is the lower the wax precipitation temperature. As a measure of this benefit the apparent viscosity drops at 30°C from 181 to 73 Pa.s equivalent to 60% reduction suggesting much saving to be made in reduced heating and/or overcoming the problem towards the crude oil gelling just before shutdown.

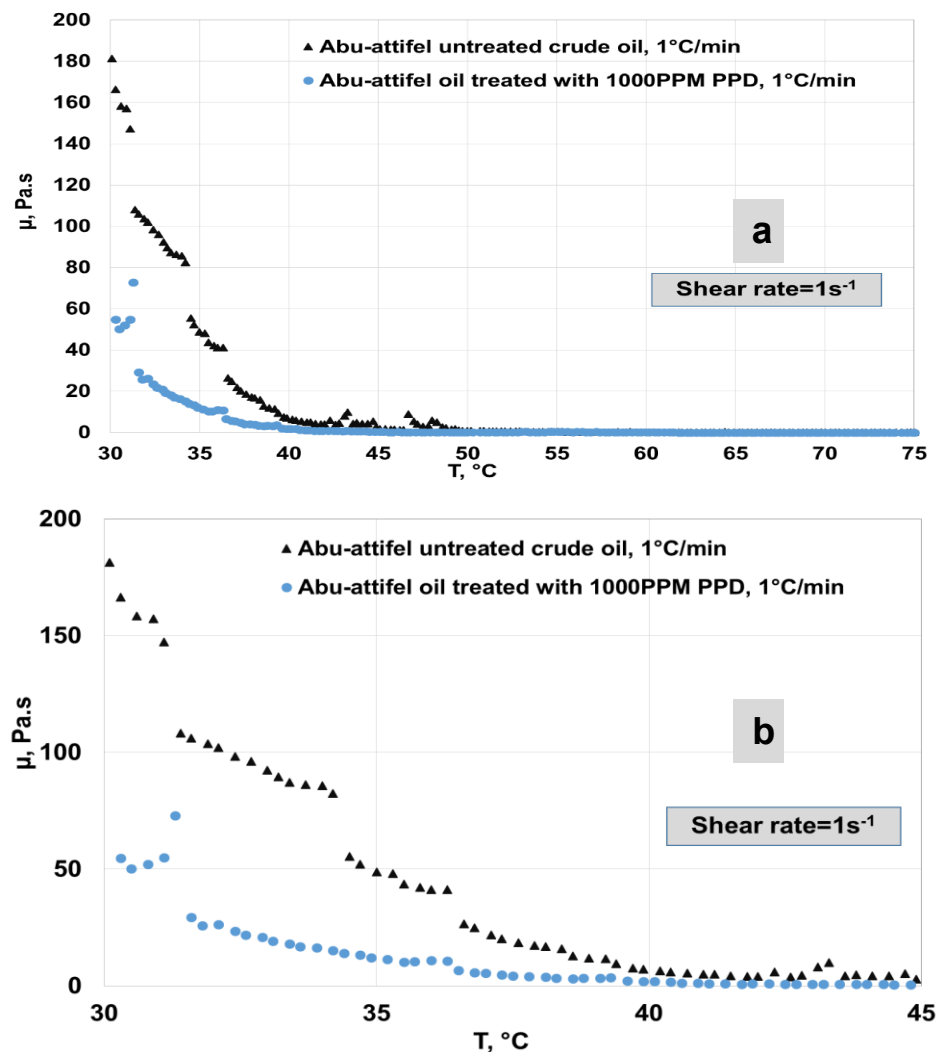


**Figure 4.4.1b:** Reduction in apparent viscosity upon dosing with PPD1000 PPM at the low shear rate of  $1 \text{ s}^{-1}$  and cooling rate of  $1^\circ\text{C}/\text{min}$  (a) 70-30 °C and (b) expanded scale in 45-30 °C range.

- Dosing with wax inhibitor ROA remains effective in reducing the apparent viscosity, particularly below 40°C further emphasizing the wax inhibition function of ROA, as shown in Figure 4.4.1c&d. Interestingly and observed earlier there is not much gain in increasing the dosage from 500 to 1000 PPM, important when the high cost of these additives is considered. As a measure of this benefit the apparent viscosity drops at 30°C from 181 to 74 Pa.s equivalent to 60% reduction suggesting much saving to be made in reduced heating and/or overcoming the problem towards the crude oil gelling just before shutdown. Also this shows than rather using PPD at the higher 1000 or 2000 PPM, consideration on a cost basis should made as the addition is only at 500 PPM. The evidence is shown in the comparative Figure 4.4.1e&f.

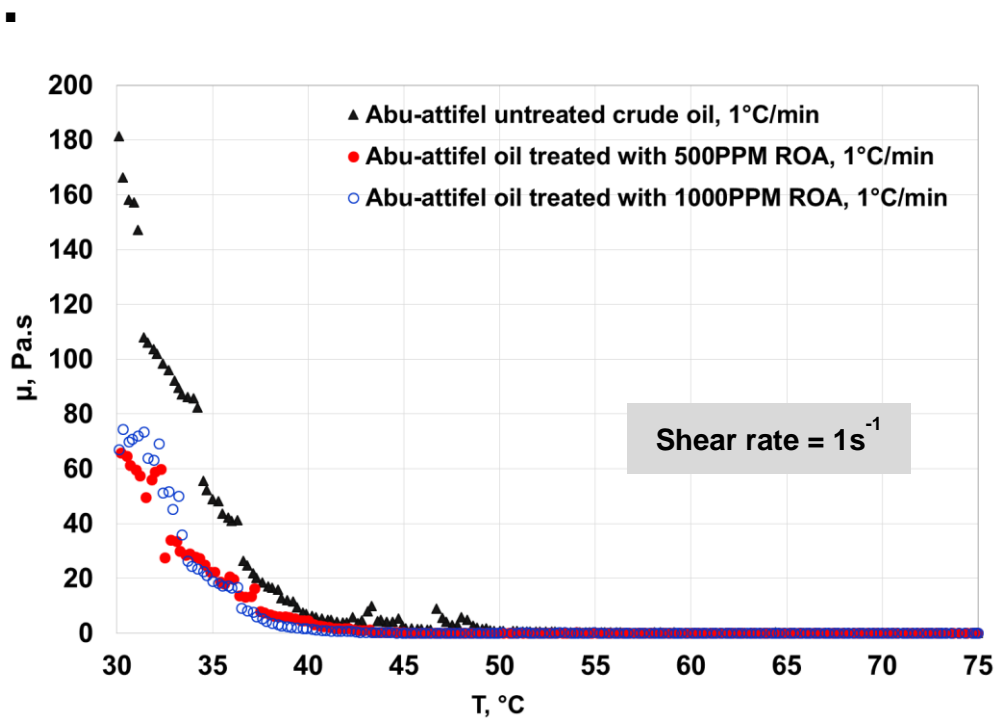


**Figure 4.4.1c:** Apparent viscosity upon dosing with ROA at shear rate of  $1 \text{ s}^{-1}$  and cooling rate of  $1^\circ\text{C}/\text{min}$ .

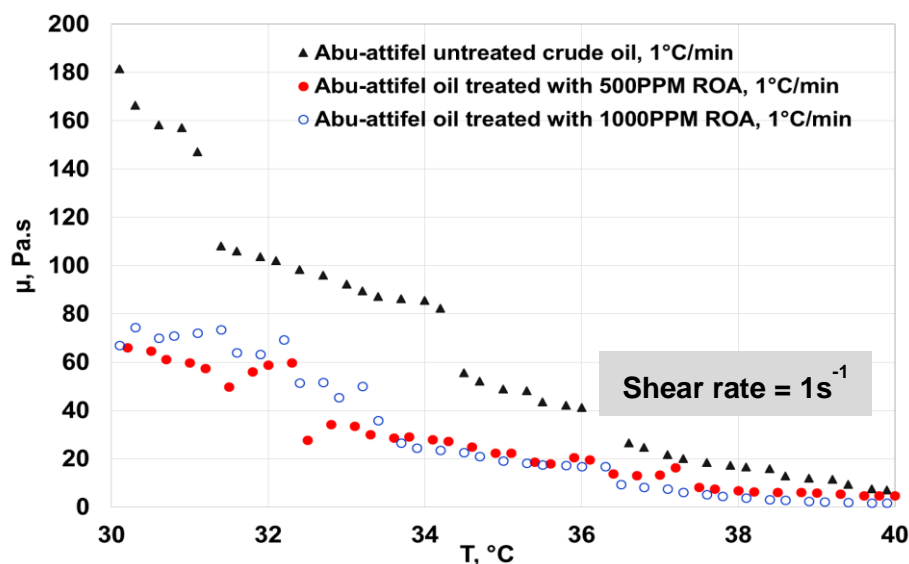


**Figure 4.4.1d:** Reduction in apparent viscosity upon dosing with ROA at the low shear rate of  $1 \text{ s}^{-1}$  and cooling rate of  $1^\circ\text{C}/\text{min}$  ( $70\text{--}30^\circ\text{C}$  and expanded scale in  $40\text{--}30^\circ\text{C}$  range).

▪ Comparison of dosing PPD with ROA:

Here, the evidence is given for the effectiveness of the ROA wax inhibitor dosing of 500 PPM compared with PPD dosing of 1000 PPM, particularly in the temperature region below  $40^\circ\text{C}$  when the network forms and the wax inhibitor functions, inserting itself between the wax crystals.

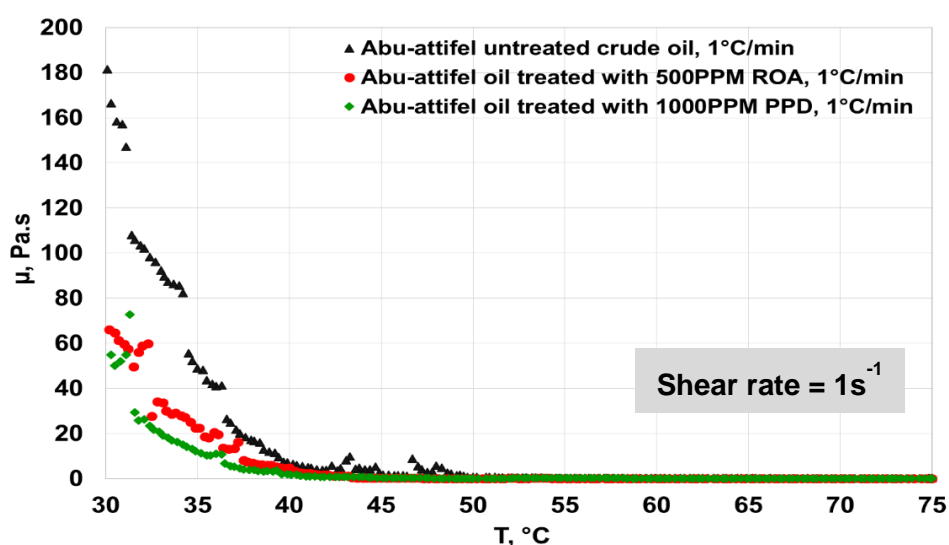


**Figure 4.4.1e:** Reduction in apparent viscosity upon dosing with ROA and PPD at the low shear rate of  $1 \text{ s}^{-1}$  and cooling rate of  $1^\circ\text{C}/\text{min}$ .

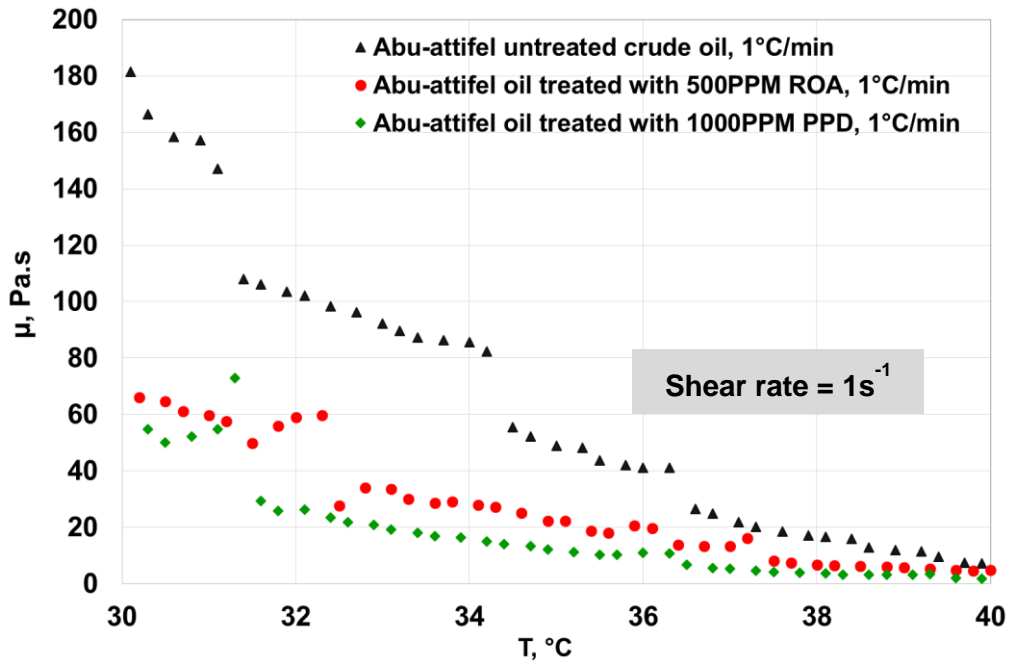


**Figure 4.4.1f:** Reduction in apparent viscosity upon dosing with ROA and PPD at the low shear rate of  $1 \text{ s}^{-1}$  and cooling rate of  $1^\circ\text{C}/\text{min}$ .

#### 4.4.2 Conclusion

Concerning the restarting of gelled waxy crude oil pipeline, the restarting pressure required to initiate flow after shutdown were determined for Abu-attifel crude oil which is taken as example, dilution with light crude oil, dosage with wax inhibitor or pour point depressant were investigated, characteristic and reliability of these options were compared under pipeline flow conditions and presented here.

#### 4.5 Rheology of treated and untreated Abu-attifel crude oil cooled statically, i.e. during shut down conditions.

The purpose of these experiments as explained earlier was to replicate the conditions at shutdown of the pipeline. Upon power failure, flow in the pipe will cease after decelerate towards the zero flow investigated above. This is considered the worst condition. These conditions are mimicked here rheologically by cooling the oil down from its normal operating temperature of  $75\text{-}80^\circ\text{C}$  down to the paraffin wax appearance temperature, at cooling rate typical of the environment of Abu-attifel crude oil that is  $0.5\text{-}1.0^\circ\text{C}/\text{min}$  and then applying incremental

stress from zero to study yielding, i.e. how the flow restarts and at what stress yield value. Such rheological experiment is obtained using a controlled stress rheometer as described in the experimental chapter. Such rheological method is a model of a pipeline restart as pressure and restart stresses ( $\tau_{rst}$ ) in the pipelines are related by the simple force balance:

$$\Delta p \pi R^2 = 2 \pi R L \tau_{rst} \quad (4.5.1)$$

where:

$R$ ,  $L$  is the pipe radius and length (m) respectively.

$\Delta p$  is the pressure difference (Pa)

$\tau_{rst}$  is the restart yield stress (Pa)

A further attribute of such a rheological approach is that it permits to assess the effect of the rate of increase of stress on yielding, effectively assessing the benefit of restarting pumping at a low or high rate of pressure increase. As discussed in the literature review, the yielding of waxy crude oils undergoes several stages as shown in Figure 4.5.1

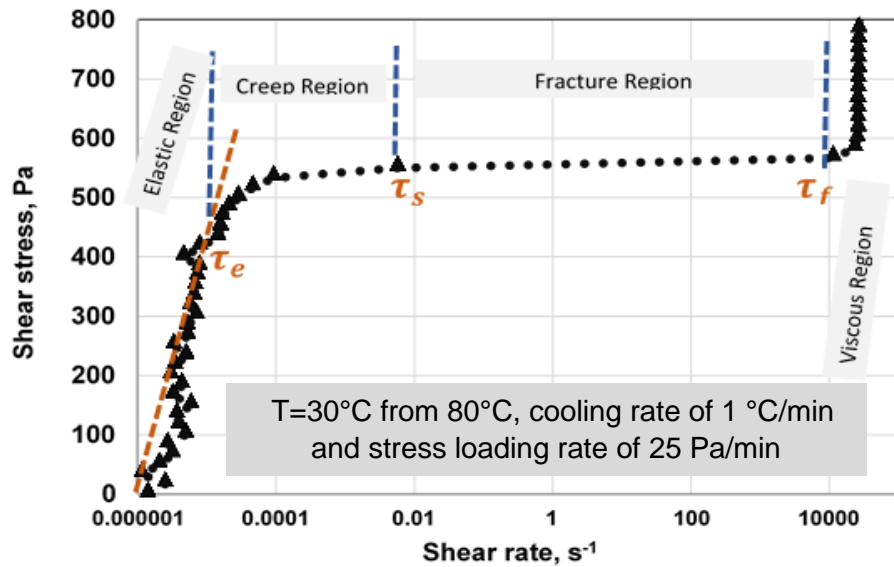


**Figure 4.5.1:** Yielding of Abu-attifel crude oil at 30°C.

This Figure (4.5.1) shows first an elastic deformation up to the elastic yield stress  $\tau_e$ , followed by a creep region where the gel network is stretched until it begins to fracture at a static yield stress  $\tau_s$ , followed by the fracture propagating throughout the network until all the network disintegrate at a fragmentation yield stress  $\tau_f$ . The restart stresses ( $\tau_{rst}$ ) can thus be in principle any of these three stresses but, it is clear that the elastic stress is the most conservative. Strictly, flow only begins once the gel disintegrates completely, that is at  $\tau_{rst}=\tau_f$  but in the context of this work  $\tau_e$  is a good approximation. In the present research, these three yield stresses can be identified for all conditions and the complete data set is given in the appendices. The identification is a simple mathematical manipulation:  $\tau_e$  is the end of the linear elastic region,  $\tau_s$  and  $\tau_f$  can be found by calculating the first and second derivative (slope and change of slope) at each point after  $\tau_e$ . Such simple processing is not presented here as the purpose of the work is to assess the effect of additives on the changes of the yielding. Typical values will however be given as shown in the concluding part of this section (Table 4.5.1). Data obtained are now presented.

#### 4.5.1 Presentation of data

Before making the presentation, it is important to help future researchers to mention that many experiments were carried out to systematically measure the effect of dilution with the light crude oil Sirtica and dosing with the wax inhibitor ROA and the pour point depressant PPD at (i) various concentrations, (ii) a range of temperatures near and below the paraffin wax appearance temperature (40, 35 and 30°C), (iii) two cooling rates to reach these temperatures from the hot initial temperature of 80°C and finally (iv) two stress loading rate (25 and 100Pa/min). All the data are given in the appendices. The purpose here is to arrive at the optimal solution as far as concentration is concerned but taking into consideration all these parameters whose functioning mechanism differ. Dilution as explained earlier is merely a reduction of the wax content. Wax inhibitors function by preventing the formation of crystal network, inserting themselves between the crystals. Pour point depressants interact with the wax causing it to precipitate at lower temperatures.

Clearly at the outset, all these parameters should help but the strongest hypothesis is that the wax inhibitor should be the most effective.

a) Abu-attifel untreated crude oil

Prior to treating Abu-attifel crude oil with (light crude dilution, dosing with PPD and WI chemical), yield stress of Abu-attifel untreated crude oil were measured using stress controlled mode at temperature of 30°C, stress loading rate of 100 Pa/min and cooling rate of 1°C/min, the average percentage difference between three consecutive runs were determined and results were tabulated (see Appendix C0) and graphically presented in Figure 4.5.2.

As can be seen from the presented data, the magnitude of difference between runs is strongly related to the flow curve region (shear stage) as depicted in Figure 4.5.2. At elastic and creep stress range the variation magnitude were relatively high (63%), however at fracture region the average % difference between the three runs is 159%, as the viscous flow commences the % difference between the three runs was as low as 22%.

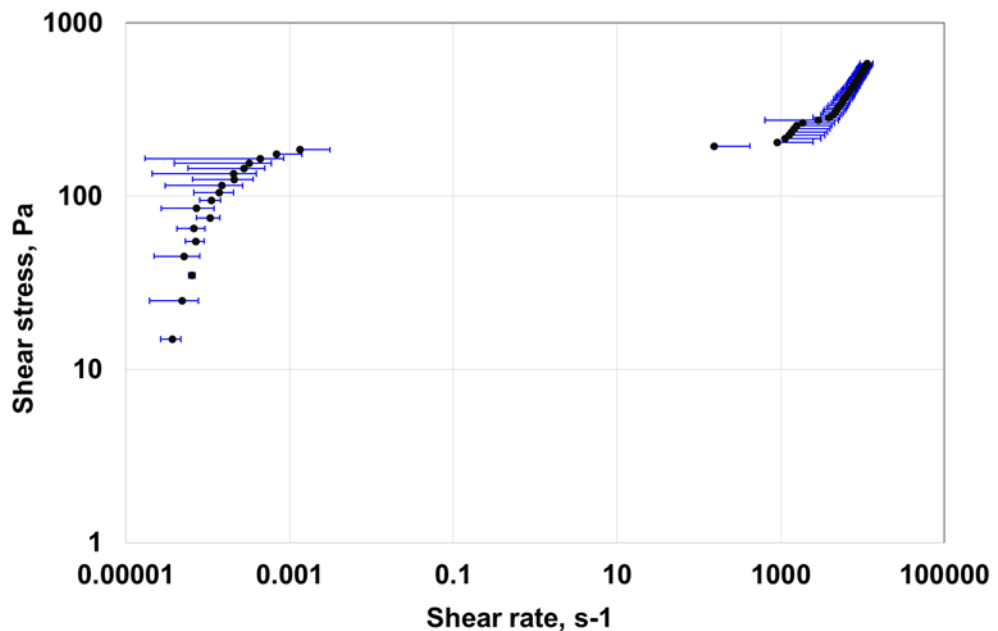


**Figure 4.5.2:** Variation of shear stress with shear rate for Abu-attifel untreated crude oil at 1°C/min.

b) Comparative effect of addition of ROA at 40°C: As shown in Figure 4.5.3 and as expected near the wax appearance temperature the benefit of addition of the wax inhibitor is very pronounced as it combines the viscosity reduction discussed earlier, hence the very low measured yield stress.

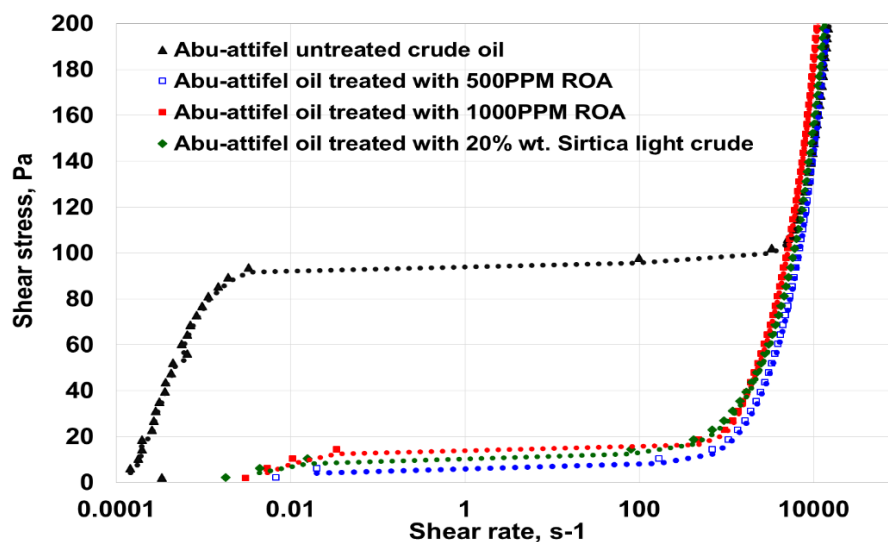


**Figure 4.5.3:** Yielding of Abu-attifel crude oil at 40°C upon addition of Sirtica and ROA (cooling rate= 0.5°C/min and stress loading rate=25Pa/min).

c) Comparative effect of addition of PPD at 40°C: As shown in Figure 4.5.4, PPD is less effective in lowering the yield stress. This is consistent with its function which is to lower the pour point, confirming that ROA is the most appropriate as it affect the strength of the wax network that forms.



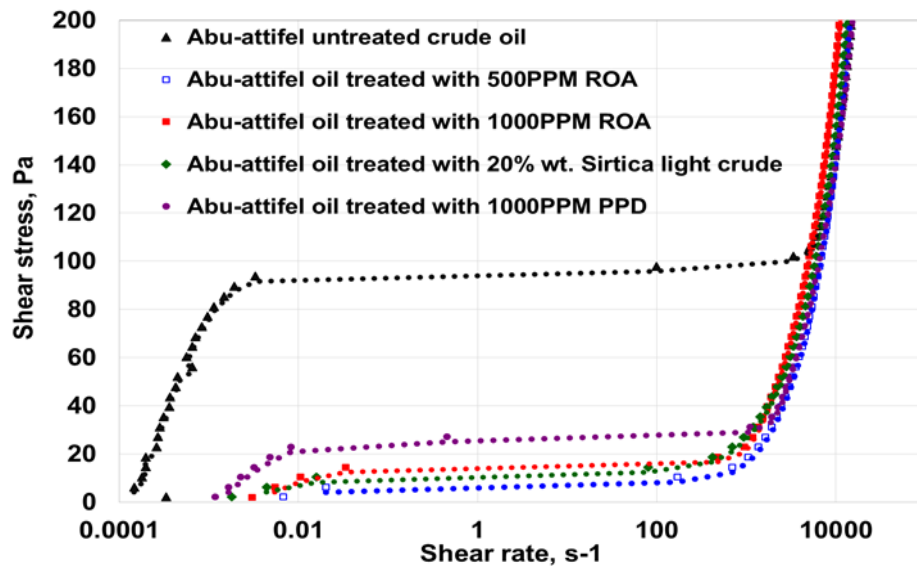


**Figure 4.5.4:** Yielding of Abu-attifel crude oil at 40°C upon addition of Sirtica, ROA and PPD (cooling rate= 0.5°C/min and stress loading rate=25Pa/min).

d) Comparative effect of dilution with Sirtica and addition of ROA

at 35°C: Figure 4.5.5 provides a comparison of the effects of dilution with Sirtica and the dosing with the wax inhibitor ROA at the concentration deemed from the normal pumping conditions (dynamic cooling at 10 and 50 s<sup>-1</sup>) and near shutdown conditions (dynamic cooling at 1s<sup>-1</sup>) to be beneficial on the basis of reduction of apparent viscosity. The question is does the same treatment ease yielding of the oil now cooled and immobile in the pipeline? As shown from Figure 4.5.5, the answer is yes with ROA at both 500 PPM and 1000 PPM but no with dilution with Sirtica. The rationale for this is that whereas the wax inhibitor has achieved its function of preventing the formation of a strong gel, Sirtica has not because it merely reduces the wax content, a condition not sufficient to prevent the formation of a strong gel. Indeed, from the literature review, it has been shown that strong gel form with crude oils that have a range of wax content. This is an important research finding as previous work have not made such comparative measurements. As an approximate guide to the yield values, Figure 4.5.5 shows that yield stresses of order 215Pa with

Abu attifel, 120Pa for Abu-attifel crude oil treated with 500 PPM ROA and 75Pa for Abu-attifel crude oil treated with 1000 PPM ROA, equivalent to decreases in restart pressures of 44%, and 65% respectively.

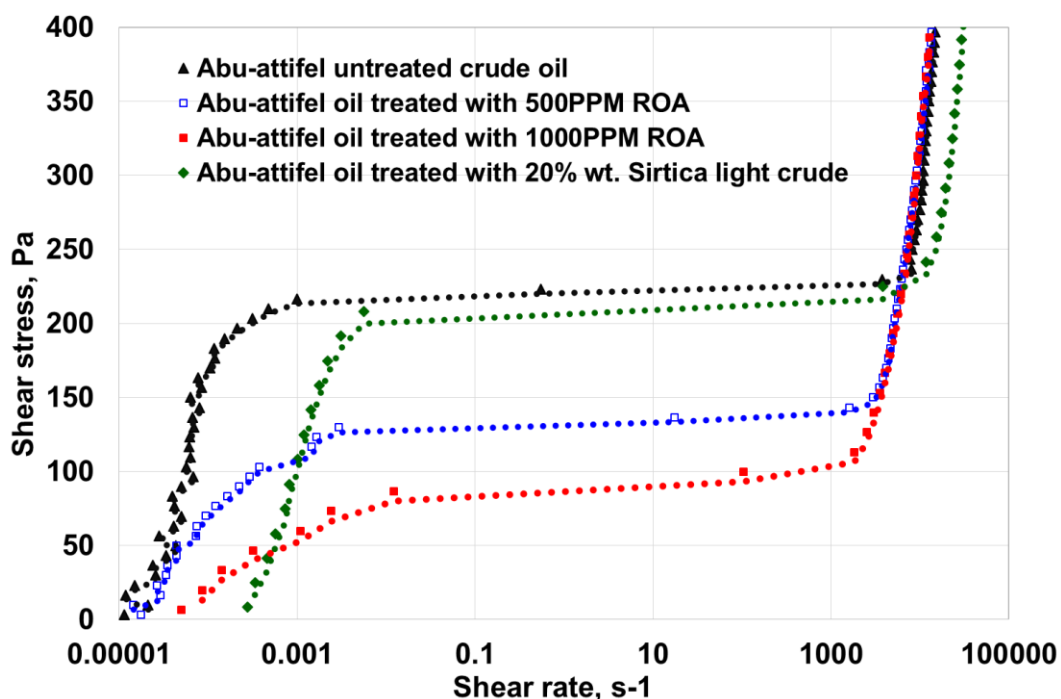


**Figure 4.5.5:** Yielding of Abu-attifel crude oil at 35°C upon addition of Sirtica and ROA (cooling rate= 0.5°C/min and stress loading rate=25Pa/min).

e) Comparative effect of addition of ROA at 30°C: Having established the benefit on yielding of the addition of ROA at 35°C, it is important to assess if that benefit is sustained on further decrease of temperature, here at 30°C. Interestingly, as observed from Figure 4.5.6 that 500 PPM is no longer sufficient with the yield stress approximately being the same as with the untreated Abu-attifel crude oil. Addition of 1000 PPM remains beneficial with the yield stress now dropping from 550 Pa for untreated Abu-attifel crude oil to 420Pa, equivalent to 24% in restart pressure decrease. For “insurance” purposes, it is thus necessary to use the larger dosage of ROA. Accurate values at temperature of 30°C are given in Table 4.5.1.

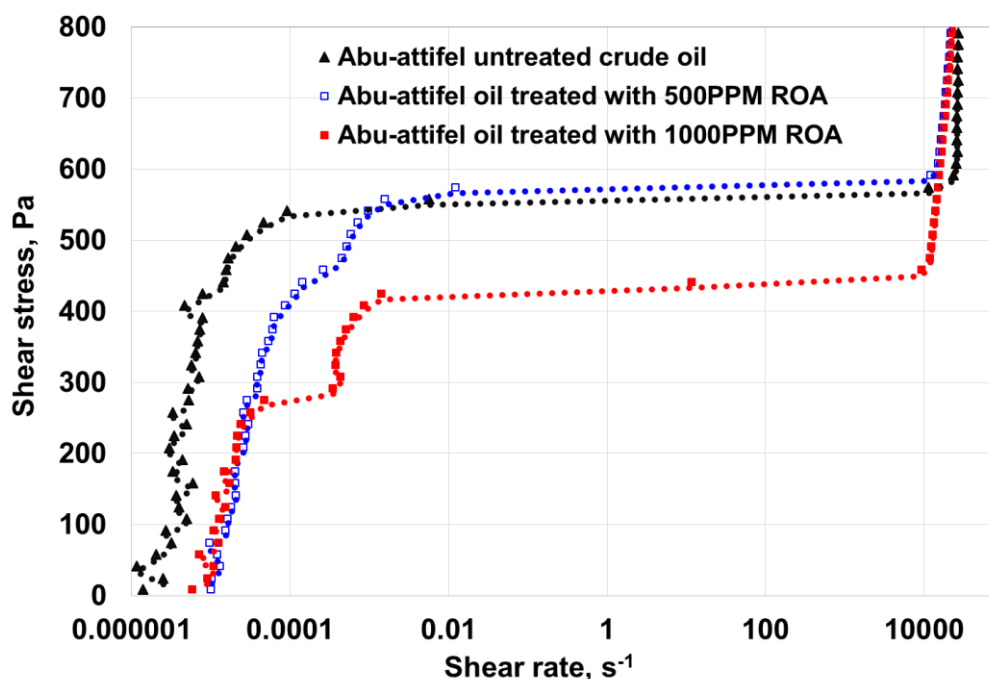


**Figure 4.5.6:** Yielding of Abu-attifel crude oil at 30°C upon addition of wax inhibitor ROA (cooling rate= 0.5°C/min and stress loading rate=25Pa/min).

As can be seen in Figures 4.5.3 - 4.5.6, the effect of temperature on the yielding of Abu-attifel treated with chemicals was enhanced, however at different levels as the temperature was increased from 30°C to 40°C as compared with Abu attifel untreated, which is considered as a double effect (thermal and chemical) on morphology and strength of wax crystals, as proved by microscope and rheology measurements carried in this research.

*b) Effect of increasing cooling (0.5 to 1.0°C/min):* As shown in Figure 4.5.7, the observations made earlier at the lower cooling rate of 0.5°C/min hold also at 1.0°C/min and the necessity of using ROA at 1000 PPM rather than 500 PPM to ensure effectiveness at low temperature (30 °C). At 40 °C, Figure 4.5.8 show how very effective is ROA even at the lower dosage at 500 PPM and the comparatively less effectiveness of dilution with Sirtica or dosing with PPD for the reasons explained earlier: lowering the wax content (with dilution) or the wax precipitation temperature (dosing with PPD) are less effective solutions.

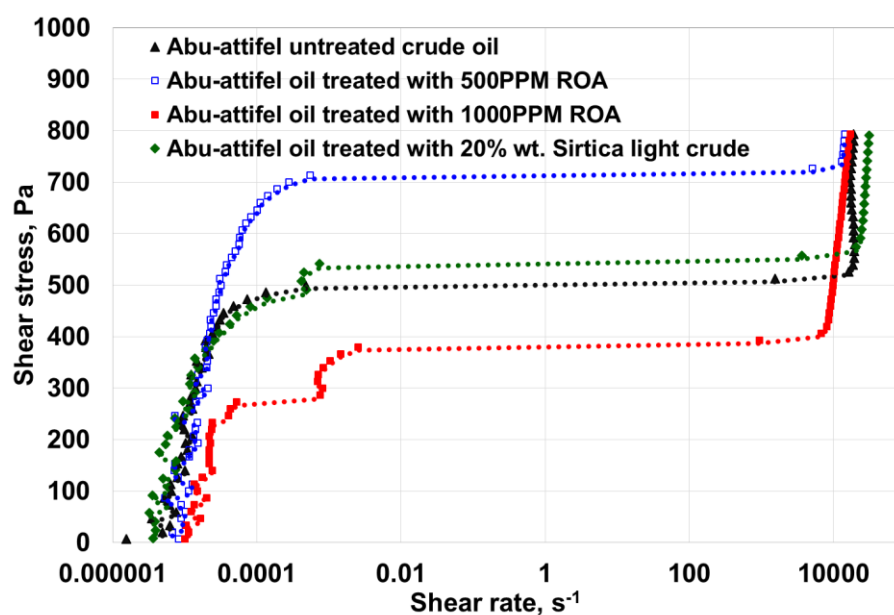


**Figure 4.5.7:** Yielding of Abu-attifel crude oil at 30°C upon addition of Sirtica and ROA at the higher cooling rate (cooling rate= 1°C/min and stress loading rate=25Pa/min).

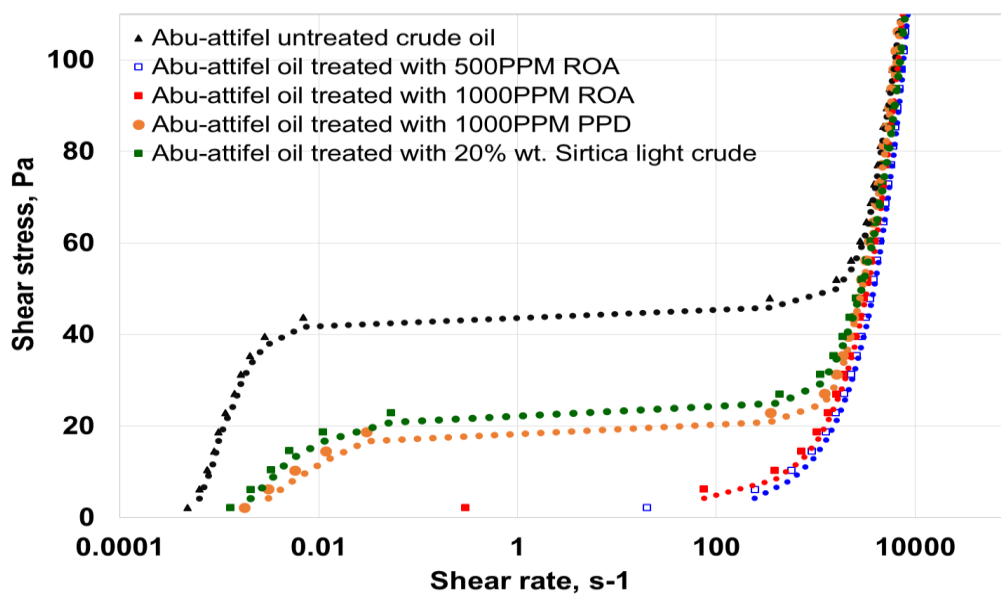


**Figure 4.5.8:** Yielding of Abu-attifel crude oil at 40°C upon addition of Sirtica, ROA and PPD at the higher cooling rate (cooling rate= 1°C/min and stress loading rate=25Pa/min).

c) Effect of increasing stress loading rate (25 to 100Pa/min): Having established that the dosing with the wax inhibitor at 1000 PPM was required for effectiveness at low temperature (30°C), the next consideration was to assess whether it is more effective to restart flow at low or high stress (pressure) rate as explained earlier. As shown in Figure 4.5.9, at 100 Pa/min, yielding begins at 375 Pa, the network fracturing and moving into the viscous state at 395 Pa. In comparison at 25 Pa/min (see Table 4.5.1), yielding started at 380Pa/min and the wax crystals network fractured at 420Pa/min, suggesting that restart at high stress (pressure) loading rate is more effective. This is an important conclusion of relevance to guiding restart operation in the field. Noting from the above figure that yielding of the untreated crude starts at 675Pa, fracturing and moving into the viscous regime at 708 Pa stress, it is observed that ROA addition at 1000 PPM resulted in a 44% drop in the yield stress which is a tremendous benefit in restart pumping pressures reduction.

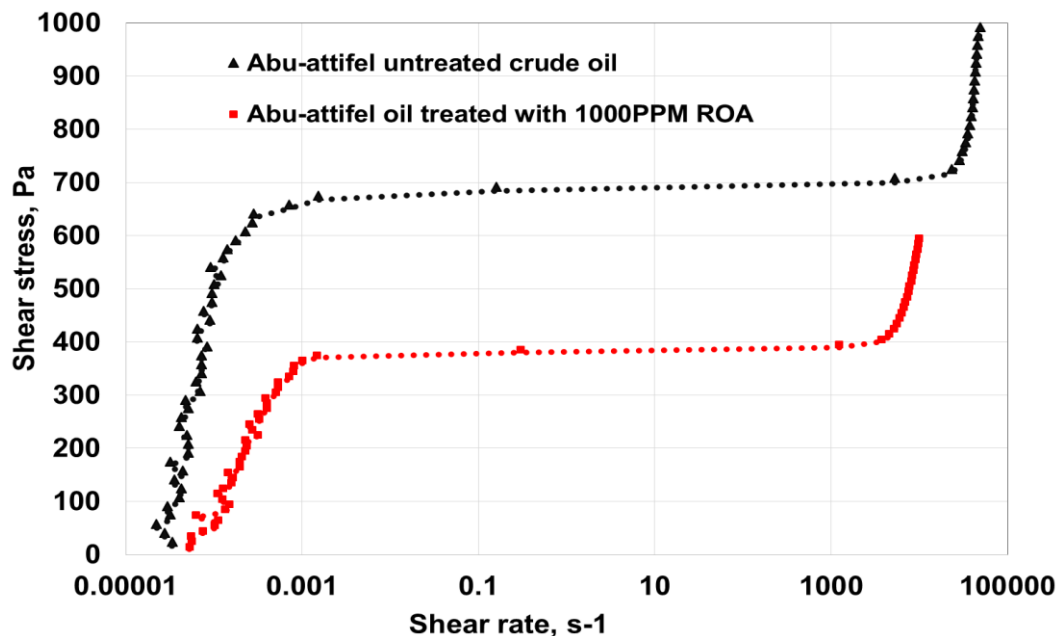


**Figure 4.5.9:** Yielding of Abu-attifel crude oil dosed with 1000 PPM ROA at 30°C (cooling rate= 1°C/min and stress loading rate=100Pa/min).

#### 4.5.2 Conclusion

The controlled stress rheological data have shown that, yielding of waxy crude oils can be reduced by diluting with a light oil or dosing with the wax inhibitor of (WI) and or a pour point depressant (PPD). The extent however, varies and it was found here that the most effective reduction in yielding is achieved by the dosing with the wax inhibitor which retains its function even when the temperature is reduced, the requirement being that a higher dosage is necessary to ensure effectiveness at low temperatures. Thus, ROA added at 1000 PPM is effective and retain its effectiveness down to 30°C, reducing the yield stress by as much as 40% (see Table 4.5.1 below giving reduction at 1.0°C/min). This translates directly into a 40% reduction in restart pressures and should be considered for application subject to cost of addition of ROA at 1000 PPM dosing.

**Table 4.5.1:** Comparative yielding of Abu-attifel crude oil treated with ROA1000 PPM (T=30°C and cooling rate=1°C/min).

	<b>Abu-attifel untreated crude oil</b>	<b>Abu-attifel oil treated with 1000 PPM ROA</b>	<b>% Decrease</b>
<b>Elastic Yield Stress</b>	340Pa @25Pa/min 542Pa @100Pa/min	233Pa @25Pa/min 325Pa @100Pa/min	31.5% 40%
<b>Static Yield Stress</b>	500Pa @25Pa/min 675Pa @100Pa/min	380Pa @25Pa/min 625Pa @100Pa/min	24% 7.4%
<b>Fracture Yield Stress</b>	540Pa @25Pa/min 725Pa @100Pa/min	420Pa @25Pa/min 691Pa @100Pa/min	22.2% 4.7%

#### **4.6 Gel structure of treated and untreated Abu-attifel crude oil at shutdown.**

##### **Mechanisms of Wax Alteration & Inhibition on Gel Network**

Having established the benefit of dosing with wax inhibitor ROA, the next phase of the research was to provide the evidence that the effect is attributable to changes in the gel network. Thus here microscopic observations undertaken at temperature near and below the wax appearance temperature are presented, comparing the structure of untreated Abu-attifel crude oil with Abu-attifel crude oil diluted with light crude oil Sirtica and dosed with pour point depressant PPD and wax inhibitor ROA. The method used is as described in the experimental chapter, that is a Cross Polarised Microscope was used with a cell holding the samples to be viewed, operating at controlled cooling rate from the hot initial temperature of 80°C down to WAT and below it. Clearly the observations of interests are those at near WAT (40°C) and below it (35 and 30°C). Following classical crystallization theory, at supersaturation the wax crystal will form as nuclei that can grow depending on temperature and cooling rate. At low cooling rate; and increasing cooling time the crystals will grow more whereas, a high cooling rate, the growth is limited. Image analysis of the microscopic observations was based on this simple principle. Thus, size distributions of the crystals were measured throughout the range of conditions. Although, the size distributions are more discerning, it was found that the number and average size of the crystals were sufficient to arrive at understanding of the main mechanisms. The complete data set, including images, size distributions, number density and average area is given in the appendices, here the main findings are presented and discussed.

#### 4.6.1 Presentation of data

As just explained, the aim here is to underpin the rheological observations which showed that only ROA played a significant role in the yielding process reducing significantly. Dilution with the light oil Sirtica and dosing with the pour point depressant PPD at 1000 PPM and 2000 PPM were effective as far as lowering the apparent viscosity during flow, i.e. at the conditions denominated as dynamic cooling at shear rate 10-50 s<sup>-1</sup>, descriptive of normal production and dynamic cooling at 1 s<sup>-1</sup>, descriptive of very slow flow approaching shutdown. Yielding data in comparison are those denominated by static cooling, i.e. no flow with the aim of measuring stresses to make them flow.

The observations are presented as photographs for the same temperature and cooling conditions and show the following:

- Crystallisation of waxy crude oils follow classical theory that is crystal nuclei are allowed to grow when slow cooling is imposed as shown below in Figure 4.6.1 where for Abu-attifel crude oil the average area of the crystals has grown from 34.3 µm<sup>2</sup> to 264 µm<sup>2</sup> upon cooling from 1 down to 0.1 °C/min. At the intermediate cooling rate of 0.5 °C/min, the average area was 62.4 µm<sup>2</sup>. [PLEASE NOTE NUMBER DENSITY ARE x 10<sup>-3</sup> per µm<sup>2</sup>]

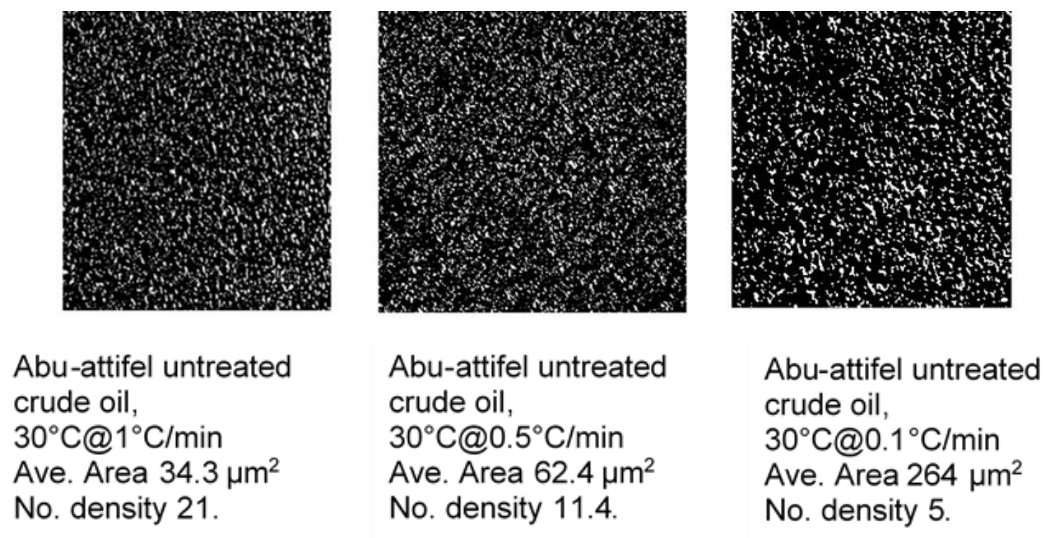


**Figure 4.6.1:** Effect of cooling rate on crystal average area of Abu-attifel untreated crude oil. Scale: X100 magnification, whole width of the photographs covers 1380 µm.



- Crystallisation of Abu-attifel crude oil diluted with the light crude oil Sirtica does not show any changes in the microstructure of the wax crystal network (see Figure 4.6.2) which remains similar to the one depicted in Figure 4.6.1 for the untreated Abu-attifel crude oil. This confirms that dilution with a light oil merely reduces the wax content not the mechanism of gel formation.

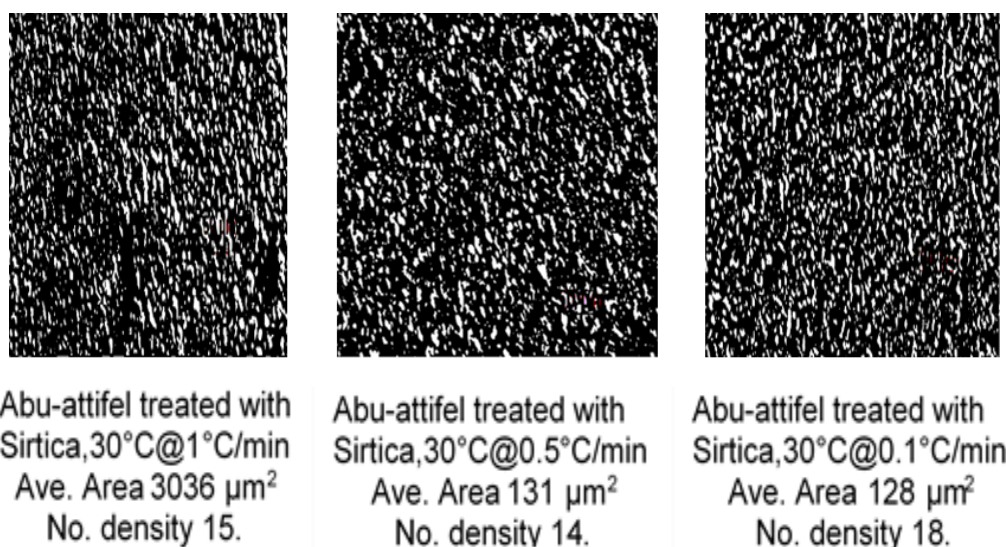
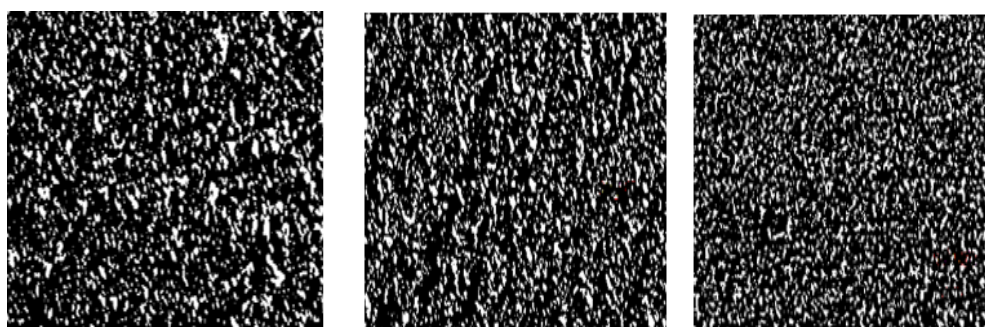


**Figure 4.6.2:** Microstructure and crystal average area of Abu-attifel crude oil diluted with 20% Sirtica at 30°C for a range of cooling rates. Scale: The whole width of the photographs covers 1380  $\mu\text{m}$  and X100 magnification.

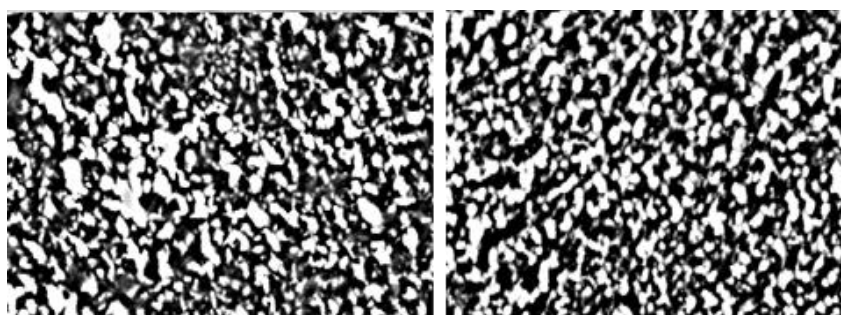
- Crystallisation of Abu-attifel crude oil dosed with the pour point depressant PPD at 2000 PPM reveal also no change in the mechanism of gel formation (see Figure 4.6.3) suggesting and proving that pour point depressants merely reduce the onset of wax precipitation but do not affect the formation of gel network. Pour point depressants work on the premise that they hinder the formation of crystals network upon cooling hence lowering the WAT as explained in the literature review with supporting evidence from other studies.



Abu-attifel treated with  
2000PPM PPD,  
30°C@1°C/min  
Ave. Area 99  $\mu\text{m}^2$   
No. density 8.4.

Abu-attifel treated with  
2000PPM PPD,  
30°C@0.5°C/min  
Ave. Area 82  $\mu\text{m}^2$   
No. density 18.

Abu-attifel treated with  
2000PPM PPD,  
30°C@0.1°C/min  
Ave. Area 89  $\mu\text{m}^2$   
No. density 10.



Abu-attifel untreated crude oil  
30°C@0.1°C/min  
Ave. Area 264  $\mu\text{m}^2$   
No. density 5 ( $10^{-3}\mu\text{m}^{-2}$ ).

Abu-attifel treated with 2000PPM PPD,  
30°C@0.1°C/min  
Ave. Area 89  $\mu\text{m}^2$   
No. density 10 ( $10^{-3}\mu\text{m}^{-2}$ )

**Figure 4.6.3:** Microstructure and crystal average area of Abu-attifel crude oil dosed with PPD 2000 PPM at 30°C for a range of cooling rates. Scale: The whole width of the photographs covers 1380  $\mu\text{m}$  and X100 magnification.

- Crystallisation of Abu-attifel crude oil dosed with the wax inhibitor ROA shows a drastic change (Figure 4.6.4) in the microstructure of the gel network at both 500 and 1000 PPM addition and confirm their effect on reducing yielding. Zooming on the microstructure as shown in Figure 4.6.5 reveals that the network is now disrupted as a result of the wax inhibitor lodging themselves between the individual crystals, forming weaker agglomerates rather than well knitted network. Furthermore, this disruption starts from the onset of crystallization as shown in Figure 4.6.6 taken at 40°C, the WAT2

temperature for paraffin wax being (39-40°C) as measured at the onset in the DSC experiments.

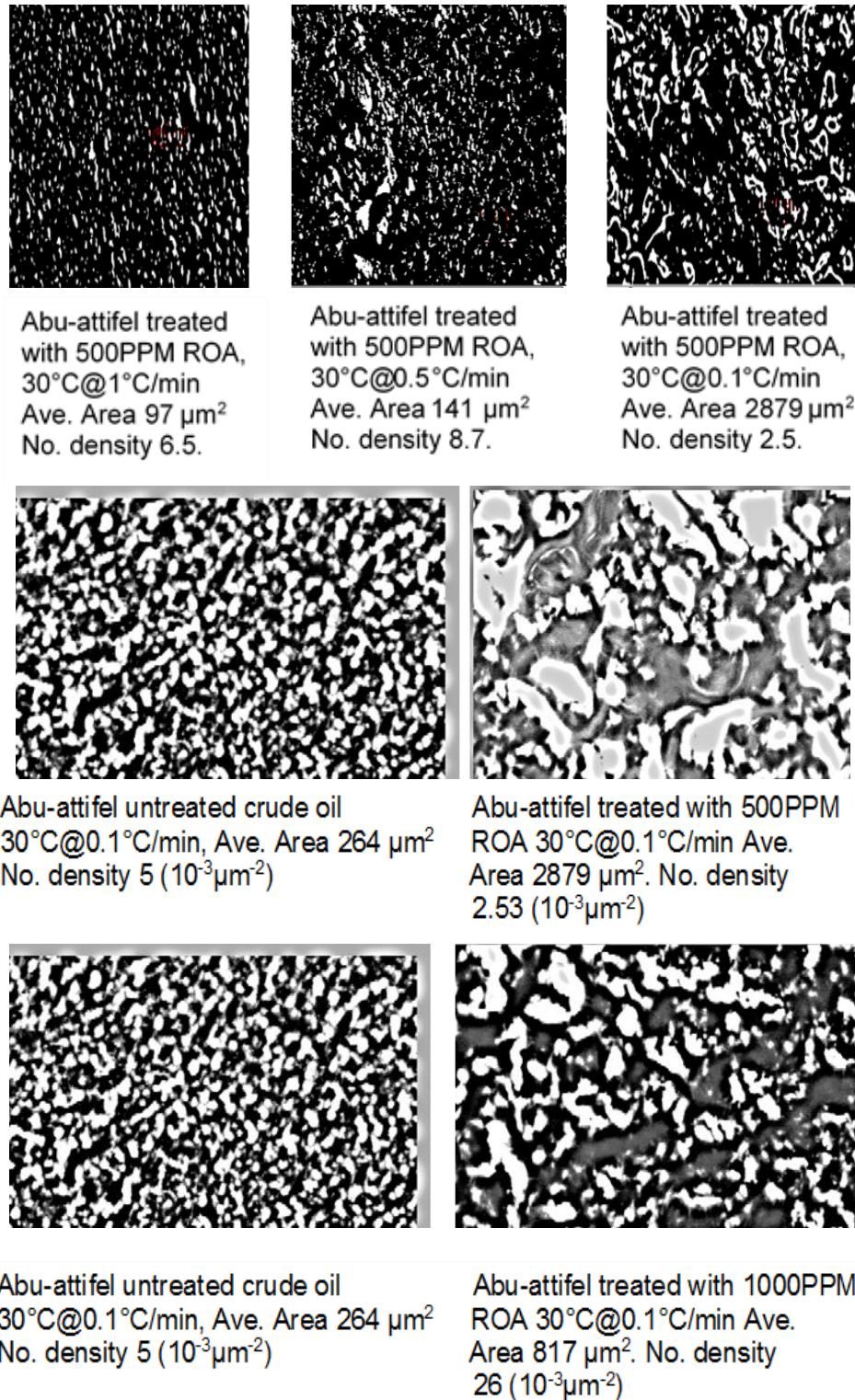


**Figure 4.6.4:** Microstructure and crystal average area of Abu-attifel crude oil dosed with ROA 500 PPM at 30°C for a range of cooling rates. Scale: The whole width of the photographs covers 1380  $\mu\text{m}$  and X100 magnification.



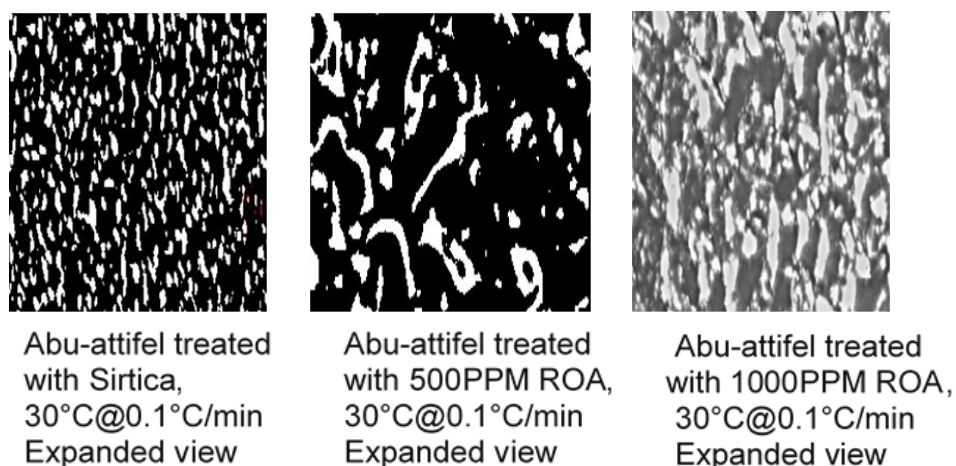


**Figure 4.6.5:** Expanded view of Microstructure and crystal average area of Abu-attifel crude oil dosed with Sirtica and ROA. 111

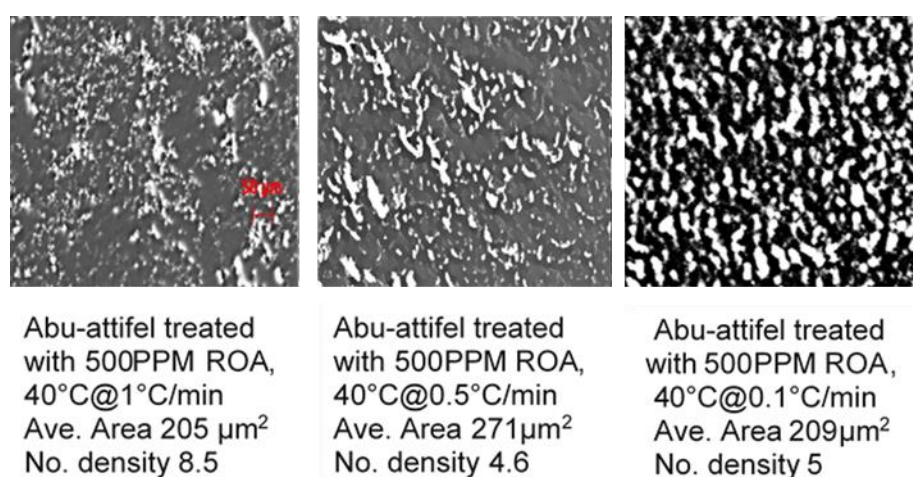


**Figure 4.6.6:** Microstructure and crystal average area of Abu-attifel crude oil dosed with ROA 500 PPM at 40°C. Scale: The whole width of the photographs covers 1380  $\mu\text{m}$  and X100 magnification.

## 4.6.2 Conclusion

Cross polarized microscopic observation of gelled samples of Abu-attifel crude oil diluted with a light crude oil and dosed with a wax inhibitor and a pour point depressant have revealed that the most critical changes in structure occurs with the addition of the wax inhibitor. This is consistent with the function of wax inhibitors which in principle is to prevent the formation of a strong network. The microscopic observations have shown the wax crystals to assemble in large disconnected weak agglomerates rather than a network of individual strong crystals. This

support the rheometric data which have shown yielding to be reduced upon the addition of the wax inhibitor ROA.

#### **4.7 Oscillatory Rheology of treated and untreated Abu-attifel crude oil cooling statically, i.e. during shut down conditions.**

Having established from the above rheological characterization, the benefit of addition of wax inhibitors on reducing both the apparent viscosity during normal pumping, near shutdown and the yield stress at shutdown, oscillatory rheology was used in an effort to provide further underpinning of the yielding process. First, the principle behind this technique is introduced to help the presentation and discussion of the data

##### **4.7.1 Principles**

Oscillatory rheology is used to extract the viscoelastic behaviour of materials that is the viscous and elastic component of a material, here a waxy crude oil gel. Essentially, the approach is to apply a time varying sinusoidal (rather than a linear) strain  $\gamma$  with an amplitude  $\gamma_0$  and measure the ensuing stress  $\tau$  which too must vary with time. Expressed mathematically, these strain and stress will be:

$$\gamma = \gamma_0 \sin \omega t \quad (4.7.1)$$

$$\tau = \tau_0 \sin (\omega t + \delta) \quad (4.7.2)$$

Eq. (4.7.2) expresses that the stress response lags by a phase angle. In order to study yielding, the strain that is applied must have a low amplitude to avoid destroying the gel from the start. For low amplitudes, Eq. (4.7.2) can be transformed into:

$$\tau = G' \sin \omega t + G'' \cos \omega t \quad (4.7.3)$$

The two quantities  $G'$  and  $G''$  are thus the outputs from oscillatory experiments.  $G'$  expresses the elastic component of the gel (the storage modulus) and  $G''$  the viscous component (loss modulus). An example from the measured data is given in Figure 4.7.1. In this Figure, the temperatures

given (30, 35, 40, 45°C) are those where the measurements were carried out, the oil being initially hot at 80°C, cooled down to these temperatures at a fixed cooling rate, 1°C/min in this example.

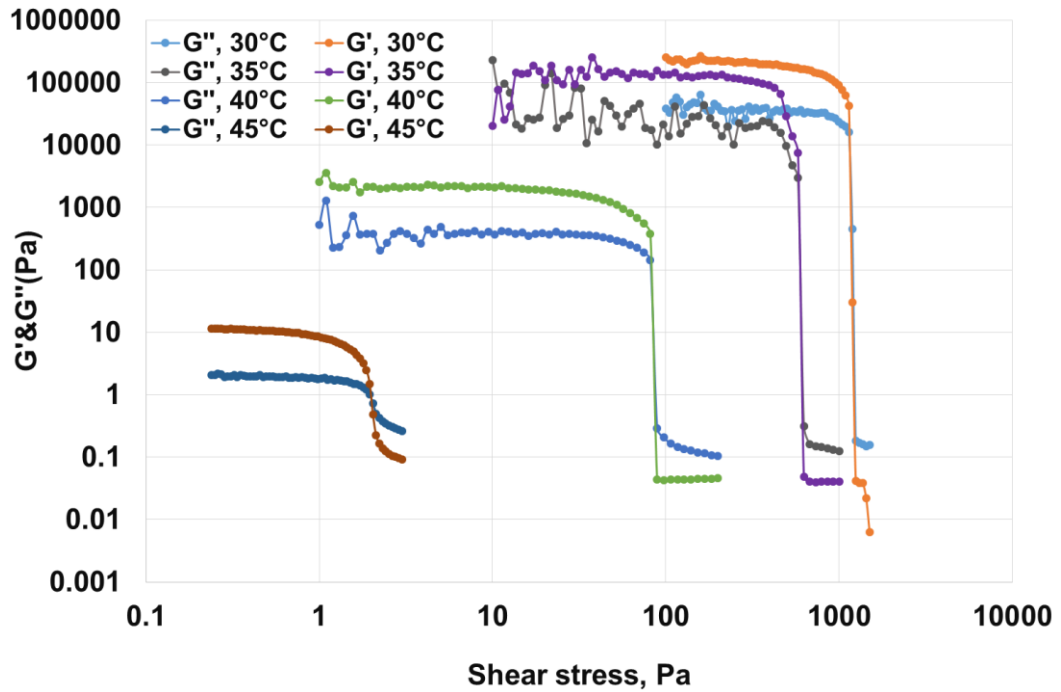


**Figure 4.7.1:**  $G'$  and  $G''$  as measured for Abu-attifel untreated crude oil at various temperatures. (Frequency= 0.5 Hz and cooling rate= 1°C).

The addition of 500 PPM ROA has clearly modified the wax structure of Abu-attifel crude oil at various temperature as shown in Figure 4.7.2. It can be seen that at 45°C that  $G''$  is larger than  $G'$  on account that at this temperature, the oil is above the paraffin wax appearance temperature (39-40 °C). It will be thus more viscous than elastic. Pursuing the argument at 40, 35 and 30°C, the elastic component now dominates as the oil has gelled.

An interesting feature of Figure 4.7.2 is that these  $G'$  and  $G''$  cross over, meaning that at crossing point the elastic and viscous component are the same but switching to the viscous component becoming larger upon an increase in shear stress. This point signifies the stress at end of fracture,  $\tau_f$  described earlier in the controlled stress rheology section (see Figure 4.5.1). Above this critical stress, a large drop in the stresses is observed meaning that the gel is completely destroyed and has moved to the viscous region.

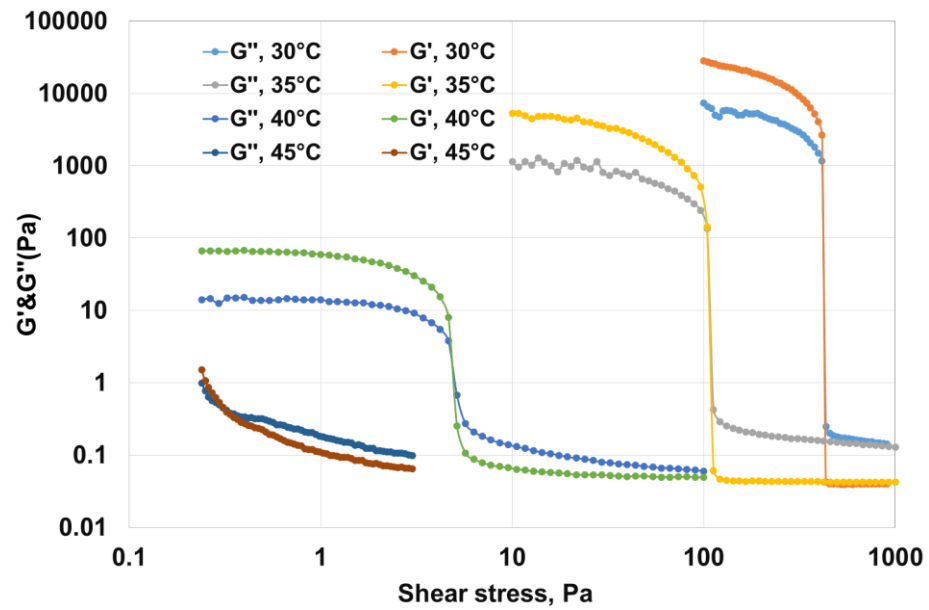


**Figure 4.7.2:**  $G'$  and  $G''$  as measured for Abu-attifel crude oil with 500 PPM ROA at various temperatures. (Frequency=0.5Hz and cooling rate=1°C/min).

It is clear from Figure 4.7.2 that similar experiments can be conducted but at a fixed stress which will lead to measuring the changes of  $G'$  and  $G''$  with the cold temperatures as shown in the example of Figure 4.7.3, giving the gel point.

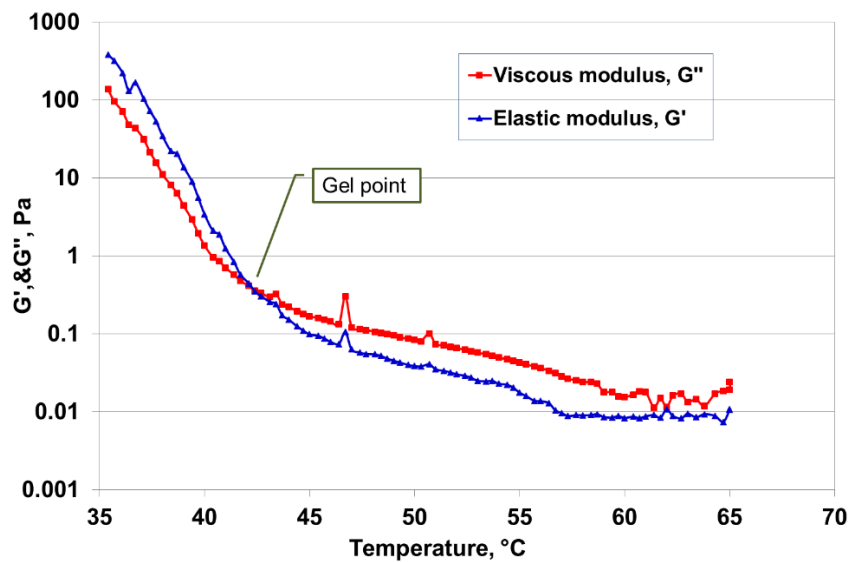


**Figure 4.7.3:**  $G'$  and  $G''$  as measured for Abu-attifel crude oil with 20% of Sirtica at various temperatures. (Frequency= 0.2 Hz, Shear stress= 0.3Pa and cooling rate= 1°C).

#### 4.7.2 Presentation of data

Following from the rationale presented above, the following observations can be made from the wide range of data collected in this mode (see Appendices for the complete data set which covers temperatures of 30, 35, 40 and 45 °C, cooling rates of 0.5 and 1°C/min for Abu-attifel crude oil diluted with 20% Sirtica and dosed with the wax inhibitor and the pour point depressant).

##### Effect of temperature on Abu untreated:

- The cooling rate at 0.5°C/min ( longer cooling time) resulted a higher storage module than the one of 1°C/min. This the result of the low cooling rate allowing crystal growth, an observation made earlier by CPM and further confirmed here by rheology.
- The magnitude of diffrence between the storage module at cooling rate of 0.5 and 1°C/min is minimum at 30°C (lowest temperature) and become higher with increasing temperature for 40°C and 45°C. This a corollary of the fact that at lower temperature, more wax precipitates, increasing the solid component of the gel, again an observation made earlier by CPM and confirmed further here by rheology. (see Figure 4.7.4)

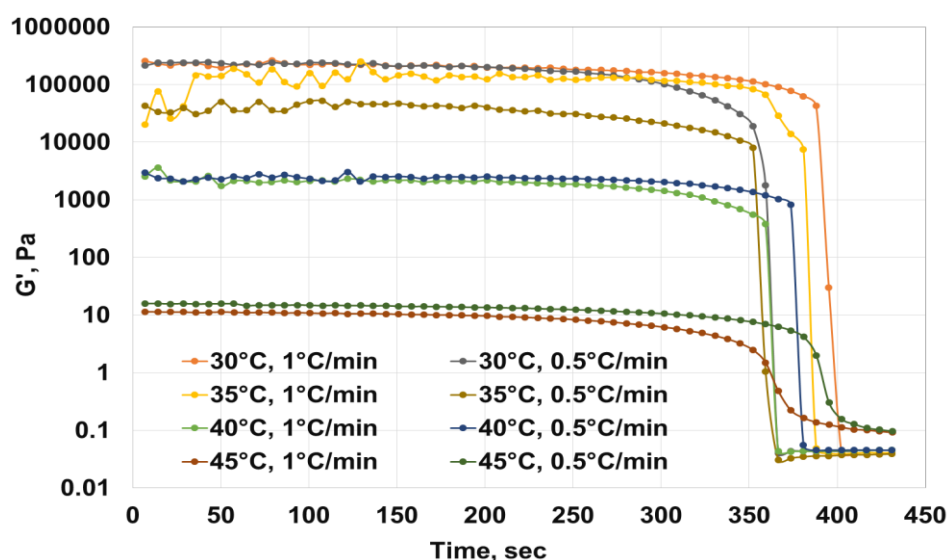


**Figure 4.7.4:** Elastic modulus of Abu-attifel untreated crude oil.



- Elastic yield stress of Abu-attifel crude oil was found from the  $G'$  and  $G''$  vs. shear stress at the point where the viscoelastic linear region ceases. The static and fracture yield stresses from the turning point of the linear viscoelastic region and the cross over point of  $G'$  and  $G''$  respectively (see Figure 4.7.1).
- The effect of temperature on yield stresses ( $\tau_e$ ,  $\tau_s$  and  $\tau_f$ ) is found to be as follow:
  - At 35°C, yield stresses ( $\tau_e$ ,  $\tau_s$  and  $\tau_f$ ) have decreased by 69%, 49% and 50.5% respectively of the values, at 30 °C.
  - At 40°C, the decreases were 97%, 93% and 91% respectively of the values, at 30°C.
  - At 45°C, Abu-attifel crude oil became liquid with negligible stresses ( $\tau_e$ ,  $\tau_s$  and  $\tau_f$ ) as (0.07, 1.9 and 2.2 Pa) , respectively. See appendix j for yield stress data.

*Effect of Treatment with Sirtica, PPD and ROA:*

- The experimental data of Figure 4.7.5 have confirmed that the wax inhibitor ROA was the most effective at reducing yield stress in comparison with diluting with light crude oil Sirtica or dosing with the pour point depressant PPD 1000 PPM or 2000 PPM for the reasons explained earlier and further confirmed here: the wax inhibitor affecting wax network structure whereas Sirtica affecting wax content and the PPD reducing the wax precipitation temperature (see Figure 4.7.6).

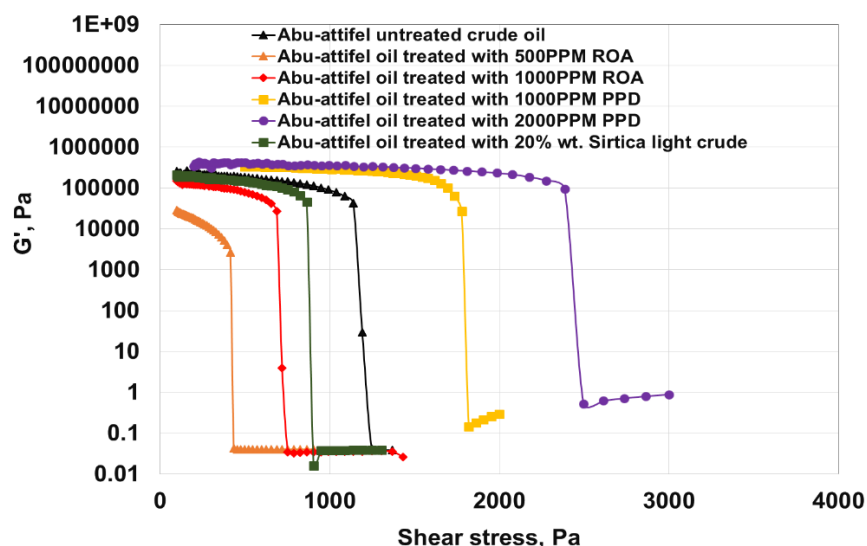


**Figure 4.7.5:** Elastic modulus of Abu-attifel crude oil treated with chemicals at 30°C and cooling rate of 1°C/min.

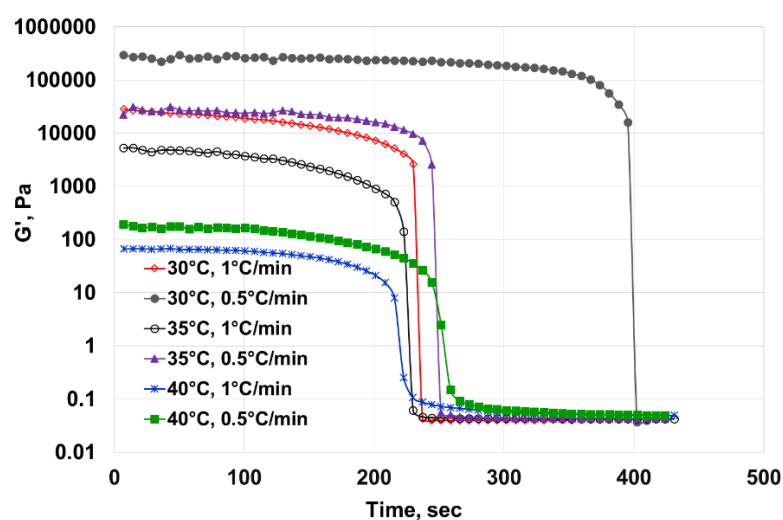


**Figure 4.7.6:** Elastic modulus of Abu-attifel crude oil + 500 PPM ROA.

### 4.7.3 Conclusion

In an effort to further check the findings of this research oscillatory rheological data were collected on the same samples viewed under the cross polarised microscopy and tested in control stress rheology. The data showed conclusively that ROA is the most effective as a wax inhibitor can alter the structure of waxy crude oil. Dilution with a light crude oil or dosing with a pour point depressant did not show significant effect on the network structure confirming their role as reducing wax content (Sirtica) and lower gelation temperature (PPD).

## CHAPTER 5: CONCLUSION & RECOMMENDATIONS

### 5.1 Context

This work was undertaken with the aim of finding a practical solution to the multi-millions of dollars problem of the gelation of waxy crude oils based on a fundamental study of how to reduce the pressure necessary to restart a gelled pipeline. Gelling occurs as a result of the loss of power and heating, causing a normally hot waxy oil being pumped in pipelines to cool down below the wax precipitation temperature. Typically, as it is the case for Abu-attifel crude oil (representative of many other waxy crude oils throughout the world - waxy crude oils accounts about one third of the world oil production), the hot oil temperature is 80°C and the wax appearance or precipitation temperature (WAT) is 40°C. Upon cooling, say at a conservative 0.5°C/min, the temperature will drop to this critical temperature of 40°C within 80 minutes, not practically long enough to remedy a serious power failure and loss of heating. Clearly as an *insurance* policy is required against such potentially catastrophic problem (if the problem is not fixed in a reasonable time, the wax will harden threatening the pipeline viability altogether). This is the context and the aim is to mitigate against this, using, (i) dilution with a light crude oil that is produced nearby, in this case Sirtica oil, (ii) dosing with a chemical known for reducing the pour point temperature and (iii) dosing with a wax inhibitor known for weakening the structure of the gel formed.

### 5.2 Research Strategy

The strategy adopted for this research was to approach the problem in its entirety by:

1. Splitting the production situation leading to shut-down into 3 stages:
  - I. Normal full production, i.e. high shear rate pumping, the shear rate being easily calculated from first principle as  $= 8V/D = 8(4Q/\pi D^2)/D$ ,  $D$ , being the diameter of the pipe and  $Q$ , the volumetric flow rate of the crude oil through the pipe. Typically, the range of shear rates for such a stage is 10-50 s<sup>-1</sup>, taking into consideration low and high production rates.

- II. Decelerating production, which starts immediately after the power fails and the pump stops. Such situation was deemed here to be not zero but near zero, that is of order  $1 \text{ s}^{-1}$ .
- III. Ceased production, when the flow ceases, that is when the shear rate is zero.

Clearly stage (i) and (ii) concern a pure shear flow and the parameter of concern is the apparent viscosity as it controls pressure thus power. The research question was then “Would the addition of a light crude oil, a pour point depressant or a wax inhibitor reduce apparent viscosity hence flow ability?” If the answer is yes, then the investment in this addition is worthwhile.

As for stage (iii), the research question does not concern a pure shear flow but the yielding of a gelled waxy crude oil and it is “Would the addition of a light crude oil, a pour point depressant or a wax inhibitor reduce the yield stress?”, the yield stress being the equivalent to pipe restart pressure as defined from the simple force balance equation:  $\Delta p \pi R^2 = 2\pi R L \tau_{rst}$ .

2. Carrying out the rheological work corresponding to the normal full production, decelerating and ceased production stages described above to discern working mechanism of the dilution with a light crude oil, dosing with a pour point depressant or dosing with a wax inhibitor and which is the most effective.
3. Underpinning the numerical data obtained above by structural microscopic observations of the wax structure below the wax precipitation temperature to verify the mechanism by which yielding is reduced if any.

### 5.3 Conclusions with recommendation imbedded

Based on the outcomes of this research, the strategy was proven to be sound as it gave both an evaluation of the extent of the reduction of apparent viscosity for stages (i) and (ii) and of the yield stress hence, the pumping power specifically, the conclusions are as follows, embodied along fundamental concepts:

*a) On the crystallisation of waxy crude oils*

- Waxy crude oils do not always exhibit a single wax appearance temperature but several and this depends on the paraffins molecular weight range in the waxy crude oil. With Abu-attifel crude oil, two such WAT were identified; the first (WAT1) can be attributed to the highest molecular weight paraffins (associated with asphaltenes), while the second (WAT2) is attributed to the remaining lower carbon number wax molecules.
- Cooling is found to be the most critical parameter, it controls crystal number, size and growth, with low cooling rates leading to the formation of large crystals, strongly knitted together, and thus requiring higher stress to break. Thus, low cooling rates (longer cooling time) as they occur in practice add further to the problem as the result is that high restart pressure will be required.

*b) On the crystallisation of waxy crude oils with additives*

- It was clear from the data collected here, that the dilution with a light crude oil does not change the crystallisation mechanism as the net result is a new waxy crude oil with reduced wax content.
- The data collected here, reveals that pour point depressant played a role in affecting crystallisation. It co-crystallised with wax crystals in the crude causing an increase of crystal size and a reduction in the crystal number density. Further research would be helpful to identify the role of chemical composition on the working mechanism.
- It was clear from the microscopic results obtained here, that wax inhibitor by their very function have successfully changed the structure hence, reduced the important parameter-the yield stress as shown in the rheology results. Optimum concentration of chemical best be determined through monitoring the blend characteristics through thermal and rheological measurements since the flow behaviour characteristic might change at a certain

dose of chemical, therefore defining the range of chemical dosing and the resulting blend properties has to be determined and accounted for.

*c) On the appropriate rheological technique to evaluate yielding*

- Yielding of waxy crude oil is a complex deformation that shows three separate regions: an elastic region first followed by a creep region then by a fracture region. In other words, waxy crude oil gels are resistant to stress as a result of their crystal structure strength, with the crystal bound together in a network that need fracturing before disintegrating totally into loose crystals in the oil bulk. It is worthy for future research to be able to view this in situ which is a challenging task as it requires a rheometer with structure viewing cells.
- The controlled stress method was found to be well suited for this research, as it determines the required stress that should be applied to the gelled wax starting from zero stress and then increased at a specific rate towards the elastic, static and finally the flow stress. Such technique is simple, yet it allows for investigating the effect of changing the stress loading rate, which equivalent in practice to the pumping pressure rating.
- Oscillatory rheometry complemented the controlled stress technique in characterising the flow behaviour. With such tests, the elastic and viscous moduli ( $G'$  and  $G''$ ) can be determined to underpin further the constant stress data and to be used in mathematical modelling.

*d) On the structural microscopic observations*

- Microscopic observations of untreated and treated Abu crude oils provide important structural details such average crystal size, size distribution and crystal density. The data given here, helped to study and quantify the effect of temperature and cooling rate on the waxy crude characteristics.

e) The experimental method protocol proposed and implemented in this research in which Thermal analysis, Microscopy and Rheology were integrated in a systematic approach which can be considered as replacement to old primitive method of pour point test used for chemical performance and selection.

f) *On the limits of this research*

- Although, this research has provided sound solution in mitigating wax gelation based on fundamental principle, this solution has to be tested for other crudes due to the complex nature of waxy crude oils. Therefore further research should be undertaken using (i) crude oils which contain wax and asphaltenes (ii) other wax inhibitors types to find which aspect of the wax inhibitor chemistry is most effective. The testing protocol proposed in this research will help in the development of new wax inhibitors much needed by the industry.
- Although, the apparent viscosity and yield stresses measured here provided a reliable guide to approximating reduction in power required for pumping, the problem of restart flow requires a fuller mathematical analysis so that the whole sequence of pressures required from restart to steady flow is computed precisely. The rheological data presented which split here in these 3 shear rates regimes, provide the basis to develop rheological models for this complex problem.
- Finally, and importantly, it is worth to note that the dilution with light crude oil and addition of chemicals is considered as a complementary to the current heating method in case of power failure or furnaces malfunction, however a cost benefit study would complement the finding of this work.

## References

- Abdelrahim, A.M.A. 2011. Rheology and Pumping of Waxy Crude Oils. PhD thesis. School of Engineering, Design and Technology, University of Bradford.
- Alderman, N.J., Gavignet, A., Guillot, D. and Maitland, G.C.1988. High-Temperature, High-Pressure Rheology of Water-Based Muds. SPE Paper 18305.
- Alfonso, P.G., Luis, A. B. P., Blanca, G. A., Gerardo, M. G., Gustavo, B. C., and Carlos, R. 2012. Effect of structural characteristics of modified waxy corn starches on rheological properties, film-forming solutions, and on water vapor. Starch. 64(1): 27-36.
- Al-Yaari, M. 2011. Paraffin Wax Deposition: Mitigation and Removal Techniques. Saudi Arabia Section Young Professionals Technical Symposium. Dehran, Saudi Arabia: SPE 155412:1-10.
- Al-Sabagh, A.M., El-Hamouly, S.H., Khidr, T.T.,El-Ghazawy, R.A. and Higazy, S.A. 2013. Preparation the Esters of Oleic Acid-Maleic Anhydride Copolymer and Their Evaluation as Flow Improvers for Waxy Crude Oil. J. Dispersion Sci. Technol., 34: 1585–1596
- American Society for Testing and Materials (ASTM). 2008. Annual Book of ASTM Standards; ASTM: West Conshohocken, PA, Vol. 05.01.
- Amhamed A. I. 2009. Rheology and Pipelines Start up Pressures of Waxy Crude Oils. PhD thesis. School of Engineering, Design and Technology, University of Bradford.
- Atta, A. M., Al-Shafy, H. I., and Ismail, E. A., 2011. Influence of Ethylene Acrylic Alkyl Ester Copolymer Wax Dispersants on the



Rheological Behavior of Egyptian Crude Oil. *Journal of Dispersion Science and Technology*, 32:1296–1305

- Boger, L. T., D. V., 1991. The measurement and description of the yielding behavior of waxy crude oil. *J. Rheol.* 35, (6):1121–1156.
- Barnes, H.A., Hutton, J.F., and Walters, K. 1989. *An introduction to Rheology*. Elsevier science publishers B. V., N3
- Barnes, H.A., 1997. Thixotropy—a review. *Journal of Non-Newtonian fluid mechanics*, 70(1): 1-33
- Barnes, H. A., Hutton, J.F., and Walters, K. 1989. *An introduction to Rheology*. Elsevier, Amsterdam.
- Barnes, H.A. 1999. The yield stress-a review or ‘παντα ρει’-everything flows? *J. Non-Newt. Fluid Mech.* 81: 133-178.
- Barnes, H. A. & WALTER, K. 1985. The yield stress myth. *Rheol. Acta* (24): 323- 326.
- Bassane, J.F.P., Sad, C.M.S., Neto, D.M.C., Santos, F.D., Silva, M., Tozzi, F.C., Filgueiras, P.R., Castro, E.V.R.D., Romao, W., Santos, M.F.P., Silva, J.O.R.D. and V.L. Jr. 2016. Study of the effect of temperature and gas condensate addition on the viscosity of heavy oils. *J. Petrol. Sci. Eng.*142: 163–169.
- Benziane, M. M., Wahab, S. A. A., Benaicha, M. and Belhadri, M. 2012. Investigating the rheological properties of light crude oil and the characteristics of its emulsions in order to improve pipeline flow. *Fuel*, 95: 97-107.
- Borghi, G. P., Corraera, S., Merlini, M., and Carniani, C. 2003. Prediction and Scale up of Waxy Oil Restart Behavior. Paper SPE

80259 presented at the SPE International Symposium on Oilfield Chemistry, Houston, 5 – 8 February.

- Bummer, B.L., 1971. Improved paraffin prevention techniques reduce operating costs, powder river basin, Wyoming. In: Rocky Mountain Regional Meeting of the Society of Petroleum Engineers of AIME. Billings, 1971. American Institute of Mining, Metallurgical, and Petroleum Engineers.
- Bello, O.O., Fasesan, S.O., Teodoriu, C., Reinicke, K.M., 2006. An evaluation of the performance of selected wax inhibitors on paraffin deposition of Nigerian crude oils. *Pet. Sci. Technol.* 24:195–206.
- Birdwell, B.F. 1964 Effects of various additives on crystal habit and other properties of petroleum wax solutions, Ph.D. dissertation, University of Texas, Austin.
- Carmen Garca, M., 2001. Paraffin deposition in oil production. In: SPE International Symposium on Oilfield Chemistry. Houston, 2001. Society of Petroleum Engineers.
- Chanda, D., Sarmah, A., Borthakur, A., Rao, K.V., Subrahmanyam, B. and Das, H.C., 1998. Combined effect of asphaltenes and flow improvers on the rheological behaviour of Indian waxy crude oil. *Fuel*, 77(11):1163-1167.
- Cheng, D. C.-H., 1986. Yield stress: a time dependent property and how to measure it. *Rheol. Acta* 25: 542-54.
- Chang, C., BOGER, D.V., and NGUYEN, Q. D., 1998. The yielding of waxy crude oils. *Ind. Eng. Chem. Res.* 37(4): 1551-1559.

- Chang, C., Boger, D.V., and Nguyen, Q.D. 2000. Influence of Thermal History on the Waxy Structure of Statically Cooled Waxy Crude Oil. SPE Journal 5 (2): 148 – 157.
- Chen, S. K., Qye, G., Sjöblom, J. 2007. Rheological properties of model and crude oil systems when wax precipitate under quiescent and flowing conditions. Dispersion Sci. Technol.28 (7): 1020-1029.
- Coussot, P., and Boyer, S. 1996. Determination of yield stress fluid behavior from inclined plane test. J.Rheol. Acta, 34: 534-543.
- Carniani, C., and Merlini, SM. 1996. Basic Design of Waxy Oil Transportation through Improved Lab Testing. Paper SPE 36836 presented at the SPE European Petroleum Conference in Milan, Italy, 22 -24 October.
- Cipelletti, L., Manley, S., Ball, R. C. and Weitz, D. A. 2000. Universal Aging Features in the Restructuring of Fractal Colloidal Gels. Phys. Rev. Lett. 6(84): 2276-2278.
- Cawkwell, M.G., and Charles, M.E. 1989. Characterization of Canadian Arctic “Thixotropic Gelled Crude Oils Utilizing an Eight-Parameter Model”. *J. Pipelines* 7: 251-264.
- Coutinho, J.A., Lopes da Silva, J.A., Ferreira, A., Rosário Soares, M. and Daridon, J.L. 2003. Evidence for the aging of wax deposits in crude oils by Ostwald ripening. Petroleum science and technology, 21(3-4):381-391.
- Davenport, T. C. and R. J. Russell.1960. The Full-Scale Pumping of Admiralty Fuel Oil and its Relation to Laboratory Tests. J. Inst. Petroleum. 46 (437):143-160

- Davenport, T. C. and Somper, R. S. H. 1971. The Yield Value and Breakdown of Crude Oil Gels. *J. Inst. Pet.* 57 (554): 86-105.
- Dehaghani, A. H. S. and Badizad, M. Hasan. 2016. Experimental study of Iranian heavy crude oil viscosity reduction by diluting with heptane, methanol, toluene, gas condensate and naphtha. *Petroleum* 2: 415-424.
- Dobbs, J. B. 1999. A unique method of paraffin control in production operations. *J. SPE* 55647 presented at SPE rocky mountain regional meeting held in Gillette. Wyoming, May 15-18.
- Dirand, M., Chevallier, V., Provost, E., Bouroukba, M. and Petitjean, D. 1998. Multicomponent paraffin waxes and petroleum solid deposits: structural and thermodynamic state. *Fuel*, 77(12): 1253-1260.
- Da Silva, J.A.L. and Coutinho, J.A. 2004. Dynamic rheological analysis of the gelation behaviour of waxy crude oils. *Rheologica Acta*, 43(5): 433-441.
- Ding, J., Zhang, J., Li, H., Zhang, F., and Yang, X. 2006. Flow Behavior of Daqing Waxy Crude Oil under Simulated Pipelining Conditions. *Energy & Fuels* (20): 2531-2536.
- Deshmukh, S. and Bharambe, D. P. 2008. Synthesis of polymeric pour point depressants for Nada crude oil (Gujarat, India) and its impact on oil rheology. *Fuel Processing Technology* 89(3): 227-233.
- Deshmukh, S. and Bharambe, D. P. 2012. Wax Dispersant Additives for Improving the Low Temperature Flow Behavior of Waxy Crude Oil. *Energy Sources, Part A*, 34:1121–1129

- Duffy, D.M., Moon, C., and Rodger, P.M. 2004. Computer-assisted design of oil additives: hydrate and wax inhibitors. *Molecular physics J.* 203-210 Journal.
- Ekweribe, C. K. 2008. Quiescent Gelation of Waxy Crudes and Restart of Shut-In Subsea Pipelines. Ms. Thesis, University of Oklahoma.
- Edwards, R. T. 1957. Crystal Habit of Paraffin Wax. *Ind. Eng. Chem.* 49 (4): 750–757.
- Elhaddad, E. E., Bahadori, A., El-Sayed Abdel-Raouf, M. and Elkatatny, S. 2015. A new experimental method to prevent paraffin–wax formation on the crude oil wells: A field case study in Libya. *Hem. ind,* 69(3): 269-274.
- El-Gamal, I. M., and Gad, E. A. 1997. Low temperature rheological behavior of Umbaraka waxy crude and influence of flow improver. *Revue de l'institute Francais du petrole,* (3): 369-379.
- Elsayed, A. Z. A. and El-Shiekh, T. M. 2010. Effect of cooling rate on the flow behaviour of waxy crude oils. *Energy sources.* 32: 197-207.
- Emre, Özkol and Halloran, J. 2013. Rheological Characterization of Aqueous 3Y-TZP Inks Optimized for Direct Thermal Ink-Jet Printing of Ceramic Components. *Journal of the American Ceramic Society.* 96 (4).
- Facron, A., A. 2017. The development of a knowledge-based wax deposition, three yield stresses model and failure mechanisms for re-starting petroleum field pipelines. PhD thesis, university of Bradford. Faculty of engineering and informatics.

- Frenier, W. W., Zainuddin, M., and Venkatesan, R. 2010. Organic Deposits in Oil and Gas Production. Society of Petroleum Engineers.
- Farag, R.K. 2008. Poly (Cinnamoyloxy Ethyl Methacrylate-Co-Octadecyl Acrylate) as Flow Improver for Egyptian Waxy Crude Oils. *Int. J. Polym. Mater*, 57: 189–202.
- Gateau, P., Henaut, I., Argilier, J.F. 2004. Heavy oil dilution. *Oil Gas Sci. Technol.* 59: 503–509.
- Gang, C., Yongfei, L., Wei, Z., Kun, Q., Yang, Ning. and Jie, Z. 2015. Investigation of cyclohexanone pentaerythritol ketal as a clean flow improver for crude oil. *Fuel Process. Technol.* 133: 64–68.
- Ghannam, M.T., Hasan, S. W., Abu- Jdyil, B. and Esmail, N. 2017. Rheological properties of heavy & light crude oil mixtures for improving flowability. *Rheologica Acta*, V 56 (3): 177-188.
- Ghannam, M.T., Hasan, S.W., Abu-Jdayil, B. and Esmail, N. 2012. Rheological properties of heavy & light crude oil mixtures for improving flowability. *Journal of Petroleum Science and Engineering*. 81: 122-128.
- Gill, F., and Russell, R.J. 1954. Pump Ability of Residual Fuel Oils. *Ind. Eng. Chem.*
- Giri, A., M. and Rabah, A., A. 2018. Rheolog behaviour of waxy crude oils under oscillatory shear and effect of plant seed oil. *International Journal of Engineering Trends and technology (IJETT)*. (58): 165-175.

- Garcia, M. D., Orea, M., Carbognani, L., and Urbina A. 2001. The effect of paraffinic fractions on crude oil wax crystallization. *Pet. Sci. Technol.*(19): 189 -196.
- Gutiérrez. G. S., Alonso, M.M. and Gadea, J. 2013. Rheological behaviour of gypsum plaster pastes with polyamide powder wastes. *Construction and Building Materials*. 38.
- El-GAMAL, I. and GAD, E.A.M. 1998. Low temperature rheological behaviour of Umbaraka waxy crude and influence of flow improver. *J. colloids and surfaces*. 81-191.
- Henaut. I., Vincke, O., and Brucy, F. 1999. Waxy Crude Oil Restart: Mechanical Properties of Gelled Oils. Paper SPE 56771 presented at the SPE Annual Technical Conference and Exhibition, Houston, 3 -6 October.
- Hamouda, A. A., and Viken, b. k. 1993. Wax deposition mechanism under high – pressure and in presence of light hydrocarbons. Paper SPE 25189, presented at the INT, Symposium. On oil field chem., New Orleans, La march 2-5.
- Holder, G.A., and Winkler, J. 1965a. Wax Crystallisation from Distillate Fuels: I. Cloud and Pour Phenomena Exhibited by Solutions of Binary n-Paraffin Mixtures.
- Holder, G.A., and Winkler, J. 1965b. Wax Crystallisation from Distillate Fuels:
- II. Mechanism of Pour Depression. *J. Inst. Petrol*. 51: 235.
- Houwen, O.H. and Geehan, T. 1986. Rheology of Oil-base Muds. SPE Paper 15416.

- HY, Li., QY, Huang., F, Zhang. and JJ, Zhang. 2003. Determination of wax content in crude oil using differential scanning calorimetry. J Univ Pet. (27):60–67.
- Jin, W. Jing, J. Wu, H. Yang, L. Li,Y. Shu X. and Wang, Y. 2014. Study on the Inherent Factors Affecting the Modification Effect of EVA on Waxy Crude Oils and the Mechanism of Pour Point Depression. Journal of Dispersion Science and Technology, (35):1434–1441.
- Karan, K., Ratulowski, J and German, P. 2000. Measurement of Waxy crude Properties Using Novel Laboratory Techniques. SPE, Annual Technical Conference and Exhibition, 1-4 October.
- Kané, M., Djabourov, M., Volle, J., Lechhairec, J., and Frebourg, G. 2003. Morphology of Paraffin Crystals in Waxy Crude Oils Cooled in Quiescent Conditions and Under Flow. Fuel. 82: 127–135.
- Kané, M., Djabourov, M., Volle, J.-L. 2004. Rheology and structure of waxy crude oils in quiescent and under shearing conditions, Fuel 83: 1591–1605.
- Keleşoğlu, S., Pettersen, B. H. and Sjöblom, Johan. 2012. Flow properties of water-in-North Sea heavy crude oil emulsions. Journal of Petroleum Science and Engineering, 100: 14-23.
- Kelland, M.A. 2009. Production Chemicals for the Oil and Gas Industry. CRC Press.
- Khidr, T.T and Mahmoud, S.A., 2007. Dispersion of waxy gas oil by some nonionic surfactants. J. Dispersion Sci. Technol. 28: 1309–1315.



- Khalkhal, F., Carreau, P. J. 2011. Scaling behavior of the elastic properties of non-dilute MWCNT–epoxy suspensions. *Rheol. Acta*. 50: 717-728.
- Kriz, P., Andersen, S.I. 2005. Effect of asphaltenes on crude oil wax crystallisation. *Energy Fuels* 19, 948–953.
- Hou, I., and Zhang, J. 2007. Viscoelasticity of gelled waxy crude oil. *J cent. South univ. tech* 14(s1): 414-417.
- Lin, M.Z., Li, C.X., Yang, F. 2008. Research on the properties of gelling process of waxy crude oil. *Chem. Res. Chin. Univ.* 29 (11): 2239–2244.
- Lin, M., LI, C., Yang, F. and Ma, Y. 2011. Isothermal structure development of Qinghai waxy crude oil after static and dynamic cooling. *Journal of petroleum science and engineering*. (77): 351-358.
- Liu, T. Fang L, Liu X, Zhang X. 2015. Preparation of a kind of reactive pour point depressant and its action mechanism. *Fuel*. 143:448–54.
- Lei, H. and Jin-jun, Z. 2007. New Method for rapid thixotropy measurement of waxy crude. *Journal Central South University* 14 part 1: 3.
- Lee, H.S., Singh, P., Thomason, W.H. and Fogler, H.S. 2008. Waxy Oil Gel Breaking Mechanisms: Adhesive versus Cohesive Failure. *Energy & Fuels* 22: 480–487.
- Ilyin, S.O., Arinina, M.P., Polyakova, M.Yu., Kulichikhin, V.G. and Malkin, A.Ya. 2016. Rheological comparison of light and heavy crude oils. *Fuel*, 186 (15): 157-167.

- Lorge, O., Djabourov, M., Brucy, F. 1997. Crystallisation and gelation of waxy crude oils under flowing conditions. *Revue de l'institut Français du Pétrole*. 52: 235-239.
- Magda, J. El-Gendy H, Oh K, Deo M, Montesi A, Venkatesan, R. 2009. Time-dependent rheology of a model waxy crude oil with relevance to gelled pipeline restart. *Energy Fuels* 23(3):1311–1315.
- Malkin, A., Kulichikhin, V., and Ilyin, S. 2017. A modern look on yield stress fluids. vol. 56 (3): 177-188.
- Manka, J.S., Ziegler, K.L. 2001. Factors affecting the performance of crude oil wax control additives. In: *SPE Production and Operations Symposium*. Oklahoma, Society of Petroleum Engineers.
- Mujumdar A, Beris AN, Metzner AB. 2002. Transient phenomena in thixotropic systems. *J Non-Newtonian Fluid Mech* 102(2):157–178.
- Mewis, J. and Wagner, NJ. 2009. Thixotropy. *Adv Colloid Interface Sci* 147–148:214–227.
- Mohamed, F. 2003. Rheology and start-up pressure of waxy crude oils. Dissertation for Degree of MPhil, University of Bradford.
- Morozov, E.V., Falaleev, O.V and Martyanov O.N. 2016. New insight into the wax precipitation process: in situ NMR imaging study in a cold finger cell. *Energy Fuels* (30): 9003–9013.
- Mendes, R. 2015. Rheological behavior and modeling of waxy crude oils in transient flows. PhD thesis, University Paris-Est.
- Mezger, T.G. 2006. *The rheology handbook: for users of rotational and oscillatory rheometers*. Vincentz Network GmbH & Co KG.

- Musser B. J., and Kilpatrick P. K. 1998. Molecular Characterization of Wax Isolated from a Variety of Crude Oils. *Energy & Fuels* 12: 715-725
- Mujumdar A, Beris AN, Metzner AB. 2002. Transient phenomena in thixotropic systems. *J Non-Newtonian Fluid Mech* 102(2):157–178
- Misra, S., BARUAH, and Singh, K. 1995. Paraffin problems in crude oil production and transportation a review, *SPE production& facilities*, Feb.50-54.
- Najah, T., El-Moudir, W. 2006. Libyan crude oils, their characteristics and suitability for further processing. Presented at the OAPEC/IFP Seminar, Rueil-Malmaison, France, June.
- Nguyen, Q.D., and Boger, D.V. 1992. Measuring the flow properties of yield stress fluids. *Annu. Rev. Fluid Mech.* 24: 47-88.
- Nguyen, Q.D., and Boger, D. V. 1983. Yield Stress Measurement for Concentrated Suspensions. *J. Rheol.* 27: 321-349.
- Nguyen, Q. D., and Boger, D. V. 1985. Direct Yield Stress Measurement with the Vane method. *J. Rheol.* 29: 335-347.
- Newberry, M. E. 1982. Chemical Treatments for Paraffin Control in the Oilfield. Paper presented at the Southwestern Petroleum Short Course, Lubbock.
- Oh, K., Jemmett, M., Deo, M. Yield behavior of gelled waxy oil: effect of stress application in creep ranges. 2009. *Ind. Eng. Chem. Res.* (48): 8950–8953.

- Oliveira, M.C. Carvalho, R. M. Carvalho, A. B. Couto, B. C. Faria, F and Cardoso, R. L. P. 2010. Waxy crude oil emulsion gel: impact on flow assurance. *Energy Fuels*, 24: 2287–2293

Onur, Y., Catalina, N. C., Gürbüz, G., 2011. Rheological behaviour of acrylate/montmorillonite nanocomposite latexes and their application in leather finishing as binders. (70).

- Pedersen, K. S., Aa Fredenslund, and P. Thomassen. 1989. *Properties of Oils and Natural Gases*-Gulf Publ. Company, Houston.
- Pedersen, K. S., and Rønningsen, H. S. 2003. Influence of Wax Inhibitors on Wax Appearance Temperature, Pour Point, and Viscosity of Waxy Crude Oils. *Energy & Fuels*, 17: 321-328.
- Price, R. C. 1971. Flow Improvers for Waxy Crudes. *J. Inst. Petrol.*, 57: 106-109.
- Paso, K.G. 2005. Paraffin Gelation Kinetics. PhD Dissertation, University of Michigan.
- Paso, K.G. and Fogler, H.S. 2004. Bulk stabilization in wax deposition systems. *Energy & fuels*, 18(4): 1005-1013.
- Patton, C.C. 1970. Paraffin deposition from refined wax-solvent systems. *Soc.Petrol. Eng. J.*, 17–24.
- Ronningsen, H.P. 1992. Rheological Behavior of Gelled, Waxy North Sea Crude Oils. *J. Petr.Sci. and Eng.* 7: 177-213.
- Ronningsen, H.P., Bjorndal, B., Hansen, A.B., and Pedersen, W.B. 1991. Wax Precipitation from North Sea Crude Oils. 1. Crystallisation and Dissolution Temperatures and Newtonian and Non-Newtonian Flow Properties. *Energy & Fuels*. 5: 895 – 908.

- Rønningsen, H.P., 2012. Production of waxy oils on the Norwegian continental shelf: Experiences, challenges, and practices. *Energy&Fuels* 26: 4124–4136.
- Radlinski, A. P., Barre, L., Espinat, D. 1996. Aggregation of n-alkanes in organic solvents. *Mol. Struct. J.* 383: 51-56
- Ranalli, G. 1995. *Rheology of the Earth*. second edition, chapman&hall.
- Russell, R.J. and Chapman, E.D. 1971. The Pumping of 85°F Pour Point Assam (Nahorkatiya) Crude Oil at 65°F. *J. Inst. Pet.* 57: 117.
- Singh P., Venkatesan R., Fogler H. S.and Nagarajan NR. 2000. Formation and Aging of Incipient Thin Film Wax-Oil Gels. *AIChE J.* 46 (5): 1059.
- Singhal, H.K., Sahai, G.C., Pundeer, G.S. and Chandra, K. 1991. Designing and selecting wax crystal modifier for optimum field performance based on crude oil composition, in: *Annual Technical Conference and Exhibition of the Society of Petroleum Engineers*. Dallas.
- Sivakumar, P., Sircar, A., Deka, B., Silviya Anumegalai, A., Suresh Moorthi,P. and Yasvanthrajan N. 2018. Flow improvers for assured flow of crude oil in midstream pipeline -A review .*Journal of Petroleum Science and Engineering* 164: 24–30.
- Shenghai, W., Chuncheng, Y., Xiufang, B. 2012. Magnetoviscous properties of Fe<sub>3</sub>O<sub>4</sub> silicon oil based ferrofluid. *Journal of Magnetism and Magnetic Materials*. 324(20).

- Shih, W.H., Shih, W. Y., Kim, S.I., Liu, J. and Aksay, I. A. 1990. Scaling behavior of the elastic properties of colloidal gels. *Phys. Rev. A*. 42: 4772–4779.
- Soni, H.P., Kiranbala, Bharambe, D.P., 2008. Performance-based design of wax crystal growth inhibitors. *Energy and Fuels* 22: 3930–3938.
- Solomon, M.J., and Spicer, P.T. 2010. Microstructural regimes of colloidal rod suspensions, gels, and glasses. *The Royal Society of Chemistry*. 6: 1391-1400.
- Stickel, J, J., and Powell, R L. 2005. Fluid mechanics and rheology of dense suspensions. *Annual Review of Fluid Mechanics*. V. 37, 37: 129-149.
- Schramm, G. 1994. A practical approach to rheology and rheometry (pp. 32–45). Gebrueder Haake GmbH, Karlsruhe, Germany.
- Sulaiman, S.A., Biga, B.K. and Chala, G.T. 2017. Injection of non-reacting gas into production pipelines to ease restart pumping of waxy crude oil. *J. Petrol. Sci. Eng.* (152): 549–554.
- Sun, G., Zhang, J. and Li, H. 2014. Structure behaviors of waxy crude oil emulsion gels. *Energy and fuels*. (28): 3718-3729.
- Thomason, W.H. 2000. Start-Up and Shut-In Issues for Subsea Production of High Paraffinic Crudes. Paper OTC 11967 presented at the Offshore Technology Conference, Houston, 1- 4 May.
- Tinsley, Jack F., Prud'homme, R. K., Guo. X., Adamson, D. H., Callahan, S., Amin, D., Shao, S., Kriegel, R. M. and Saini, R. 2007. Novel Laboratory Cell for Fundamental Studies of the Effect of

Polymer Additives on Wax Deposition from Model Crude Oils.  
Energy & Fuels, 21:1301-1308

- Uhlherr, P.H.T., Guo J., Tiu C., Zhang, X.-M., Zhou, J.Z.-Q., and Fang, T.-N., 2005. The shear-induced solid-liquid transition in yield stress materials with chemically different structures. J. Non-Newt. Fluid Mech.125: 101-119.
- Visintin, R.F.G., Lapasin, R., Vignati, E., D Antona, P., and Lockhart, T.P. 2005. Rheological Behavior and Structural Interpretation of Waxy Crude Oil Gels. *Langmuir*. 21: 6240 – 6249.
- Venkatesan, R., Östlund, J.A., Chawla, H., Wattana, P., Nydén, M. and Fogler, H.S. 2003. The effect of asphaltenes on the gelation of waxy oils. Energy & fuels, 17(6): 1630-1640.
- Venkatesan, R., Nagarajan, N.R., Paso, K., Yi, Y.B., Sastry, A.M. and Fogler, H.S. 2005. The strength of paraffin gels formed under static and flow conditions. Chemical Engineering Science, 60(13): 3587-3598
- Verschuur, E., Verheul, C. M., and Hartog, A. P. D. 1971. Pilot-Scale Studies on Restarting Pipelines Containing Gelled Waxy Crudes. J. Inst. Pet. 57 (555): 139-146.
- Venkatesan, R. and Fogler, H.S. 2004. Comments on analogies for correlated heat and mass transfer in turbulent flow. AIChE journal, 50(7), PPM.1623-1626.
- Venkatesan, R., Östlund, J.A., Chawla, H., Wattana, P., Nydén, M. and Fogler, H.S. 2003. The effect of asphaltenes on the gelation of waxy oils. Energy & fuels, 17(6) :1630-1640.

- Venkatesan, R., Singh, P., and Fogler, H.S. 2002. Delineating the Pour Point and Gelation Temperature of Waxy Crude Oils. SPE J. 349 – 352.
- Wang, K., Wu, Chien-C., Creek, J., Shuler, P. and Tang, Y. 2003. Evaluation of effects of selected wax inhibitors on paraffin deposition. Petroleum science and technology.21 (3 & 4): 369–379.
- Wardhaugh, L. T. and Boger, D. V. The Measurement and Description of the Yielding Behaviour of Waxy Crude Oil. J. Rheol. 1991. 35 (6): 1121-1156.
- Wei, B. 2015. Recent advances On mitigating wax problem using polymeric wax crystal modifier. Journal of Petroleum Exploration and Production Technology. (5): 391-401.
- Webber, R.M. 2001. Yield properties of wax crystal structures formed in lubricant mineral oils. Industrial & Engineering Chemistry Research, 40(1): 195-203.
- Wu, C., Zhang, J., Li, W., Wu, N. 2005. Simulation guiding the improvement of EVA- type pour point depressant. Fuel, (84): 2039-2047.
- Yang, F., Li, C. and Wang, D. 2013a. Studies on the structural characteristics of gelled waxy crude oils based on scaling model. Energy Fuels, 27: 1307–1313.
- Yang, F., Chen Li., Chuanxian Li, and Wang, D. 2013b. Studies on the structural characteristics of gelled model oils. Energy Fuels, 27: 3718–3724. Licence
- Zhao, Y., Kumar L., Paso, K., Safieva, Jamilia., Sariman., M Z., B., and Sjöblom., J. Gelation Behaviour of Model Wax–Oil and Crude



Oil Systems and Yield Stress Model Development. 2012. *Energy Fuels* (26): 6323-6331

- Zhang, J.J. and Liu, X. 2008. Some advances in crude oil rheology and its application. *Journal of Central South University of Technology*. (15): 288-292.
- Zhang, D.M., Jiang, B. L., Zhang, L. X., Yang, M. S., Ding, Y.F., Zhi, S. J. and Li, I. 2011. The influence of composite nanometer-sized material on waxy deposit property of waxy crude oil. *Oil gas storage transp.* (30): 249- 453.
- Zhu, L., Sun, N. L., Papadopoulos, K. and De, Kee, D. (2011). A slotted plate device for measuring static yield stress. *J. Rheol.* (30): 249- 453.

# Appendix

## Appendix 1: DSC Data

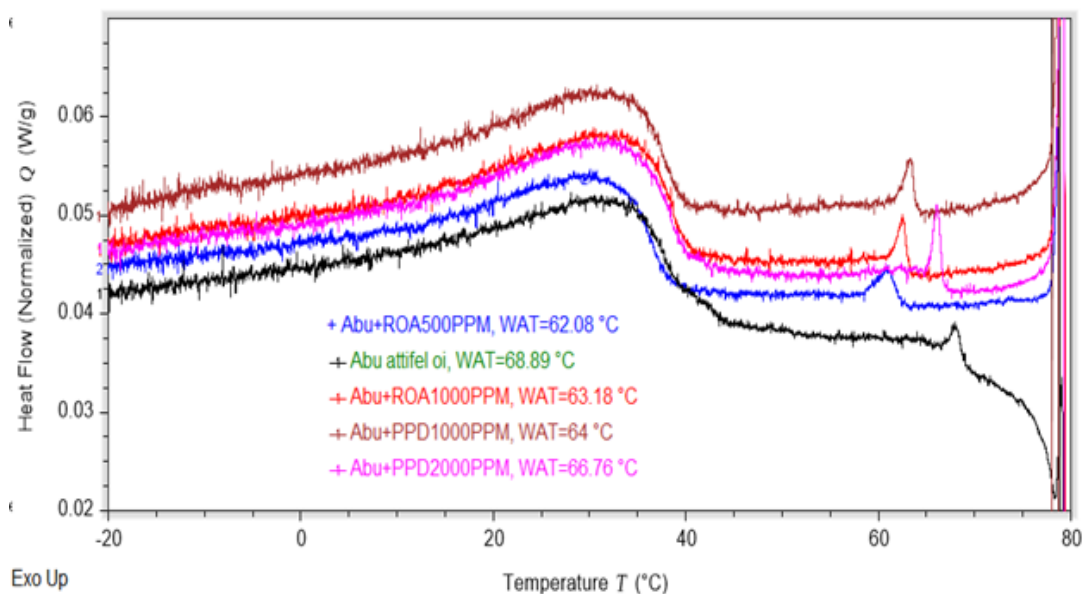


**Figure 1.1:** Wax appearance temperature for Abu-attifel crude oil untreated and treated with chemicals at cooling rate of 0.5 °C/min

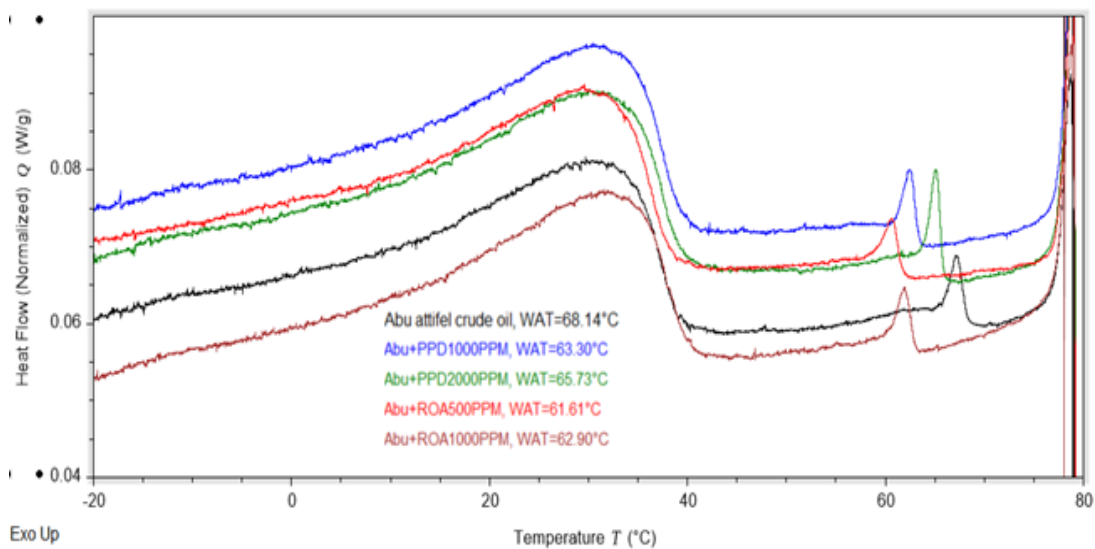


**Figure 1.2:** Wax appearance temperature for Abu-attifel crude oil untreated and treated with chemicals at cooling rate of 1 °C/min

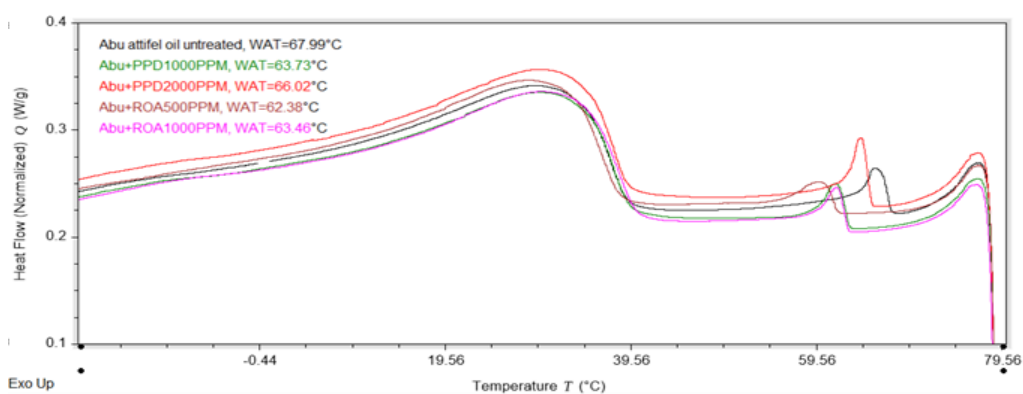


**Figure 1.3:** Wax appearance temperature for Abu-attifel crude oil untreated and treated with chemicals at cooling rate of 5 °C/min

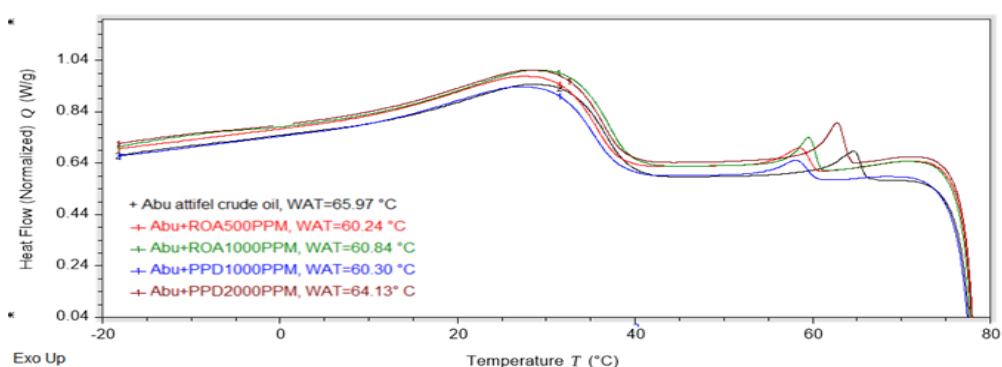


**Figure 1.4:** Wax appearance temperature for Abu-attifel crude oil untreated and treated with chemicals at cooling rate of 15 °C/min

## Appendix 2: Controlled Stress Rheometry

**Appendix 2.1:** The entire set covered the following conditions (see Tables below).

### 1: Controlled stress mode (viscosity and yield stress measurement)

**Table 1.1:** Dynamic cooling (1s-1)

	(80- T <sub>test</sub> )			
Shear rate, s-1	1			
Test Temp.	30	35	40	45
Abu-attifel crude oil untreated				
Abu-attifel oil treated with Sirtica oil 20%vol.				
Abu-attifel oil treated with ROA500 PPM				
Abu-attifel oil treated with ROA1000 PPM				
Abu-attifel oil treated with PPD1000 PPM				
Abu-attifel oil treated with PPD2000 PPM				

**Table 1.2:** Dynamic cooling (10s-1&50s-1)

temperature	(85- 30C)			
Cooling rate	0.5		1	
Shear rate, s-1	10	50	10	50
Abu-attifel crude oil untreated				
Abu-attifel oil treated with Sirticaoil 20%vol.				
Abu-attifel oil treated with ROA500 PPM				
Abu-attifel oil treated with ROA1000 PPM				
Abu-attifel oil treated with PPD2000 PPM				

**Table 1.3:** static cooling at various cooling rates & various stress loading rates

(75- T <sub>test</sub> )																
Cooling rate, c/min	0.5								1c							
SLR, Pa	25				100				25				100			
Test Temp.	30	35	40	45	30	35	40	45	30	35	40	45	30	35	40	45
Abu-attifel crude oil untreated																
Abu-attifel oil treated with Sirticaoil 20%vol.																
Abu-attifel oil treated with ROA500 PPM																
Abu-attifel oil treated with ROA1000 PPM																
Abu-attifel oil treated with PPD1000 PPM																
Abu-attifel oil treated with PPD2000 PPM																

**Appendix 2.2:** Here are presented the data at 30C and cooling rate 1C/min and stress loading rate 25Pa/min. The remaining data can be found in the CD attached to the thesis.

**Table 2.2.1 Abu-attifel untreated crude oilat 1°C/min and 25 Pa/min**

	Time s	Temperature °C	Shear Stress Pa	Shear Rate 1/s	Instantaneous Viscosity Pas	Strain
1, 1	16.02	30	6.807	1.54E-06	4.43E+06	0.007856
1, 2	48.07	30	19.95	4.87E-06	4.10E+06	0.007856
1, 3	80.07	30	33.24	6.20E-06	5.36E+06	0.008123
1, 4	112	30	46.52	3.48E-06	1.34E+07	0.008389
1, 5	144.1	30	59.78	7.61E-06	7.85E+06	0.008522
1, 6	176.1	30	73.34	6.08E-06	1.21E+07	0.008788
1, 7	208	30	86.62	5.24E-06	1.65E+07	0.008922
1, 8	240.1	30	99.88	6.47E-06	1.54E+07	0.009321
1, 9	272.1	30	113.1	6.34E-06	1.78E+07	0.009454
1, 10	304	30	126.7	7.91E-06	1.60E+07	0.009853
1, 11	336.1	30	140	1.01E-05	1.39E+07	0.009987
1, 12	368.1	30	153.2	7.96E-06	1.92E+07	0.01039
1, 13	400	30	166.5	9.00E-06	1.85E+07	0.01065
1, 14	432.1	30	180	1.09E-05	1.65E+07	0.01119
1, 15	464.1	30	193.3	1.04E-05	1.87E+07	0.01119
1, 16	496	30	206.6	1.29E-05	1.61E+07	0.01158
1, 17	528.1	30	219.8	9.92E-06	2.22E+07	0.01198
1, 18	560.1	30	233.4	8.69E-06	2.68E+07	0.01225
1, 19	592	30	246.6	9.56E-06	2.58E+07	0.01265
1, 20	624.1	30	259.9	1.28E-05	2.03E+07	0.01292
1, 21	656.1	30	273.2	1.21E-05	2.27E+07	0.01318
1, 22	688	30	286.4	1.26E-05	2.28E+07	0.01332
1, 23	720.1	30	300	1.42E-05	2.11E+07	0.01385
1, 24	752.1	30	313.3	1.48E-05	2.12E+07	0.01451
1, 25	784	30	326.5	1.23E-05	2.65E+07	0.01491
1, 26	816.1	30	339.8	1.71E-05	1.98E+07	0.01518
1, 27	848.1	30	353.3	1.46E-05	2.41E+07	0.01585
1, 28	880	30	366.6	2.13E-05	1.72E+07	0.01624
1, 29	912.1	30	380.1	1.97E-05	1.93E+07	0.01704
1, 30	944.1	30	393.3	1.93E-05	2.04E+07	0.01758
1, 31	976	30	406.6	2.43E-05	1.67E+07	0.01824
1, 32	1008	30	419.8	2.78E-05	1.51E+07	0.01918
1, 33	1040	30	433.4	3.07E-05	1.41E+07	0.02024
1, 34	1072	30	446.6	3.48E-05	1.28E+07	0.02144
1, 35	1104	30	459.9	4.75E-05	9.68E+06	0.02304
1, 36	1136	30	473.2	7.40E-05	6.39E+06	0.02543
1, 37	1168	30	486.4	0.000135	3.61E+06	0.02956
1, 38	1200	30	500	0.000482	1.04E+06	0.04714
1, 39	1232	30	513.2	1542	0.3328	8.40E+04
1, 40	1264	30	526.5	1.64E+04	0.03218	6.06E+05
1, 41	1296	30	540	1.86E+04	0.02905	1.20E+06
1, 42	1328	30	553.3	1.94E+04	0.02858	1.82E+06

1, 43	1360	30	566.5	1.95E+04	0.0291	2.44E+06
1, 44	1392	30	579.8	1.96E+04	0.02957	3.07E+06
1, 45	1424	30	593.3	1.92E+04	0.03098	3.69E+06
1, 46	1456	30	606.6	1.91E+04	0.0317	4.30E+06
1, 47	1488	30	619.9	1.91E+04	0.03247	4.91E+06
1, 48	1520	30	633.4	1.85E+04	0.03429	5.50E+06
1, 49	1552	30	646.6	1.78E+04	0.03642	6.07E+06
1, 50	1584	30	659.9	1.77E+04	0.03719	6.63E+06
1, 51	1616	30	673.2	1.76E+04	0.03826	7.20E+06
1, 52	1648	30	686.7	1.75E+04	0.03923	7.76E+06
1, 53	1680	30	699.9	1.70E+04	0.04129	8.30E+06
1, 54	1712	30	713.2	1.71E+04	0.04163	8.85E+06
1, 55	1744	30	726.5	1.75E+04	0.04154	9.41E+06
1, 56	1776	30	739.8	1.79E+04	0.04136	9.98E+06
1, 57	1808	30	753.4	1.82E+04	0.04131	1.06E+07
1, 58	1840	30	766.6	1.85E+04	0.04139	1.12E+07
1, 59	1872	30	779.9	1.89E+04	0.04134	1.18E+07
1, 60	1904	30	793.1	1.92E+04	0.04136	1.24E+07
1, 61	1936	30	793.3	1.91E+04	0.04154	1.30E+07
1, 62	1968	30	780	1.84E+04	0.04239	1.36E+07
1, 63	2000	30	766.7	1.77E+04	0.04332	1.41E+07
1, 64	2032	30	753.2	1.71E+04	0.04411	1.47E+07
1, 65	2064	30	740	1.64E+04	0.04518	1.52E+07
1, 66	2096	30	726.7	1.57E+04	0.04616	1.57E+07
1, 67	2128	30	713.4	1.52E+04	0.0471	1.62E+07
1, 68	2160	30	699.9	1.46E+04	0.04812	1.67E+07
1, 69	2192	30	686.6	1.40E+04	0.04912	1.71E+07
1, 70	2224	30	673.4	1.34E+04	0.05023	1.75E+07
1, 71	2256	30	660.1	1.28E+04	0.05168	1.80E+07
1, 72	2288	30	646.8	1.22E+04	0.05305	1.83E+07
1, 73	2320	30	633.2	1.16E+04	0.0547	1.87E+07
1, 74	2352	30	620	1.10E+04	0.0565	1.91E+07
1, 75	2384	30	606.7	1.04E+04	0.05831	1.94E+07
1, 76	2416	30	593.4	9843	0.06029	1.97E+07
1, 77	2448	30	579.9	9247	0.06272	2.00E+07
1, 78	2480	30	566.7	8624	0.06571	2.03E+07
1, 79	2512	30	553.4	7939	0.06971	2.05E+07
1, 80	2544	30	539.9	7205	0.07493	2.08E+07
1, 81	2576	30	526.6	6607	0.07971	2.10E+07
1, 82	2608	30	513.3	6204	0.08275	2.12E+07
1, 83	2640	30	500.1	5882	0.08502	2.14E+07
1, 84	2672	30	486.8	5577	0.08729	2.15E+07
1, 85	2704	30	473.2	5304	0.08922	2.17E+07
1, 86	2736	30	460	5027	0.0915	2.19E+07
1, 87	2768	30	446.7	4765	0.09376	2.20E+07
1, 88	2800	30	433.5	4522	0.09587	2.22E+07
1, 89	2832	30	419.9	4274	0.09824	2.23E+07
1, 90	2864	30	406.6	4040	0.1006	2.24E+07
1, 91	2896	30	393.4	3819	0.103	2.26E+07
1, 92	2928	30	380.1	3605	0.1054	2.27E+07
1, 93	2960	30	366.6	3392	0.1081	2.28E+07
1, 94	2992	30	353.3	3188	0.1108	2.29E+07
1, 95	3024	30	340	2986	0.1139	2.30E+07

1, 96	3056	30	326.8	2797	0.1168	2.31E+07
1, 97	3088	30	313.2	2608	0.1201	2.32E+07
1, 98	3120	30	300	2426	0.1236	2.32E+07
1, 99	3152	30	286.7	2256	0.1271	2.33E+07
1, 100	3184	30	273.4	2087	0.131	2.34E+07
1, 101	3216	30	259.9	1916	0.1356	2.34E+07
1, 102	3248	30	246.6	1751	0.1409	2.35E+07
1, 103	3280	30	233.3	1586	0.1472	2.35E+07
1, 104	3312	30	220.1	1425	0.1545	2.36E+07
1, 105	3344	30	206.8	1268	0.1631	2.36E+07
1, 106	3376	30	193.2	1104	0.175	2.37E+07
1, 107	3408	30	180	946.5	0.1901	2.37E+07
1, 108	3440	30	166.7	790.5	0.2109	2.37E+07
1, 109	3472	30	153.4	634.6	0.2417	2.37E+07
1, 110	3504	30	139.9	481.3	0.2906	2.38E+07
1, 111	3536	30	126.6	347.2	0.3647	2.38E+07
1, 112	3568	30	113.3	239.9	0.4724	2.38E+07
1, 113	3600	30	100.1	172.8	0.5791	2.38E+07
1, 114	3632	30	86.8	123.3	0.7037	2.38E+07
1, 115	3664	30	73.23	86.33	0.8484	2.38E+07
1, 116	3696	30	59.94	54.54	1.099	2.38E+07
1, 117	3728	30	46.65	30.1	1.55	2.38E+07
1, 118	3760	30	33.36	8.667	3.849	2.38E+07
1, 119	3792	30	20.06	4.28	4.687	2.38E+07
1, 120	3824	30	6.755	0.2858	23.63	2.38E+07

### Appendix 3: Oscillatory Shear Rheometry

The entire set covered the following conditions (see Table below).

**Table 3.1:** Oscillatory test (yield stress measurement)

(80- T <sub>test</sub> )																	
Cooling rate, c/min	0.5								1c								
SLR, Pa	25				100				25				100				
Test Temp.	30	35	40	45	30	35	40	45	30	35	40	45	30	35	40	45	
Abu-attifel crude oil untreated																	
Abu-attifel oil treated with Sirticaoil 20%vol.																	
Abu-attifel oil treated with ROA500 PPM																	

Abu-attifel oil treated with ROA1000 PPM																
Abu-attifel oil treated with PPD1000 PPM																
Abu-attifel oil treated with PPD2000 PPM																



Following are presented the data at 30C and cooling rate 1C/min. The remaining data can be found in the CD attached to the thesis.

**Table 3.2:** Oscillation results for Abu-attifel untreated crude oil at 1°C/min and at 30°C

	Time s	Temperature °C	Frequency Hz	Shear Stress Pa	Strain	Phase Angle °	Viscous Modulus Pa	Elastic Modulus Pa	Complex Modulus Pa
1, 1	7.072	30	0.5	100	0.000386	8.41	3.79E+04	2.56E+05	2.59E+05
1, 2	14.27	30	0.5	104.7	0.000448	8.17	3.32E+04	2.31E+05	2.34E+05
1, 3	21.46	30	0.5	109.6	0.000495	12.74	4.89E+04	2.16E+05	2.22E+05
1, 4	28.64	30	0.5	114.8	0.00048	13.87	5.73E+04	2.32E+05	2.39E+05
1, 5	35.84	30	0.5	120.2	0.000498	11.86	4.96E+04	2.36E+05	2.41E+05
1, 6	43.02	30	0.5	125.8	0.000588	8.11	3.02E+04	2.12E+05	2.14E+05
1, 7	50.2	30	0.5	131.7	0.000655	11.71	4.08E+04	1.97E+05	2.01E+05
1, 8	57.39	30	0.5	137.9	0.000626	11.71	4.47E+04	2.16E+05	2.20E+05
1, 9	64.58	30	0.5	144.4	0.000631	12.34	4.89E+04	2.23E+05	2.29E+05
1, 10	71.77	30	0.5	151.1	0.000651	11.54	4.65E+04	2.28E+05	2.32E+05
1, 11	78.97	30	0.5	158.3	0.000582	13.75	6.46E+04	2.64E+05	2.72E+05
1, 12	86.14	30	0.5	165.7	0.000691	9.5	3.96E+04	2.37E+05	2.40E+05
1, 13	93.33	30	0.5	173.4	0.000769	9.12	3.57E+04	2.23E+05	2.26E+05
1, 14	100.5	30	0.5	181.6	0.000809	9.15	3.57E+04	2.22E+05	2.24E+05
1, 15	107.7	30	0.5	190.1	0.000825	11.34	4.53E+04	2.26E+05	2.31E+05
1, 16	114.9	30	0.5	199	0.000862	10.3	4.13E+04	2.27E+05	2.31E+05
1, 17	122.1	30	0.5	208.4	0.000942	9.28	3.57E+04	2.18E+05	2.21E+05
1, 18	129.3	30	0.5	218.2	0.00099	9.13	3.50E+04	2.18E+05	2.20E+05
1, 19	136.5	30	0.5	228.5	0.001009	4.95	1.95E+04	2.26E+05	2.26E+05
1, 20	143.6	30	0.5	239.2	0.001089	9.55	3.64E+04	2.17E+05	2.20E+05

1, 21	150.8	30	0.5	250.4	0.001209	6.64	2.39E+04	2.06E+05	2.07E+05
1, 22	158	30	0.5	262.2	0.001215	9.49	3.56E+04	2.13E+05	2.16E+05
1, 23	165.2	30	0.5	274.5	0.001262	9.93	3.75E+04	2.14E+05	2.18E+05
1, 24	172.4	30	0.5	287.4	0.001306	6.78	2.60E+04	2.19E+05	2.20E+05
1, 25	179.6	30	0.5	300.9	0.001425	11.3	4.14E+04	2.07E+05	2.11E+05
1, 26	186.8	30	0.5	315	0.00149	9.44	3.47E+04	2.09E+05	2.11E+05
1, 27	193.9	30	0.5	329.8	0.001549	10.59	3.91E+04	2.09E+05	2.13E+05
1, 28	201.1	30	0.5	345.3	0.001712	10.05	3.52E+04	1.99E+05	2.02E+05
1, 29	208.3	30	0.5	361.5	0.001797	11.09	3.87E+04	1.97E+05	2.01E+05
1, 30	215.5	30	0.5	378.5	0.001875	11.35	3.97E+04	1.98E+05	2.02E+05
1, 31	222.7	30	0.5	396.3	0.002007	7.88	2.71E+04	1.96E+05	1.97E+05
1, 32	229.9	30	0.5	414.9	0.002126	9.95	3.37E+04	1.92E+05	1.95E+05
1, 33	237.1	30	0.5	434.4	0.002174	10.55	3.66E+04	1.97E+05	2.00E+05
1, 34	244.3	30	0.5	454.8	0.002384	10.55	3.49E+04	1.88E+05	1.91E+05
1, 35	251.4	30	0.5	476.1	0.002567	11.67	3.75E+04	1.82E+05	1.86E+05
1, 36	258.6	30	0.5	498.5	0.002683	11.87	3.82E+04	1.82E+05	1.86E+05
1, 37	265.8	30	0.5	521.9	0.002885	10.36	3.26E+04	1.78E+05	1.81E+05
1, 38	273	30	0.5	546.5	0.003067	11.23	3.47E+04	1.75E+05	1.78E+05
1, 39	280.2	30	0.5	572.1	0.003237	10.97	3.36E+04	1.74E+05	1.77E+05
1, 40	287.4	30	0.5	599	0.003547	12.36	3.62E+04	1.65E+05	1.69E+05
1, 41	294.6	30	0.5	627.1	0.003745	10.94	3.18E+04	1.64E+05	1.68E+05
1, 42	301.8	30	0.5	656.6	0.004039	11.9	3.35E+04	1.59E+05	1.63E+05
1, 43	308.9	30	0.5	687.4	0.004358	12.03	3.29E+04	1.54E+05	1.58E+05
1, 44	316.1	30	0.5	719.7	0.004827	12.5	3.23E+04	1.46E+05	1.49E+05
1, 45	323.3	30	0.5	753.5	0.005169	12.6	3.18E+04	1.42E+05	1.46E+05
1, 46	330.5	30	0.5	788.9	0.005648	13.54	3.27E+04	1.36E+05	1.40E+05

1, 47	337.7	30	0.5	826	0.006178	14.12	3.26E+04	1.30E+05	1.34E+05
1, 48	344.9	30	0.5	864.8	0.006944	13.52	2.91E+04	1.21E+05	1.25E+05
1, 49	352.1	30	0.5	905.4	0.007763	13.98	2.82E+04	1.13E+05	1.17E+05
1, 50	359.3	30	0.5	947.9	0.009093	14.77	2.66E+04	1.01E+05	1.04E+05
1, 51	366.4	30	0.5	992.4	0.01061	14.49	2.34E+04	9.05E+04	9.35E+04
1, 52	373.6	30	0.5	1039	0.01295	15.6	2.16E+04	7.73E+04	8.03E+04
1, 53	380.8	30	0.5	1088	0.01659	17.62	1.99E+04	6.25E+04	6.56E+04
1, 54	388	30	0.5	1139	0.02502	20.6	1.60E+04	4.26E+04	4.55E+04
1, 55	395.2	30	0.5	1192	2.641	86.21	450.5	29.88	451.5
1, 56	402.4	30	0.5	1248	2410	77.08	0.1813	0.04159	0.186
1, 57	409.6	30	0.5	1307	2530	77.15	0.1681	0.03835	0.1724
1, 58	416.8	29.9	0.5	1368	2662	76.52	0.1609	0.03858	0.1655
1, 59	423.9	30	0.5	1433	2718	81.74	0.1511	0.02193	0.1527
1, 60	431.1	30	0.5	1500	2698	87.74	0.1578	0.006227	0.1579

#### Appendix 4: CPM Microscopy and Structure

The entire set covered the following conditions (see Table below).

**Table 4.1:** Microscopic analysis (CPM)

Test	Crystal size distribution (measurement)			Ave. crystal size (calculation)			No. density (calculation)		
Temp	30			35			40		
Cooling rate, C/min	0.1	0.5	1	0.1	0.5	1	0.1	0.5	1
Abu-attifel crude oil untreated									
Abu-attifel oil treated with Sirtica oil 20%vol.									
Abu-attifel oil treated with ROA500 PPM									
Abu-attifel oil treated with ROA1000 PPM									
Abu-attifel oil treated with PPD1000 PPM									
Abu-attifel oil treated with PPD2000 PPM									

Here are presented the data at 30C and cooling rate 1C/min.  
The remaining data can be found in the CD attached to the thesis.

Abu-attifel untreated crude oil 30°C , 1 °C.min			
Area	% wt	no. density	AV. Area
1.15	0.31843	96.86322	0.003662
6.85	3.543815	1077.993	0.242751
12.55	10.46214	3182.477	1.312998
18.26	16.93849	5152.52	3.092969
23.96	13.98193	4253.162	3.350069
29.66	14.44465	4393.917	4.284282
35.36	11.30711	3439.511	3.998195
41.07	7.801823	2373.237	3.204209
46.77	4.99651	1519.888	2.336868
52.47	3.526756	1072.804	1.850489
58.17	2.617951	796.3545	1.522862
63.87	2.05558	625.2869	1.312899
69.58	1.562866	475.4082	1.087442
75.28	1.037457	315.584	0.780998
80.98	0.952447	289.7249	0.771292
86.68	0.642689	195.4996	0.557083
92.39	0.765512	232.8611	0.707257
98.09	0.428175	130.2466	0.419997
103.79	0.395905	120.4303	0.41091
109.49	0.460444	140.0625	0.50414
115.19	0.349847	106.42	0.402989
120.9	0.275925	83.93363	0.333593
126.6	0.14372	43.71819	0.18195
132.3	0.135048	41.08025	0.178669
138	0.157509	47.91266	0.217362
143.71	0.10875	33.08066	0.156285
149.41	0.05601	17.03768	0.083685
155.11	0.078186	23.7834	0.121274
160.81	0.120833	36.75619	0.194312
166.51	0.04222	12.8429	0.070301
172.22	0.06397	19.45903	0.110169
177.92	0.022176	6.745717	0.039456
183.62	0.069372	21.10227	0.127381
189.32	0.071078	21.62122	0.134565
234.94	0.029284	8.9079	0.0688
280.56	0.035397	10.76741	0.09931
	100	30419	34.27147